UNIVERSIDADE FEDERAL DE SÃO CARLOS
PROGRAMA DE PÓS-GRADUAÇÃO EM BIOTECNOLOGIA

AÇÃO DA VITROCERÂMICA BIOATIVA (BIOSILICATO®) NO PROCESSO DE REPARAÇÃO ÓSSEA EM RATOS

HUELITON WILIAN KIDO

SÃO CARLOS – SP
2015

HUELITON WILIAN KIDO

AÇÃO DA VITROCERÂMICA BIOATIVA (BIOSILICATO®) NO PROCESSO DE REPARAÇÃO ÓSSEA EM RATOS

Tese apresentada ao Programa de Pós-Graduação em Biotecnologia da Universidade Federal de São Carlos, como parte dos requisitos para a obtenção do título de Doutor em Biotecnologia.

Orientadores: Profa. Dra. Ana Cláudia Muniz Rennó
Profa. Dra. Fernanda de Freitas Anibal
Co-orientador: Prof. Dr. Paulo Sérgio Bossini

SÃO CARLOS – SP
2015

Ficha catalográfica elaborada pelo DePT da Biblioteca Comunitária UFSCar
Processamento Técnico
com os dados fornecidos pelo(a) autor(a)

Kido, Hueliton Wilian
K46a Ação da vitrocerâmica bioativa (Biosilicato®) no processo de reparação óssea em ratos / Hueliton Wilian Kido. -- São Carlos : UFSCar, 2015.
131 p.

Tese (Doutorado) -- Universidade Federal de São Carlos, 2015.

1. Biosilicato®. 2. PLGA. 3. Scaffold. 4. Compósito. 5. Reparação óssea. I. Título.

UNIVERSIDADE FEDERAL DE SÃO CARLOS

Centro de Ciências Exatas e de Tecnologia
Programa de Pós-Graduação em Biotecnologia

Folha de Aprovação

Assinaturas dos membros da comissão examinadora que avaliou e aprovou a Defesa de Tese de Doutorado do candidato Hueliton Wilian Kido, realizada em 26/03/2015:

Profa. Dra. Ana Claudia Muniz Renno
UNIFESP

Profa. Dra. Cristina Kurachi
UFSCar

Prof. Dr. Clóvis Wesley Oliveira de Souza
UFSCar

Profa. Dra. Ana Maria de Guzzi Plepis
USP

Profa. Dra. Renata Neves Granito
USP

DEDICATÓRIA

A toda a minha família, em especial a minha querida esposa, que esteve ao meu lado durante toda a realização deste estudo, sempre me auxiliando com muito amor, compreensão e carinho.

AGRADECIMENTOS ESPECIAIS

Às minhas orientadoras, Professoras Dra. Ana Cláudia Muniz Rennó e Dra. Fernanda de Freitas Anibal, pela oportunidade concedida, pela confiança, amizade e ensinamentos que contribuíram para o meu crescimento profissional. A vocês, a minha eterna gratidão, respeito e admiração.

Ao meu co-orientador, Professor Dr. Paulo Sérgio Bossini, pela sua amizade, confiança, ensinamentos e conselhos que foram essenciais para a minha formação pessoal e profissional.

AGRADECIMENTOS

A Deus, pelas bênçãos concedidas.

Aos meus pais, Toshiyuki Kido e Roseli Stagliano Kido, por todo o amor e carinho, por acreditarem e vivenciarem junto comigo todos os meus sonhos.

Aos meus avós, Admar (em memoria) e Gonçalina, pelo amor, carinho e lições de vida que contribuíram para a minha formação pessoal.

Ao meu irmão Huilian, minha cunhada Nana, minha prima Carol e aos meus tios Carlinhos, Alice, Tico, Roberto e Rita, pelo carinho, auxílio e por toda a alegria que é proporcionada durante nossos encontros familiares.

A minha esposa, Carina Colturato Kido, por estar sempre ao meu lado, me aconselhando e me aturando em todos os momentos difíceis. Sem você eu não conseguiria realizar esse sonho de fazer o doutorado. A você, o meu carinho e amor incondicional.

Aos professores, alunos e funcionários do Departamento de Fisioterapia da UFSCar, em especial ao professor Dr. Nivaldo Antônio Parizotto, por ter disponibilizado toda a estrutura do seu laboratório, permitindo que eu fizesse parte do seu grupo de pesquisa, onde tive a oportunidade de obter os ensinamentos que foram essenciais para a realização deste estudo. A você, a minha eterna gratidão, respeito e admiração.

Aos professores e alunos do Departamento de Genética e Evolução da UFSCar, especialmente ao Dr. Iran Malavazi e Dr. Anderson Ferreira da Cunha, Krissia Goddoi e Marina Rocha, pela disponibilidade, auxílio e ensinamentos essenciais para a realização deste trabalho.

Aos professores, alunos e funcionários do Departamento de Morfologia e Patologia da UFSCar, Dra. Karina Rossi, Dr. Clovis Souza, Beto, Cidinha e a todo o grupo de pesquisa da Dra. Fernanda de Freitas Anibal, pela confiança, ensinamentos e contribuição para o presente estudo.

Aos professores, alunos e funcionários do Departamento de Biociências da UNIFESP – Baixada Santista, especialmente às minhas queridas amigas Ângela Maria, Kelly Maria e Lívia Maria, pelo carinho, amizade e contribuição para a realização deste trabalho.

A professora Dra. Ana Maria de Guzzi Plepis e a Dra. Virgínia C. Amaro Martins do Instituto de Química da USP, pela disponibilidade, atenção e pela contribuição para a realização deste estudo.

Aos alunos do Departamento de Educação Física, Antônio de Aquino, Cynthia Castro e Karina Silva, pela amizade e pelos momentos agradáveis que passamos juntos.

A todos os meus queridos amigos do Laboratório de Recursos Terapêuticos, especialmente à Carla Tim, Patricia Brassolatti e Paulo Armelin, pelo carinho, pelas contribuições para a realização deste trabalho, pelos ensinamentos que foram essenciais para o meu desenvolvimento profissional e pelos momentos agradáveis e divertidos proporcionados durante nossos encontros.

Aos professores, alunos e funcionários do Laboratório de Materiais Vítreos, em especial ao Dr. Edgar Dutra Zanotto, Dr. Oscar Peitl e Dr. Murilo Crovace pela disponibilidade, atenção e desenvolvimento das amostras utilizadas neste trabalho científico,

Aos servidores da UFSCar, especialmente ao Roberto e Revair do Biotério Central e a Suely e Iolanda do Departamento de Fisioterapia, pela disponibilidade e por toda a atenção concedida.

Aos professores, alunos e funcionários do programa de Pós-graduação em Biotecnologia da UFSCar, em especial ao Dr. Trevelin e a secretária Cláudia Pastega, pela disponibilidade, atenção e por ter proporcionado condições para que eu pudesse desenvolver o meu projeto de pesquisa. A todos, a minha eterna gratidão.

Aos meus queridos amigos de São Carlos, Nininha, Mauro, Romano, Margarido, Ricardo, Raffaela, aos amigos da Rep. do Cogu e aos amigos pernas-de-pau do Tangará Futebol Clube (vulgo Canelite F.C), pela amizade e pelos momentos agradáveis que fizeram a diferença durante a minha estadia em São Carlos.

Aos meus amigos da UFMS, Wilter, Maria, Caio, Kexu, Erissoso, pelo carinho e amizade.

Aos meus grandes amigos de Santa Fé do Sul, Eliane, Adriana, Rodrigo, Mônica, Pulha, Tainan e Boca, pela amizade, carinho e pelos momentos prazerosos que passamos juntos.

Ao Pedro, Mariana, Bruno, Suely e Hamilton, pela amizade, apoio e por todos os momentos divertidos proporcionados em nossos encontros.

À Fundação de Amparo a Pesquisa do Estado de São Paulo (FAPESP) pela bolsa concedida.

A todas as pessoas que contribuíram de forma direta ou indireta para a realização deste trabalho.

Muito obrigado!

“As coisas mais maravilhosas que podemos experimentar são as misteriosas. Elas são a origem de toda verdadeira arte e ciência. Aquele para quem essa sensação é um estranho, aquele que não mais consegue parar para admirar e extasiar-se em veneração, é como se estivesse morto: seus olhos estão fechados”.

(Albert Einstein)

RESUMO

O presente estudo teve como objetivo principal avaliar a ação de duas diferentes apresentações (*scaffold* altamente poroso ou compósito contendo PLGA) de uma vitrocerâmica bioativa do sistema quaternário P_2O_5-Na_2O-CaO-SiO_2 (Biosilicato®) sobre o processo de reparação óssea em um modelo de defeito ósseo tibial em ratos. Para isto, foram realizados dois estudos, sendo que o primeiro teve como objetivo avaliar os efeitos dos *scaffolds* altamente porosos de Biosilicato® sobre o processo de regeneração óssea por meio da avaliação histopatológica, imunohistoquímica e ensaio imunoenzimático. Neste estudo, 80 ratos machos *Wistar* (12 semanas de idade e peso corporal de aproximadamente 300 g) foram divididos em dois grupos (controle e Biosilicato®) e eutanasiados após 3, 7, 14 e 21 dias do procedimento cirúrgico. A avalição histopatológica revelou que ambos os grupos apresentaram uma resposta inflamatória similar no período de 3 e 7 dias após a cirurgia. Durante todos os períodos experimentais, a degradação dos *scaffolds* de Biosilicato® foi observada principalmente na região periférica do material, o que possibilitou o desenvolvimento do tecido ósseo neoformado para o interior destes materiais. A Análise imunohistoquímica demonstrou que os *scaffolds* de Biosilicato® estimularam a síntese da ciclooxigenase 2 (COX-2), fator de crescimento endotelial vascular (VEGF) e fator de transcrição relacionado a runt-2 (Runx2). Além disso, o ensaio imunoenzimático revelou que o grupo Biosilicato® não apresentou diferença estatística significativa nos níveis do fator de necrose tumoral alfa (TNF-α) em todos os períodos avaliados quando comparado ao grupo controle. Ainda, o grupo Biosilicato® apresentou uma maior concentração da interleucina 4 (IL-4) 14 dias e uma menor concentração da interleucina 10 (IL-10) 21 dias após a cirurgia, quando comparado ao grupo controle. O segundo estudo teve como objetivo investigar os efeitos do compósito de Biosilicato® e ácido poli-láctico-co-glicólico (PLGA) sobre o processo de reparo ósseo através das análises histopatológica, morfométrica, imunohistoquímica e de expressão gênica (PCR em tempo real, qRT-PCR). Neste estudo, 80 ratos machos *Wistar* foram distribuídos em dois grupos (Biosilicato® e Biosilicato®/PLGA) e eutanaziados após 3, 7, 14 e 21 dias do processo de implantação dos materiais. Os achados principais mostraram que a incorporação do PLGA na vitrocerâmica Biosilicato® teve um efeito significativo na estrutura morfológica do material, levando a diminuição do pH e acelerando a perda de massa após incubação do material em solução tampão fosfato (PBS). Além disso, a avaliação histológica revelou que o grupo Biosilicato®/PLGA apresentou uma maior degradação do material, acompanhada pela maior formação de osso quando comparado ao grupo somente com Biosilicato® no período de 21 dias. Na analise imunohistoquímica nenhuma diferença na imunomarcação de Runx2, receptor ativador do ligante nuclear fator kappa-B e osteoprotegerina foram observadas entre o grupo Biosilicato® e Biosilicato®/PLGA. Ainda, a análise de qRT-PCR demonstrou que o grupo Biosilicato®/PLGA induziu a expressão de genes osteogênicos (proteína morfogenética óssea 4, fator de transcrição relacionado a runt-2, e osteocalcina) 21 dias após cirurgia. Diante dos resultados encontrados nos dois estudos, é possível concluir que ambos os materiais utilizados neste estudo, *scaffold* de Biosilicato® altamente poroso e compósito de Biosilicato® e PLGA, foram eficazes em estimular o reparo de um defeito ósseo tibial em ratos, demonstrando serem alternativas promissoras para tratamento de fraturas ósseas.

Palavras-Chave: Biosilicato®, PLGA, *scaffold*, compósito, reparação óssea.

ABSTRACT

The present study aimed to evaluate the effect of two different Biosilicate® (P_2O_5-Na_2O-CaO-SiO_2 system) presentations - highly porous scaffold and composite material – on a tibial bone defect model in rats. Two studies were performed; the first one aimed at evaluating the effect of highly porous scaffolds on bone regeneration using histopathological analysis, immunohistochemistry and immunoenzymatic assay. In this study, 80 male *Wistar* rats (12 weeks old and body weight of approximately 300 g) were divided in two groups (control and Biosilicate®) and euthanized after 3, 7, 14 and 21 days post-surgery. The histopathological evaluation revealed that both groups presented similar inflammatory responses after 3 and 7 days. At all time points, the scaffold degradation was observed, mainly in the border of the material, allowing the ingrowth of newly formed bone. The immunohistochemical analysis showed that the Biosilicate® scaffolds induced the synthesis of (i) cyclooxigenase 2 (COX-2), (ii) vascular endothelial growth factor (VEGF) and (iii) runt-related transcription factor 2 (RUNX-2). Additionally, the immunoenzymatic assay indicated that the Biosilicate® group did not presented significant statistical difference in the levels of tumor necrosis factor alpha (TNF-α) in all evaluated periods compared to the control group. In addition, the Biosilicate® group presented a higher concentration of interleukin 4 (IL-4) at day 14 and a lower concentration of interleukin 10 (IL-10) 21 days after the surgery when compared to the control group. The second study aimed at investigating the effects of Biosilicate®/ poly lactic-co-glycolic acid (PLGA) composites on the process of bone repair using histopathological, morphometric, immunohistochemical and gene expression (Real-Time PCR, qRT-PCR) analyses. In this study, 80 male *Wistar* rats were distributed in two groups (Biosilicate® and Biosilicate®/PLGA) and euthanized 3, 7, 14 and 21 days after the material implantation. The main findings showed that the incorporation of PLGA into the Biosilicate® had a significant effect in the material morphological structure, leading to a pH decrease and accelerating the mass loss upon incubation in phosphate buffered saline (PBS). Moreover, the histological evaluation revealed that the Biosilicate®/PLGA group presented a higher material degradation accompanied by a higher bone formation when compared to the plain Biosilicate® after 21 days. The immunohistochemical analysis did not show any difference in the immunolabeling for Runx2, RANKL and OPG between Biosilicate® and Biosilicate®/PLGA. In addition, the qRT-PCR indicated that the Biosilicate®/PLGA induced the osteogenic gene expressions (bone morphogenetic protein 4, Runt-related transcription factor 2 and osteocalcin) at 21 day after surgery. The results evidenced by the present studies suggest that both materials (highly porous Biosilicate® scaffolds and Biosilicate®/PLGA composites) were effective in inducing the repair of tibial bone defects in rats, demonstrating that these materials are promising alternatives for treating bone fractures.

Key-words: Biosilicate®, PLGA, *scaffold*, composite, bone repair.

LISTA DE ABREVIATURAS E SÍMBOLOS

ABNT = Associação Brasileira de Normas Técnicas

ALP = Fosfatase alcalina

ANOVA = Análise de variância

ºC = Graus Celsius

Ca = Cálcio

cm = Centímetro

cm^2 = Centímetro Quadrado

g = Grama

BG = Grupo Biosilicato®

BG/PLGA = Grupo Biosilicato® e ácido poli-láctico-co-glicólico

BGs = Vidro bioativos

$CaCO_3$ = Carbonato de cálcio

CaO = Óxido de cálcio

CaP = Fosfato de cálcio

cDNA = Ácido desoxirribonucleico complementar

CG = Grupo controle

Cox-2 = Ciclooxigenase-2

CPC = Cimento de fosfato de cálcio

Ct = Ciclo de threshold

DNA = Ácido desoxirribonucleico

EDTA = Ácido etileno diamino tetra-acético

HCA = Hidroxicarbonatoapatita

HE = Hematoxilina e Eosina

IgG = Imunoglobulina G

M = Massa molar

mg/kg = Miligrama por Quilograma de Massa Corporal

mm = Milímetro

mW = MiliWatts

Na = Sódio

O = Oxigênio

P = Fósforo

PBS = Solução de Tampão Fosfato

pH = Potencial Hidrogeniônico

rpm = Rotação por Minuto

Si = Silício

UFSCar = Universidade Federal de São Carlos

USP = Universidade de São Paulo

IL-10 = Interleucina 10

IL-4 = Interleucina 4

LaMaV = Laboratório de Materiais Vítreos

Na_2HPO_4 = Monoidrogenofosfato de sódio

Na_2O = Óxido de sódio

OC = Osteocalcina

P_2O_5 = Pentóxido de fósforo

PBS = Solução tampão fosfato

PCR = Reação em cadeia da polimerase

PLGA = Ácido poli-láctico-co-glicólico

PVA = Poli (álcool vinílico)

RANKL = Receptor ativador do ligante nuclear fator kappa-B

RNA = Ácido ribonucleico

RPS 18 = Proteína Ribossomal S18

Runx2 = Fator de transcrição relacionado a Runt-2

SD = Desvio padrão

SE = Erro padrão da média

MEV = Microscopia eletrônica de varredura

SiO_2 = Dióxido de silício

TNF = Fator de necrose tumoral-α

UNIFESP = Universidade Federal de São Paulo

VEGF = Fator de Crescimento Endotelial Vascular

W = Watts

≤ = Menor ou Igual

µm = Micrômetro

µm² = Micrômetro Quadrado

% = Porcentagem

LISTA DE FIGURAS

LISTA DE TABELAS

SUMÁRIO

PARTE II

APRESENTAÇÃO DA TESE

A presente tese foi estruturada na forma de artigos, dividida em três partes principais e redigida de acordo com as normas metodológicas da Associação Brasileira de Normas Técnicas (ABNT).

A primeira parte é constituída de uma contextualização, objetivos e detalhamento da metodologia empregada. A segunda parte é composta por dois estudos, redigidos em inglês, baseados fundamentalmente nas colocações expostas na primeira parte. O primeiro trabalho aborda a ação de um *scaffold* de Biosilicato® altamente poroso sobre o processo de reparação óssea, denominado: *"Porous bioactive scaffolds: characterization and biological performance in a model of tibial bone defect in rats"*, redigido e estruturado de acordo com as normas do periódico *"Journal of Materials Science: Materials in Medicine"*, no qual foi publicado. O segundo trabalho aborda os efeitos da utilização do compósito de Biosilicato® e microesferas de ácido poli-láctico-co-glicólico (PLGA) no processo de consolidação óssea, denominado: *"Porous poly (D,L-lactide-co-glycolide) acid/Biosilicate® composite scaffolds for bone tissue engineering"*, redigido e estruturado de acordo com as normas de publicação do periódico *"Journal Materials Research Part B"*, no qual será submetido. A terceira parte é composta pelas considerações finais, referências bibliográficas e anexos.

PARTE I

1. INTRODUÇÃO

2. OBJETIVOS

3. MATERIAIS E MÉTODOS

1. INTRODUÇÃO

O reparo de fraturas ósseas, oriundas de traumas ou decorrentes de processos patológicos, representa um grande desafio para as clínicas médias e odontológicas (FURIA *et al.*, 2010). A consolidação de fraturas é uma interação extremamente complexa que envolve a participação coordenada de células hematopoiéticas e imunes, juntamente com precursores de células esqueléticas, vias biológicas e moléculas que interagem para produzir uma resposta frente à fratura óssea (PAPE *et al.*, 2010). Múltiplos fatores regulam esta cascata de eventos moleculares por afetarem diferentes células da linhagem osteoblástica através de vários processos, tais como a migração, proliferação, quimiotaxia, diferenciação, inibição e síntese de proteína extracelular (DIMITRIOU *et al.*, 2005; GIANNOUDIS *et al.*, 2007; PAPE *et al.*, 2010).

As interações coordenadas desses diferentes elementos originam as complexas vias de reparação óssea. Qualquer déficit celular ou molecular que ocorra em determinada fase do processo de consolidação do osso, altera a sequência fisiológica do processo e pode resultar em complicações no reparo da fratura (GIANNOUDIS *et al.*, 2007). Além disso, vários fatores, tais como fraturas cominutivas, fraturas de longa extensão ou infecções podem prejudicar a consolidação óssea e conduzir a um atraso no processo de reparo, ou mesmo, levar a não união de fraturas (PHIEFFER; GOULET, 2006). Nestes casos, implantes autógenos e alógenos têm sido utilizados para estimular a consolidação de fraturas (BHATT; ROZENTAL, 2012). No entanto, a disponibilidade limitada de implantes de osso autógeno e a possibilidade de doença infecciosa ou rejeição do tecido

associada com a utilização de implantes alógenos são restrições cruciais relacionadas à reparação óssea (PULEO *et al.*, 1991).

No intuito de superar estas limitações, materiais sintéticos têm sido utilizados para estimular a regeneração do tecido ósseo (DE LONG *et al.*, 2007; HAK, 2007). Dentre os materiais sintéticos, os vidros bioativos, como por exemplo, o Bioglass® 45S5, estão entre os materiais mais utilizados na odontologia e ortopedia (XIN *et al.*, 2010). Estes materiais têm a capacidade de se ligar e integrar ao osso, formando uma camada de hidroxicarbonatoapatita (HCA) sobre a sua superfície (HENCH; POLACK, 2002). Durante a formação de HCA, ocorre a dissolução dos íons de cálcio e sílica solúvel a partir de vidro bioativo e estes produtos iónicos são capazes de estimular a divisão celular dos osteoblastos, a produção de fatores de crescimento e proteínas de matriz extracelular, contribuindo para o crescimento do tecido ósseo (JONES, 2013).

Apesar dos efeitos benéficos na formação óssea, o uso dos vidros bioativos tem sido limitado devido a suas propriedades mecânicas pobres (JAMES, 1995). Considerando este um ponto importante a ser estudado, Zanotto *et al.* (2004) desenvolveram uma vitrocerâmica bioativa totalmente cristalizada (Biosilicato®, aplicação de patente WO 2004/074199) pertencente ao sistema quaternário P_2O_5-Na_2O-CaO-SiO_2.

Estudos demonstraram que o Biosilicato® é biocompatível (KIDO *et al.*, 2013) e pode promover o aumento da formação de tecido ósseo *in vitro* em um sistema de cultura de células osteogênicas (MOURA *et al.*, 2007). Além disso, Granito *et al.* (2009) constataram que Biosilicato® promoveu uma melhor reorganização do tecido ósseo quando comparado ao Bioglass 45S5®, ao utilizar um modelo de defeito ósseo em tíbia de ratos 15 dias após a cirurgia. Um estudo realizado por Bossini *et al.*

(2011) demostrou que Biosilicato® aumentou a quantidade de osso neoformado, a angiogênese e a deposição de colágeno em defeito ósseo tibial em ratas com osteoporose. Além disso, foi verificado que Biosilicato® pode estimular o processo de consolidação óssea através da ativação de imunomarcadores relacionados com a proliferação de células ósseas, tais como COX-2, BMP-9 e RANKL (PINTO *et al.*, 2013).

Pensando no uso clínico dos biomateriais para favorecer a regeneração óssea, especialmente em casos de perda óssea de grande extensão, pesquisas na área da engenharia de tecidos têm conduzido ao desenvolvimento de implantes com estruturas porosas tridimensionais, conhecidas como *scaffolds* (LEACH *et al.*, 2006). Os *scaffolds* são arcabouços destinados a proporcionar um ambiente e uma arquitetura específica para promover o crescimento de tecido biológico (SCHIEKER *et al.*, 2006; KHAN *et al.*, 2008). A composição do material e suas características estruturais, tais como a topografia e forma, são cruciais para o sucesso destes implantes (SCHIEKER *et al.*, 2006). De acordo com alguns autores, o *scaffold* deve ser biocompatível, possuir propriedades mecânicas semelhantes às do osso e degradar-se a uma taxa compatível com a remodelação óssea, de modo a servir como uma estrutura para a interação das células e à formação de matriz óssea extracelular para o crescimento de tecido ósseo (KARAGEORGIOU e KAPLAN, 2005; JONES *et al.*, 2007).

Neste contexto, *scaffolds* porosos (porosidade total de 44%) foram desenvolvidos a partir do Biosilicato® (CROVACE, 2009). Pinto *et al.* (2013) observaram que o *scaffold* de Biosilicato® foi capaz de suportar o crescimento ósseo na região de um defeito tibial em ratos, o que evidenciou o seu potencial osteogênico. No entanto, a quantidade de osso neoformado não foi diferente do

encontrado no grupo controle em todos os períodos avaliados (PINTO *et al.*, 2013), o que poderia estar relacionado com a porosidade relativamente baixa destes *scaffolds* (KARAGEORGIOU; KAPLAN, 2005; CHEN *et al.*, 2008). Baseado nos resultados apresentados por Pinto *et al.* (2013), levantou-se a hipótese de que o aumento da porosidade poderia conduzir a um melhor desempenho biológico destes *scaffolds*, uma vez que o *scaffold* com porosidade elevada possui uma maior taxa de degradação e pode permitir um maior crescimento de tecido ósseo quando comparado a *scaffolds* com menor porosidade (KARAGEORGIOU; KAPLAN, 2005; SCHIEKER *et al.*, 2006). Com isso, um *scaffold* de Biosilicato® com a porosidade total de aproximadamente 82% foi desenvolvido (CROVACE, 2009).

Embora os *scaffolds* sejam capazes de fornecer uma integridade estrutural para o local do defeito e um ambiente específico para promover o crescimento de tecido biológico, existem pesquisas no campo da ortopedia e da engenharia de tecidos que buscam novos materiais para preenchimento e reparo de defeitos ósseos irregulares (KHAN *et al.*, 2008). Um dos materiais que tem se destacado para tratamento reparo ósseo são os materiais cerâmicos injetáveis (KHAN *et al.*, 2008; FILLINGHAM *et al.*, 2012; WU *et al.*, 2012; CHEN *et al.*, 2013; NO *et al.*, 2014). Estes materiais, além de apresentarem as propriedades básicas dos *scaffolds*, podem ser aplicados para preenchimento de defeitos ósseos irregulares através de cirurgias minimamente invasivas (DREIFKE *et al.*, 2013; NO *et al.*, 2014). Apesar dessas vantagens, uma das preocupações em relação aos materiais cerâmicos injetáveis é a ausência de uma estrutura que proporcione a porosidade nesses materiais (KHAN *et al.*, 2008).

Neste sentido, alguns pesquisadores tem contornado esta limitação incorporando a materiais cerâmicos, partículas de degradação rápida, como por

exemplo, as microesferas de ácido poli-láctico-co-glicólico (PLGA), que podem degradar-se em um curto período de tempo após a aplicação do material, conduzindo ao desenvolvimento de uma estrutura rígida e porosa (HABRAKEN *et al.*, 2008; FELIX LANAO *et al.*, 2011).

Estudos *in vivo* demostraram que a porosidade criada pela degradação das microesferas de PLGA incorporadas ao cimento de fosfato de cálcio (CPC), aumenta a taxa de degradação do material e acelera a regeneração do defeito ósseo (PLACHOKOVA *et al.*, 2007; FÉLIX LANAO *et al.*, 2011). Félix Lanao *et al.* (2011) indicaram que a combinação CPC/PLGA induziu considerável porosidade e aumento da degradação do material. Adicionalmente, análises histológicas realizadas com estes compósitos injetados em côndilos femorais de coelhos por 6 e 12 semanas revelaram excelente biocompatibilidade e osteocondutividade dos materiais testados (FÉLIX LANAO *et al.*, 2011). Em outro estudo, Plachokova *et al.* (2007) investigaram compósitos de PLGA/CPC (20/80) injetados em defeitos ósseos cranianos de ratos nos períodos experimentais de 2, 4, e 8 semanas. Os resultados histológicos mostraram que a combinação PLGA/CPC também estimulou o reparo ósseo neste modelo animal (PLACHOKOVA *et al.*, 2007). Além destes, Rennó *et al.* (2013) avaliaram os efeitos de diferentes formulações do CPC (CPC, CPC/BGs, CPC/PLGA e CPC/BGs/PLGA) no reparo de defeitos ósseos no côndilo femoral de ratos após implantação de 2 e 6 semanas. Resultados histológicos revelaram que o compósito de CPC contendo BGs e PLGA (BGs/CPC/PLGA) apresentaram uma menor quantidade do implante e maior formação óssea quando comparado as demais formulações do material (CPC, CPC/BGs e CPC/PLGA) após 6 semanas de implantação, demonstrando que tanto o BGs quanto o PLGA foram essenciais para a melhor desempenho biológico do compósito.

Diante do exposto, tanto os *scaffolds* altamente porosos quanto os materiais compósitos contendo PLGA, apresentam propriedades promissoras que podem contribuir para a formação óssea. Desta forma, no intuito de utilizar as propriedades osteogênicas do Biosilicato® e na tentativa de melhorar o seu desempenho biológico, *scaffolds* altamente porosos de Biosilicato® e compósitos de Biosilicato®/PLGA foram desenvolvidos como uma alternativa inovadora para tratamento de reparo ósseo. Embora existam resultados positivos com o uso do Biosilicato®, mais estudos são necessários, uma vez que não existem trabalhos na literatura que abordem os efeitos dessas novas apresentações do material (*scaffolds* altamente porosos e compósitos) no processo de reparação óssea. Neste sentido, a hipótese deste estudo é que os *scaffold* de Biosilicato® com porosidade de 82% e os compósitos de Biosilicato®/PLGA possuem uma estrutura e composição adequada para proporcionar o crescimento de tecido ósseo neoformado, por meio da taxa compatível de degradação do material e aumento na expressão gênica e síntese proteica de fatores que contribuem para o processo de consolidação de defeitos ósseos.

2. OBJETIVOS

2.1. OBJETIVO PRINCIPAL

Diante do exposto, o presente estudo teve como objetivo avaliar a ação de duas diferentes formas de apresentação do Biosilicato® - (i) *scaffold* altamente poroso e (ii) compósito a partir da combinação com PLGA - no reparo ósseo de defeitos tibiais em ratos após os períodos experimentais de 3, 7, 14 e 21 dias.

2.2. OBJETIVOS ESPECÍFICOS

I. Avaliar a ação dos *scaffolds* sobre o processo de consolidação óssea através da análise histopatológica, imunohistoquímica (ciclooxigenase-2, fator de crescimento endotelial vascular e fator de transcrição relacionado à Runt-2) e do ensaio imunoenzimático (Interleucina 4, interleucina 10 e fator de necrose tumoral-α).

II. Avaliar os efeitos dos compósitos de Biosilicato®/PLGA no processo de consolidação de defeitos ósseos, mediante as análises histológicas (histopatológica e morfométrica), imunohistoquímicas (fator de transcrição relacionado à Runt-2, receptor ativador do ligante nuclear fator kappa-B e osteoprotegerina) e análise de expressão dos genes relacionados à regeneração óssea (fator de transcrição relacionado à Runt-2, proteína morfogenética óssea 4, fosfatase alcalina e osteocalcina).

3. MATERIAIS E MÉTODOS

3.1. MATERIAIS

3.1.1. BIOSILICATO®

A vitrocerâmica Biosilicato® utilizada neste estudo foi produzida e fornecida pelo Laboratório de Materiais Vítreos (LaMaV) da Universidade Federal de São Carlos (UFSCar), em colaboração com os professores Dr. Edgar Dutra Zanoto e Dr. Oscar Peitl Filho.

O Biosilicato® é uma vitrocerâmica do sistema P_2O_5-Na_2O-CaO-SiO_2, altamente bioativa e totalmente cristalina. Os detalhes da composição e do tratamento térmico para a cristalização do material estão descritos na patente WO 2004/074199 (ZANOTTO *et al.*, 2004).

Durante a síntese do material, foi realizada a fusão dos componentes pesados e homogeinizados em forno elétrico a 1450ºC. Após a homogeinização do fundido, o vidro resultante foi submetido a tratamentos térmicos até completa cristalização do material. Em seguida, a amostra passou por um processo de moagem, até a obtenção de um pó com granulometria média de 1,3 μm.

3.1.2. MICROESFERAS DE PLGA

As microesferas de PLGA (Purasorb®, Purac, Gorinchem, Holanda) foram preparadas usando a técnica de evaporação (Fig. 1), previamente descrita por Félix Lanao *et al.* (2011). Cada 1 g de PLGA foi dissolvido em 4 mL de diclorometano (DCM, Merck, Darmstadt, Alemanha) em um tubo de 50 mL. Foram adicionados 500 μL de água desionizada (dd$H_2$0) enquanto a solução era vigorosamente agitada em um agitador (vórtex) por 1 minuto. Em seguida, foram adicionados 6 mL de solução

a 3% de poli (álcool vinílico) (PVA) (88% hidrolizado, MW 22000, Belgica) e a solução resultante foi agitada em vórtex por mais 1 minuto. O conteúdo do tubo de 50 mL foi transferido para um béquer e um total de 394 mL de PVA (0,3%) foi adicionado vagarosamente, seguido pela adição de 400 mL de solução de álcool isopropílico a 2% (Merck, Darmstadt, Alemanha). A suspensão foi agitada por 1 hora. As microesferas resultantes do processo foram deixadas em repouso por 15 minutos e a solução restante foi decantada. Logo após, as esferas foram lavadas, decantadas novamente e a solução foi aspirada. A solução resultante foi levada ao liofilizador por 24 horas e em seguida estocada à -20ºC (FELIX LANAO *et al.*, 2011).

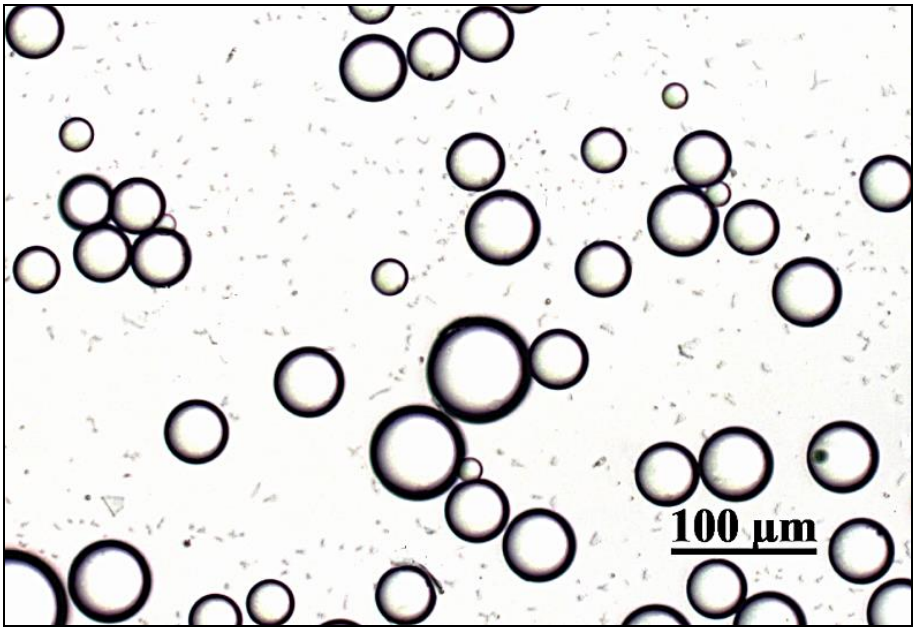

Fig. 1 Fotomicrografia representando as microesferas de PLGA.

3.2. SÍNTESE DOS *SCAFFOLDS* DE BIOSILICATO®

Os *scaffolds* foram sintetizados de acordo com Crovace (2009), onde, foi preparada uma barbotina em álcool contendo o Biosilicato®, aditivos e agentes

porogênicos (negro de fumo). Após secagem da barbotina, o pó obtido foi inicialmente prensado a uma pressão de 20 MPa até obtenção de pastilhas. Posteriormente, as pastilhas foram novamente prensadas isostaticamente a uma pressão de 100 MPa. A queima das pastilhas foi realizada em três estágios: o primeiro para remoção do ligante (2 horas em forno a 375ºC), o segundo para a remoção do agente porogênico (2 horas em forno a 610ºC) e o terceiro para a sinterização dos *scaffolds* propriamente dita (5 horas em forno a 975ºC).

Neste estudo, foram utilizados *scaffolds* com 3 mm de diâmetro e 1,5 mm de espessura, com porosidade total de aproximadamente 80%, poros totalmente interconectados com diâmetro médio de 300 µm (Fig. 2). Estas características são adequadas para a osteogênese, uma vez que permitem a passagem de células e suprimento sanguíneo através do mesmo (KARAGEORGIOU; KAPLAN, 2005).

Todos os *scaffolds* de Biosilicato® foram devidamente esterilizados em forno a 130°C durante 12 horas, antes da sua efetiva utilização.

Para a observação microestrutural, seis *scaffolds* foram incluídas em resina epoxy (EpoThin® - BUEHLER) à vácuo. As amostras foram lixadas e polidas com óxido de cério. Em seguida, as amostras foram revestidas com uma fina camada de ouro por pulverização catódica (Quorum Q150R ES) e analisados em MEV (Philips FEG XL-30). Secções transversais e longitudinais foram utilizadas para a análise. O tamanho médio dos poros e da porosidade total foi determinado por análise de imagens MEV usando o programa Image-J (versão 1.46i).

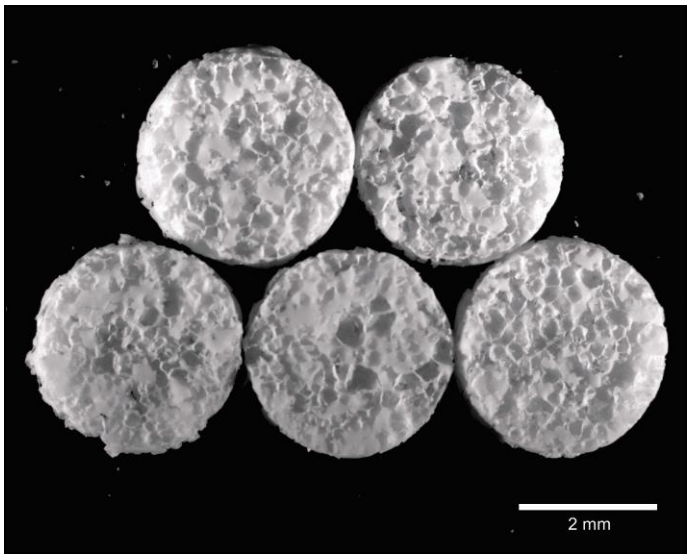

Fig. 2 Imagem dos *scaffolds* de Biosilicato® obtidas por estereomicroscópio (Leica MZ75).

3.3. SÍNTESE DOS COMPÓSITOS DE BIOSILICATO®/PLGA

As amostras de Biosilicato®/PLGA foram obtidas através da adição das microesferas de PLGA e do Biosilicato® dentro de uma seringa descartável de 5 mL. Nesta mistura, foi adicionado 280 µm de solução de Na_2HPO_4 a 1%, misturado vigorosamente por 30 segundos em um agitador odontológico (Silamat mixing apparatus, Vivadent, Schaan, Liechtenstein). Em seguida, a mistura foi injetada em um molde de teflon com dimensões de cilindros de 3 mm de diâmetro e 2 mm de espessura. Findada esta etapa, as amostras foram colocadas em estufa a 37ºC por 24 horas e estocadas em temperatura ambiente (RENNO *et al.*, 2013). Em seguida, as amostras foram removidas do molde e analisadas em microscópio eletrônico de varredura (MEV; Jeol 6310). Todas as amostras foram esterilizadas com óxido de etileno (ACECIL, Campinas, SP, Brasil) para posteriormente serem utilizadas nas análises.

Para este estudo, foram sintetizados materiais nas proporções de 70% Biosilicato®/30% PLGA e de 100% Biosilicato. Essas proporções foram obtidas baseadas em estudos prévios do nosso grupo de pesquisa (dados não publicados).

3.3.1. QUANTIFICAÇÃO DA PERDA DE MASSA E AVALIAÇÃO DO pH

Para a quantificação da porcentagem de perda de massa e estudo do pH, as amostras dos materiais (Biosilicato® e Biosilicato®/PLGA) foram pesados em balança de precisão (Quimis, São Paulo, Brasil) e imersos em solução tampão fosfato (PBS, 10mM, pH 7,6). Após os períodos de 3, 7, 14 e 21 dias, as amostras foram submetidas às análises.

No decorrer de cada período experimental, as amostras foram removidas do meio e foram secas em estufa a 37ºC antes da quantificação da massa. A perda de massa das amostras foi calculada de acordo com a seguinte fórmula:

$$\text{Perda de Massa (\%)} = [(P_t - P_0)/P_0] \times 100\%,$$

onde P_0 é o peso das amostras antes da imersão em PBS e P_t é o peso da amostra após imersão em PBS.

Logo após a remoção das amostras do meio de incubação, o pH foi mensurado (Quimis, São Paulo, Brasil).

3.4. ANIMAIS DE EXPERIMENTAÇÃO

Para a realização deste estudo, foram utilizados 160 ratos machos (*Rattus norvegicus albinus)* da linhagem *Wistar* (300-320 g), provenientes do Biotério Central da UFSCar. Os animais permaneceram durante os períodos experimentais no Biotério do Departamento de Fisioterapia, dentro de gaiolas de polipropileno, mantidos em ambiente higienizado, com iluminação em ciclo claro/escuro de 12

horas, recebendo água e ração balanceada à vontade. Esse estudo foi aprovado pela Comissão de Ética no Uso de Animais da UFSCar (protocolo nº 042/2012 e 050/2014).

3.5. DELINEAMENTO EXPERIMENTAL

Os 160 animais foram pesados e distribuídos aleatoriamente em quatro grupos experimentais para utilização em dois estudos distintos:

- **Estudo I:**

Grupo Controle: os ratos deste grupo foram submetidos à cirurgia para a confecção do defeito ósseo.

Grupo *Scaffold* de Biosilicato®: os ratos deste grupo foram submetidos ao defeito ósseo e receberam um implante de *scaffold* de Biosilicato®.

- **Estudo II:**

Grupo matriz de Biosilicato®: os ratos deste grupo foram submetidos ao defeito ósseo e receberam uma matriz com 100% de Biosilicato®.

Grupo matriz de Biosilicato®/PLGA: os ratos deste grupo foram submetidos ao defeito ósseo e receberam uma matriz com 70% de Biosilicato® e 30% de PLGA.

Todos os 4 grupos foram divididos em 4 subgrupos (compostos por 10 animais cada), para a realização das análises em diferentes períodos experimentais (3, 7, 14 e 21 dias). Estes períodos foram escolhidos no intuito de avaliar o processo de reparo ósseo durante a fase inflamatória e a fase de consolidação do tecido (HADJIARGYROU *et al.,* 1998).

3.6. PROCEDIMENTO CIRÚRGICO

Os animais foram submetidos a um procedimento cirúrgico para a confecção de um defeito ósseo circular na região proximal da tíbia (BOSSINI *et al.*, 2012; TIM *et al.*, 2013; PINTO *et al.*, 2013). Para a realização das lesões foi utilizada uma broca odontológica tipo trefina (WMA - Brasil) com 2 cm de comprimento e 3 mm de diâmetro, acionada por um micromotor (BELTEC – Brasil), com rotação de 13.500 rpm, irrigada com soro fisiológico para evitar queimadura do tecido ósseo. Os animais foram previamente anestesiados com Ketamina (80 mg/kg) e Xylazina (16 mg/kg), e a região a ser operada foi tricotomizada e limpa com iodo povidine. Os animais foram submetidos a uma incisão no terço proximal da tíbia para a exposição do osso. Em seguida, com o auxílio de um paquímetro digital, foi realizada a padronização do local do defeito ósseo (10 mm abaixo da região articular do joelho do animal). A lesão foi induzida com a trefina mantida na posição horizontal e perpendicular em relação ao eixo longitudinal do osso, de modo a penetrar a cortical medial e danificar o canal medular abaixo desta, porém, sem atingir a face contralateral, promovendo-se um orifício com 3 mm de diâmetro. O defeito ósseo foi induzido nas duas tíbias de cada animal. Logo após a confecção do defeito, os animais receberam um implante de biomaterial em cada tíbia (*scaffold* de Biosilicato® ou matriz de Biosilicato®/PLGA). Os animais do grupo controle foram submetidos ao procedimento cirúrgico, porém não receberam nenhum tipo de biomaterial. Finalizada esta etapa, a pele foi suturada e foi realizada a limpeza local com iodo povidine.

3.7. EUTANÁSIA E COLETA DAS AMOSTRAS

De acordo com cada período experimental, os animais foram anestesiados com Ketamina e Xilazina. Logo após, foi realizada a coleta sanguínea por punção cardíaca e a dissecção completa da tíbia direita e esquerda de cada animal. O sangue foi utilizado na análise de quantificação dos fatores inflamatórios, a tíbia esquerda do animal foi congelada em freezer -80ºC para posterior utilização na análise de expressão gênica e a tíbia direita foi utilizada nas análises histológicas.

3.8. ANÁLISES HISTOLÓGICAS

Para a realização das análises histológicas a tíbia direita de cada animal foi fixada em formalina tamponada a 10% (Merck, Darmstadt, Alemanha) por 24 horas. Após, as amostras foram lavadas em água por 24 horas e submetidas a um processo de descalcificação com solução aquosa a 10% de EDTA (ácido etileno diamino tetra-acético) (Merck, Darmstadt, Alemanha), onde a solução era substituída 3 vezes por semana. Após a descalcificação, as peças foram incluídas em parafina e lâminas histológicas foram confeccionadas (3 cortes semi-seriados com espessura de 5 μm para cada amostra). O plano de secção do corte foi longitudinal em relação ao osso.

3.8.1. ANÁLISE HISTOPATOLÓGICA

Os cortes histológicos de cada amostra foram corados com Hematoxilina e Eosina (HE, Merck, Darmstadt, Alemanha) e avaliados com o auxílio de um microscópio óptico (Leica Microsystems AG, Wetzlar, Alemanha). A descrição morfológica do defeito ósseo foi realizada levando em consideração os seguintes critérios: intensidade do processo inflamatório, áreas de fibrose, presença de tecido

de granulação, incorporação do biomaterial e neoformação óssea (osso primário e secundário).

3.8.2. ANÁLISE MORFOMÉTRICA

Além da análise histológica descritiva (histopatológica), foi realizada a análise morfométrica para quantificar a área de osso neoformado na extensão total do defeito ósseo. Para isto, cortes corados com HE (Merck, Darmstadt, Alemanha) foram fotografados e 3 campos padronizados na região cortical do defeito ósseo foram capturados com o auxílio de um microscópio óptico (Leica Microsystems AG, Wetzlar, Alemanha) e analisados utilizando um sistema de análise de imagem Motic Images Plus (versão 2.0). Depois de registradas, as áreas foram somadas, resultando na área total de tecido ósseo neoformado (µm²) (MATSUMOTO, *et al.*, 2009; BOSSINI *et al.*, 2012; TIM *et al.*, 2013).

3.9. ANÁLISE IMUNOHISTOQUÍMICA

Para a realização da analise imunohistoquímica os cortes histológicos foram desparafinados (xilol, Labsynth®, Diadema, Brasil) e hidratados em diferentes gradientes de etanol (Labsynth®, Diadema, Brasil). Em seguida, cada amostra foi pré-tratada num vaporizador com tampão diva Decloaker (Biocare Medical, CA, EUA) durante 5 minutos para a recuperação do antígeno. O material foi pré-incubado com 0,3% de peróxido de hidrogénio (Labsynth®, Diadema, Brasil) em solução salina tamponada com fosfato (PBS) durante 30 min a fim de inativar a peroxidase endógena e depois bloquear com 5% de soro normal de cabra em solução PBS durante 20 min. Três secções de cada espécime foram incubadas durante 2 h com anticorpo policlonal primário fator de anti-ciclooxigenase-2,

concentração de 1:200 (Santa Cruz Biotechnology, Santa Cruz, EUA), anti-crescimento endotelial vascular – VEGF, concentração de 1:200 (Santa Cruz Biotechnology, Santa Cruz, EUA), anti-fator de transcrição relacionados com o Runt 2 – Runx2, concentração de 1:200 (Santa Cruz Biotechnology, Santa Cruz, EUA), anti-receptor ativador do ligante nuclear fator kappa B – RANKL, concentração de 1:100 (Santa Cruz Biotechnology, Santa Cruz, EUA) e anti-osteoprotegerina – OPG, concentração de 1:100 (Santa Cruz Biotechnology, Santa Cruz, EUA). Em seguida, as secções foram incubadas com conjugado de biotina anticorpo secundário IgG anti-coelho (Vector Laboratories, Burlingame, CA, EUA) a uma concentração de 1: 200 em PBS durante 30 min, seguido da aplicação de pré-formado complexo biotina avidina conjugada com peroxidase (Vector Laboratories, Burlingame, CA, EUA) durante 30 min. Uma solução de solução 3-3'-diaminobenzidina (0,05%) e foram aplicadas hematoxilina de Harris. Para confirmação dos resultados, alguns cortes foram submetidos ao mesmo tratamento omitindo-se somente os anticorpos primários, estes cortes servirão como controle negativo das reações.

A marcação dos fatores estudados foram avaliados qualitativamente (presença e localização dos imunomarcadores) em 3 campos pré-determinados utilizando uma microscópio de luz óptico (Leica Microsystems AG, Wetzlar, Alemanha) e semi-quantitativamente por um sistema de scores. Na análise semi-quantitativa foi mensurada a imunomarcação nos cortes por porcentagem da área do campo avaliado em: ausente (score 1, 0%), levemente marcado (score 2, 1% a 34%), moderadamente marcado (score 3, 35% a 65%) e intensamente marcado (score 4, 66% a 100%) (MATSUMOTO *et al.*, 2012; TIM *et al.*, 2013; PINTO *et al.*, 2013).

3.10. ANÁLISE GÊNICA

A análise de expressão gênica foi realizada pela técnica de PCR em tempo real, para verificar a expressão dos genes da proteína óssea morfogenética 4 (BMP4), osteocalcina (OC), fosfatase alcalina (ALP) e fator de transcrição relacionado à Runt-2 (Runx2) durante o processo de reparo de um defeito ósseo preenchido com biomaterial. Tais genes foram selecionados por contribuírem no processo de reparo ósseo (SONG *et al.,* 2006; YAOITA *et al.,* 2000; KLOTING *et al.,* 2005; RATH *et al.,* 2008). A quantificação relativa da expressão dos genes em estudo foi normalizada através da comparação da amplificação de um controle endógeno, o gene RPS18 (Proteína Ribossomal S18).

3.10.1. EXTRAÇÃO DO RNA TOTAL

As tíbias esquerdas congeladas foram cortadas a 2 mm acima e abaixo do local do defeito e maceradas com a auxílio de um mortar e um pistilo de metal (D.L.MICOF, São Paulo, SP), mantidos em nitrogênio liquido. O “pó” proveniente das tíbias maceradas foi transferido para um cadinho de porcelana resfriado com 1 ml de trizol (Invitrogen, Carlanbad, CA), no qual foi homogeneizado com o auxílio do pistilo de porcelana. Em seguida, as amostras foram novamente homogeneizadas em tubos de ensaio de descartáveis com o auxílio do Power Gen 1000 S1 (Fisher Scientific). Passado este processo, foi iniciado o protocolo de extração de RNA de acordo com as instruções do fabricante. O RNA total obtido foi quantificado por meio da leitura em espectrofotômetro (A_{260nm} e A_{280nm}) (Nanovue Plus, GE Healthcare Life Sciences, São Paulo, Brazil) e sua integridade foi confirmada pela visualização do padrão de eletroforese das bandas 28S e 18S do RNA ribossomal, em gel de agarose-formaldeído 1%. Após a análise da integridade das bandas, o RNA total

dos espécimes de cada grupo experimental foi tratado com DNAse I (Invitrogen, Carlsbad, CA, USA), segundo a indicação do fabricante. Um micrograma de RNA total (1 µg) foi utilizado como padrão para a síntese de DNA complementar (cDNA) utilizando o kit de transcrição reversa High-capacity (Life Technologies, Carlsbad, USA), de acordo coma s instruções do fabricante. As sequencias dos primers foram desenhadas para os seguintes genes: gene endógeno RPS18 (NM_181374.2), Proteína morfogenética óssea 4 (BMP4, NM_012827.2), Fator de transcrição relacionado ao runt – 2, (Runx2, NM_053470.2), Fosfatase alcalina (ALP, J03572.1) and Osteocalcina (OC, NM_013414.1) (Table 1), usando o software Primer Express 2.0 (Applied Biosystems, Foster City, USA). Todos os primers foram inicialmente testados para avaliar a melhor concentração e eficiência na reação.

3.10.2. PCR EM TEMPO REAL

A reação de PCR em tempo real foi realizada com os primers OC, ALP, BMP4, Runx2 e RPS18 (controle endógeno) utilizando-se o kit SYBR Green PCR Master Mix (Applied Byosystems). As amostras foram processadas no Termociclador Rotor-Gene, R3000 (*Cobertt Research*) e a sequência de ciclos dos primers estudados, foram padronizadas de acordo com a temperatura de *melting* (Tm) de cada um. Os valores de Ct (Threshold cycle) foram fornecidos pelo software Rotor Gene – 6. O Ct é o ponto onde o sinal de fluorescência é notado pela primeira vez com o menor número de ciclos durante a fase exponencial da amplificação. O nível comparativo da expressão de cada condição foi dado pela unidade arbitrária e calculado pelo método de $2^{-\Delta\Delta Ct}$ (LIVAK; SCHMITTGEN, 2001).

3.11. ANÁLISE IMUNOENZIMÁTICA

A quantificação das citocinas plasmáticas foi realizada através do Ensaio Imunoenzimático (ELISA) com os kits Duo Set (R&D Systems®, Minnesota, EUA), a fim de avaliar as citocinas atuantes no processo inflamatório durante o reparo de defeito ósseo na presença dos biomateriais. Neste estudo, foram avaliadas as citocinas IL-4 (Interleucina 4), IL-10 (Interleucina 10), TNF-α (Fator de necrose tumoral alfa) por apresentarem grande importância no processo inflamatório (PAPE *et al.,* 2010). Para isto, o sangue coletado foi acondicionado em tubos sem anticoagulante por aproximadamente 2 horas até a sua coagulação. Em seguida, as amostras foram centrifugadas a 1500 rpm por 15 minutos. O soro resultante desta centrifugação foi aliquotado em microtubo e congelado a -80ºC. As citocinas foram dosadas utilizando-se pares de anticorpos e respectivos padrões recombinantes obtidos comercialmente, seguindo as recomendações do fabricante. As alíquotas de soro foram submetidas a dosagem das citocinas IL-4, IL-10 e TNF-α. As microplacas de alta afinidade foram sensibilizadas com anticorpos monoclonais anti-citocinas e permaneceram “overnight” a temperatura ambiente. Após bloqueio com PBS as placas foram lavadas e, em seguida, foram adicionados sobrenadantes e a curvas padrão de citocinas recombinantes. As placas foram mantidas a temperatura ambiente por 2 horas e após o termino deste período, foram lavadas novamente. Foram adicionados anticorpos anti-citocinas biotinilados e mantidos por mais de 1 hora a temperatura ambiente. Os resultados expressos em densidade óptica e foram convertidos em quantidade de moléculas por mL, com o auxílio da curva padra. Esta análise foi realizada no Laboratório de Parasitologia do Departamento de Morfologia e Patologia da UFSCar, sob a supervisão da Profa. Dra. Fernanda de Freitas Anibal.

3.12. ANÁLISE ESTATÍSTICA

Os dados foram analisados estatisticamente através de técnicas descritivas (tabelas e gráficos), na forma de médias, desvios (SD) ou erros padrão (SE). A normalidade da distribuição de todas as variáveis foi verificada usando o teste de Shapiro-Wilk's. Para amostras paramétricas foi utilizado o teste Two-way ANOVA ou teste t *student* para avaliar a variância da comparação entre os grupos, e nos casos significantes, o teste de Tukey foi utilizado para discriminar as diferenças geradas pelo test Two-way. Para amostras não paramétricas foi utilizado o teste de Mann-Whitney. As análises foram realizadas no programa EXCEL (2007) e no software STATISTICA (versão 7.0). Para as conclusões das análises estatísticas será utilizado o nível de significância de 5% ($p \leq 0,05$).

PARTE II

4. ESTUDO I

5. ESTUDO II

4. ESTUDO I

Porous bioactive scaffolds: characterization and biological performance in a model of tibial bone defect in rats

Hueliton Wilian Kido,[1] Carla Roberta Tim,[1] Paulo Sérgio Bossini,[5] Nivaldo Antônio Parizotto,[1] Cynthia Aparecida de Castro,[2] Murilo Camuri Crovace,[3] Ana Candida Martins Rodrigues,[3] Edgar Dutra Zanotto,[3] Oscar Peitl Filho,[3] Fernanda de Freitas Anibal,[4] Ana Claudia Muniz Rennó[5]

[1]Department of Physiotherapy, Post-Graduate Program of Biotechnology, Federal University of São Carlos (UFSCar), São Carlos, SP, Brazil

[2]Department of Physiological Sciences, Federal University of São Carlos (UFSCar), São Carlos, SP, Brazil

[3]Department of Materials Engineering, Vitreous Materials Laboratory (LaMaV), Federal University of São Carlos (UFSCar), São Carlos, SP, Brazil

[4]Department of Morphology and Pathology, Federal University of São Carlos (UFSCar), São Carlos, SP, Brazil

[5]Department of Biosciences, Federal University of São Paulo (UNIFESP), Santos, SP, Brazil

4.1. ABSTRACT

The aim of this study was to evaluate the effects of highly porous Biosilicate® scaffolds on bone healing in a tibial bone defect model in rats by means of histological evaluation (histopathological and immunohistochemical analysis) of the bone callus and the systemic inflammatory response (immunoenzymatic assay). Eighty *Wistar* rats (12 weeks old, weighing ±300 g) were randomly divided into 2 groups (n = 10 per experimental group, per time point): Control group (CG) and Biosilicate® group (BG). Each group was euthanized at 3, 7, 14 and 21 days after surgery. Histological findings revealed a similar inflammatory response in both experimental groups, 3 and 7 days after surgery. During the experimental periods (3-21 days post-surgery), it was observed that the biomaterial degradation, mainly in the peripheral region, provided the development of the newly formed bone into the scaffolds. Immunohistochemical analysis demonstrated that the Biosilicate® scaffolds stimulated cyclooxygenase-2 (COX-2), vascular endothelial growth factor (VEGF) and runt-related transcription factor 2 expression (Runx2). Furthermore, in the immunoenzymatic assay, BG presented no difference in the level of tumor necrosis factor alpha (TNF-α) in all experimental periods. Still, BG showed a higher level of interleukin 4 (IL-4) 14 days after implantation and a lower level of interleukin 10 (IL-10) in 21 days after surgery. Our results demonstrated that Biosilicate® scaffolds can contribute for bone formation through a suitable architecture and by stimulating the synthesis of markers related to the bone repair.

Key words: bioactive material, scaffold, bone repair

Publicado no periódico Journal of Material Science: Material in Medice (Anexo C)

4.2. INTRODUCTION

Although bone tissues have the ability of healing themselves, multiple factors may impair fracture consolidation, including fractures beyond critical size dimension, bone loss caused by diseases, infections or tumor resections, which may lead to the development of pseudoarthosis or even non-union fractures [1]. In this context, several surgical procedures are required to treat such clinical conditions, which are related to considerable morbidity and increased health care needs [2]. Bone grafts to enhance bone repair have been emerging as a promising alternative and include the use of autografts, allografts and synthetic bone substitutes [3-5].

Nevertheless, the limited availability of autogenous bone implants and the possibility of infectious diseases or tissue rejection associated to the use of allogenous implants are pivotal restrictions related to bone healing therapies [6]. As an alternative, synthetic bone substitutes such as calcium phosphate (CaP) ceramics [7], polymer-based materials [8], bioactive glass and glass-ceramics [9] have been developed in order to overcome these limitations [10-12].

Bioactive glasses are a well-known class of materials, with a markedly osteogenic potential, able of stimulating bone metabolism and accelerating bone healing [13-15]. These materials when immersed in body fluids promote release of ions in the medium, leading to the formation of a porous layer which is rich in silica, followed by the formation of hydroxy carbonate-apatite (HCA) layer on the surface of the material [16]. The formation of the HCA layer may contribute to the development of bone tissue, once the HCA is equivalent to inorganic mineral phase of bone [16].

Despite the osteogenic potential of the bioactive glasses, their use has been limited because of their poor mechanical properties and very high crystallization tendency when heated [17]. As an alternative, some glass-ceramics obtained by

controlled crystallization of certain glasses based on the quaternary Na_2O-CaO-SiO_2-P_2O_5 system having improved mechanical properties, including Biosilicate®, have been developed [17]. It was demonstrated that Biosilicate® is biocompatible with bone tissues and presents non-cytotoxicity [18]. Furthermore, its osteogenic effects have already been demonstrated by using both *in vitro* and *in vivo* studies [19-21]. Granito *et al.* [21] found that Biosilicate® presented higher bone volume when compared to Bioglass 45S5 in a tibial bone defect model in rats 20 days post-surgery.

The current availability of glass ceramics for the treatment of bone defects, including Biosilicate®, is still mainly in solid pieces or in the form of granules. One of the main disadvantages of those forms is that they may not have the proper porosity to allow tissue ingrowth and may not degrade according to the rate of bone tissue formation [22]. In this context, many efforts have been made to develop improved bone graft substitutes that interact more appropriately with the complex biological environment of bone tissue [23]. Biosilicate® porous scaffolds offer a three-dimensional structure which mimics the structure of the extracellular matrix of natural bone, allowing bone cell attachment, proliferation and differentiation at the region of the defect [24].

An initial *in vivo* study demonstrated that a porous Biosilicate® scaffold (total porosity of 44%) was able to support bone ingrowth in the region of the tibial bone defect, thus highlighting the osteogenic potential of the material. However, the amount of newly formed bone was not significantly different from the control group which may be related to its relatively low porosity [25].

In order to obtain more appropriate bone substitutes to be used as grafts, highly porous scaffolds may be an interesting alternative with useful properties for

biomedical applications, i.e. biodegradability and more appropriate structure to allow tissue ingrowth [26].

In this context, a new Biosilicate® scaffold, with increased porosity (total porosity of 82%), was developed [18]. It was hypothesized that this innovative osteogenic scaffold would offer a more suitable template for bone cell attraction and tissue ingrowth. Consequently, the present study aimed to evaluate the *in vivo* orthotopic response of this new porous bioactive scaffold, during different experimental set points (3, 7, 14 and 21 days after implantation) in a tibial bone defect model in rats. Histology and immunohistochemistry analyses of the factors involved in osteogenesis (COX-2, VEGF, Runx2) were used to evaluate the effects of the porous bioactive scaffold in the bone callus. Furthermore, an immunoenzymatic assay was performed to evaluate the action of the material on the systemic inflammatory response by quantifying the inflammatory cytokines levels (IL-4, IL-10 and TNF-α) in rat serum.

4.3. MATERIALS AND METHODS

4.3.1. FABRICATION AND CHARACTERIZATION OF THE BIOSILICATE® SCAFFOLDS

Biosilicate® was obtained by melting reagent grade raw materials (Na_2CO_3 – JT Baker, $CaCO_3$ – JT Baker, Na_2HPO_4 – JT Baker, and SiO2 – Zetasil 2) in a platinum crucible at 1250ºC for four hours. The glass was poured in a stainless steel mould and heat treated until it reached full crystallization in an electric furnace. More details of the synthesis of Biosilicate® are described in the WO 2004/074199 patent [27]. Glass pieces were crushed in a porcelain mortar and milled in a planetary ball mill at 550 rpm for 240 min. In this study, the Biosilicate® scaffolds were

manufactured by a method based in the addition of a porogen agent. This method was described with details in a previous work [18, 28]. This method is therefore only shortly described here: initially, 100 mL of a suspension containing 67 vol % of isopropyl alcohol anhydrous (QHEMIS), 3 vol % of polyvinyl butiral (Butvar B-98), 24 vol % of carbon black (CABOT BP-120), and 6 vol % of Biosilicate® was prepared. Then isopropyl alcohol, PVB, and Biosilicate® were mixed in an agate jar and milled in a planetary ball mill (Pulverisette 6 – FRITSCH) at 550 rpm for 1 h. The agate spheres were removed from the suspension and the pre-sieved carbon black (300–600 μm) was added and then mixed for 5 min at 150 rpm. The suspension was poured into a plastic container and dried with a heat gun (DEKEL DK1210). The resulting granulated powder was pressed in two steps, the first unixial using a cylindrical steel mould and the second isostatical. Finally, the cylindrical samples were heat treated for organics burn-out and to promote Biosilicate® sintering. Scaffolds of approximately 3 mm (diameter) by 2 mm (thickness) were obtained. Sterilization was performed in an electric oven at 130°C for 14 h.

For microstructural observation, six scaffolds were embedded in epoxy resin (EpoThin® - BUEHLER) under vacuum. The embedded samples were ground in silicon carbide paper until grit size 1200 and polished with cerium oxide. Then, they were coated with a thin layer of gold by sputtering (Quorum Q150R ES) and analyzed in SEM (Philips FEG XL-30). Both transversal and longitudinal sections of the scaffolds were analyzed. The average pore size and total porosity were determined by analysis of SEM images using the software Image-J (version 1.46i).

4.3.2. EXPERIMENTAL DESIGN

This study was conducted according to the Guiding Principles for the Use of Laboratory Animals and it was approved by the Animal Care Committee guidelines at Federal University of São Carlos (protocol 046/2012).

In this investigation, 80 male *Wistar* rats were used (12 weeks old and weighing 300 g), and were maintained under controlled conditions of temperature (24 ± 2ºC) with light-dark periods of 12 h, with free access to water and commercial diet. The experimental animals were randomly distributed into 2 groups: Control group (CG) and Biosilicate® group (BG). Each group was divided into 4 four subgroups (n = 10 animals) euthanized 3, 7, 14 and 21 days post-surgery.

4.3.3. SURGICAL PROCEDURES

Before surgery, all the animals were anesthetized by intraperitoneal injection of ketamine (40 mg/kg, Agener®, Brasília, Brazil) and xylazine (20 mg/kg, Syntec®, Cotia, Brazil). After exposing the right proximal tibia of each animal, a standardized 3.0 mm diameter non-critical bone defect was created by using a motorized drill under irrigation with saline solution [21, 25, 29]. The porous bioactive scaffolds were implanted, in the created defects in a randomization scheme. The skin was closed and sutured with 4-0 nylon monofilament (Shalon®, São Luis de Montes Belos, GO, Brazil), and disinfected with povidone iodine. The health status of the animals was monitored on a daily basis.

The animals were housed in pairs and the intake of water and food was monitored in the initial postoperative period. Moreover, the animals were observed for signs of pain, infection and activity. According to each experimental period, animals were euthanized by CO_2 asphyxiation.

The blood and the right tibia of each animal were collected for analysis. The blood samples were used for the quantification of inflammatory factors and the right tibia was taken to histological analyzes.

4.3.4. HISTOPATHOLOGICAL ANALYSIS

The right tibias were fixed in 10% buffered formalin (Merck, Darmstadt, Germany) for 24 h. Afterwards, the specimens were decalcified in 10% EDTA solution (ethylenediaminetetraacetic acid, Labsynth®, Diadema, Brazil) for 40 days, dehydrated and embedded in paraffin blocks. Three sections (5 μm) of each specimen were longitudinally sectioned (Microtome Leica Microsystems SP 1600, Nussloch, Germany) and stained with hematoxylin and eosin (H.E. stain, Merck, Darmstadt, Germany). The morphological description of the bone defect was performed with an optical microscopy (Olympus Optical Co., Tokyo, Japan) according to the following parameters: granulation tissue, inflammatory process, area of fibrosis, necrotic tissue, bone formation and biomaterial degradation.

4.3.5. IMMUNOHISTOCHEMISTRY

Histological sections (5 μm) were deparaffinized using xylene and rehydrated in graded ethanol. After, each specimen was pre-treated in a Steamer with buffer Diva Decloaker (Biocare Medical, CA, USA) for 5 min for antigen retrieval. The material was pre-incubated with 0.3% hydrogen peroxide (Labsynth®, Diadema, Brazil) in phosphate-buffered saline (PBS) solution for 30 min in order to inactivate endogenous peroxidase and then block with 5% normal goat serum in PBS solution for 20 min. Three sections of each specimen were incubated for 2 h with polyclonal primary antibody anti-Cyclooxygenase-2, anti-Vascular endothelial growth factor and

anti-Runt-related transcription factor 2, all at a concentration of 1:200 (Santa Cruz Biotechnology, Santa Cruz, USA). Afterwards, the sections were incubated with biotin conjugated secondary antibody anti-rabbit IgG (Vector Laboratories, Burlingame, CA, USA) at a concentration of 1:200 in PBS for 30 min, followed by the application of preformed avidin biotin complex conjugated to peroxidase (Vector Laboratories, Burlingame, CA, USA) for 30 min. A solution of 3-3′-diaminobenzidine solution (0.05%) and Harris hematoxylin were applied.

The expression of cyclooxygenase-2 (COX-2), vascular endothelial growth factor (VEGF) and runt-related transcription factor 2 (Runx2) were assessed qualitatively (presence and location of the immunomarkers) in five pre-determined fields using an optical light microscope (Leica Microsystems AG, Wetzlar, Germany). The analysis was performed by 2 observers (CRT and HWK) in a blinded way.

4.3.6. IMMUNOENZYMATIC ASSAY

Quantification of plasma cytokines was performed using the immunoenzymatic assay (ELISA). In this study, the cytokines interleukin 4 (IL-4), interleukin 10 (IL-10) and tumor necrosis factor alpha (TNF-α) were evaluated by their influences on the inflammatory process [30].

For this purpose, the collected blood from each animal (5 mL) was placed in tubes without anticoagulant for about 2 hours until its coagulation. Then, the samples were centrifuged at 1500 rpm for 15 minutes. The serum that resulted from this centrifugation was aliquoted into microtube and frozen at -80 ° C. Cytokines were measured using Duo Set kits (R&D Systems®, Minnesota, USA), following the manufacturer's recommendations. The serum samples were used to measure IL-4, IL-10 and TNF-α. The high affinity microplates were sensitized with monoclonal anti-

cytokines and remained "overnight" at room temperature. Afterwards, the plates were blocked (with PBS) and washed. Supernatants and standard curves (made with recombinant cytokines) were added. The plates were maintained at room temperature for 2 hours and then another washing was performed. Subsequently, biotinylated anti-cytokine antibodies were added and maintained for 1 hour at room temperature. The results were expressed in pg/mL for all cytokines evaluated.

4.3.7. STATISTICAL ANALYSIS

Data were expressed as mean values and standard deviations (SD) for each sample group. The normal distribution of all variables was checked using the Shapiro-Wilk's W test. Two-way ANOVA with Tukey post-hoc tests were used to evaluate the variance between groups. All analyses were performed using Excel (2007) and STATISTICA 7.0. For all the tests, the significance level of 5% ($p \leq 0.05$) was considered.

4.4. RESULTS

4.4.1. MATERIAL CHARACTERIZATION

The porous bioactive scaffolds which were obtained via addition of carbon black as a porogen agent are highly porous, as can be seen in the images captured via stereomicroscopy (Fig. 3a, 3b). SEM photomicrographies revealed that the macroporosity was 72 ± 6%, with an average pore size of 275 μm (Fig. 3c, 3d). The mechanical strength of the material was sufficient for handling and placing it inside the surgical site.

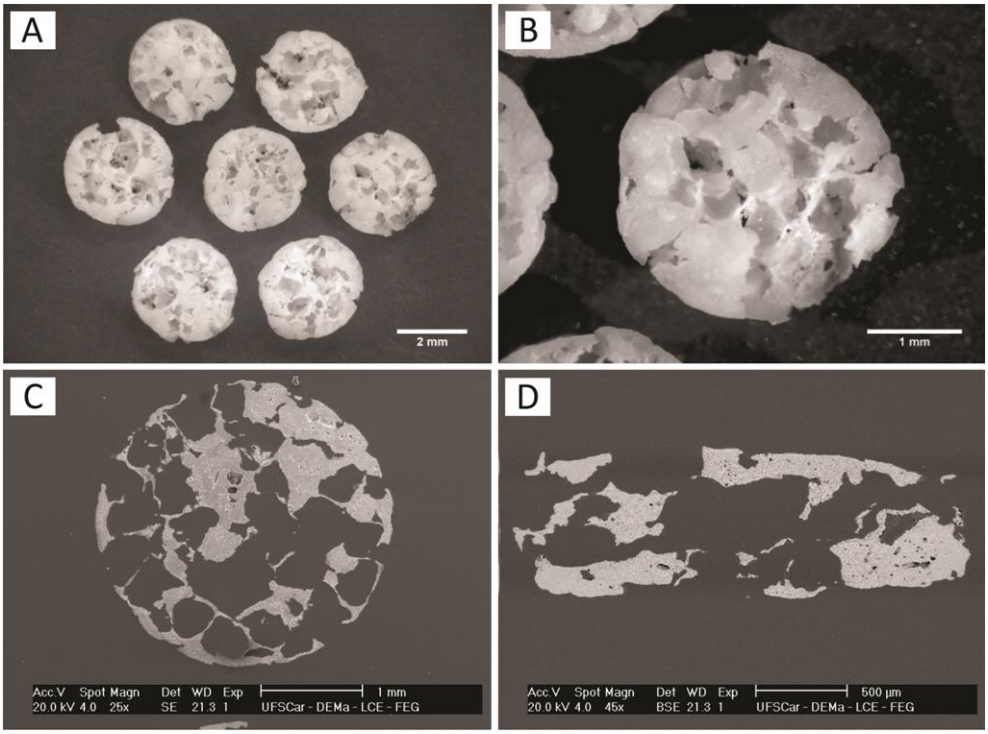

Fig. 3 Images of the Biosilicate® scaffolds obtained with the stereomicroscope Leica MZ75 (a, b) and SEM images of two scaffolds embedded in epoxy resin under vacuum: longitudinal section (c) and transversal section (d).

4.4.2. GENERAL FINDINGS

In this study, no animal of CG died and all tibia samples were used for analysis. Only two animals of BG were lost due to a respiratory depression induced by the anesthesia. The other animals rapidly returned to their normal diet and no post-operative complications were observed during the experimental period. At the end of the experiment, 38 tibial implants were retrieved, of which 35 were used for analysis (3 porous bioative scaffolds were lost due to implant fracturing during the histological processing). An overview of the number of implants placed, retrieved and used for analysis is presented in Table 1.

Table 1 Number of implants placed, retrieved and used for histological analyses for the tibial defect implants.

	Implants placed				Implants retrieved				Implants used for analysis			
	Day 3	Day 7	Day 14	Day 21	Day 3	Day 7	Day 14	Day 21	Day 3	Day 7	Day 14	Day 21
Tibial implants												
Biosilicate® *scaffolds*	10	10	10	10	9[a]	9[a]	10	10	8[b]	8[b]	9[b]	10

[a]Deviation from number of implants placed due to animal dead.
[b]Deviation from number of implants retrieved due to fracturing of implants during to the histological processing.

4.4.3. HISTOPATHOLOGICAL ANALYSIS

Representative histological sections of all experimental groups are depicted in Figures 4 and 5.

3 days

Three days after surgery, histological evaluation of CG revealed that the bone defect area was mostly filled with inflammatory cells and granulation tissue (Fig. 4b). In BG, the integrity of the implant was affected, with material degradation, especially in the borders. The presence of inflammatory cells around the material particles was observed, with ingrowth of granulation tissue (Fig. 4d).

7 days

Seven days after implantation, bone defect area of control animals was filled mostly by granulation tissue, accompanied by some inflammatory cells (Fig. 4f). Furthermore, immature newly formed bone was observed in the periphery of the defect (Fig. 4f). For BG, the degradation of the material continued, leaving lower amounts of material compared to the previous experimental set point (Fig. 4h). Furthermore, in the spaces previously occupied by the material, a discrete inflammatory process and granulation tissue was noticed (Fig. 4h). Newly formed

bone was noticed in the contact area between the edges of the bone defect and the remained implant (Fig. 4h).

14 days

For CG, the amount of granulation tissue increased in the bone defect area and some inflammatory cells still could be observed in some specimens (Fig. 5b). In addition, newly formed bone was observed into the area of the defect, mainly at the periphery (Fig. 5b). The degradation of the scaffold had continued, allowing the ingrowth of granulation tissue and newly formed bone (Fig. 5d).

21 days

After 21 days of implantation, for both experimental groups, bone defect was mostly filled with newly formed bone in both experimental groups (Fig. 5f, 5h). Some particles of the material could still be noticed the bone defect, mainly in the center of the defect (Fig. 5h).

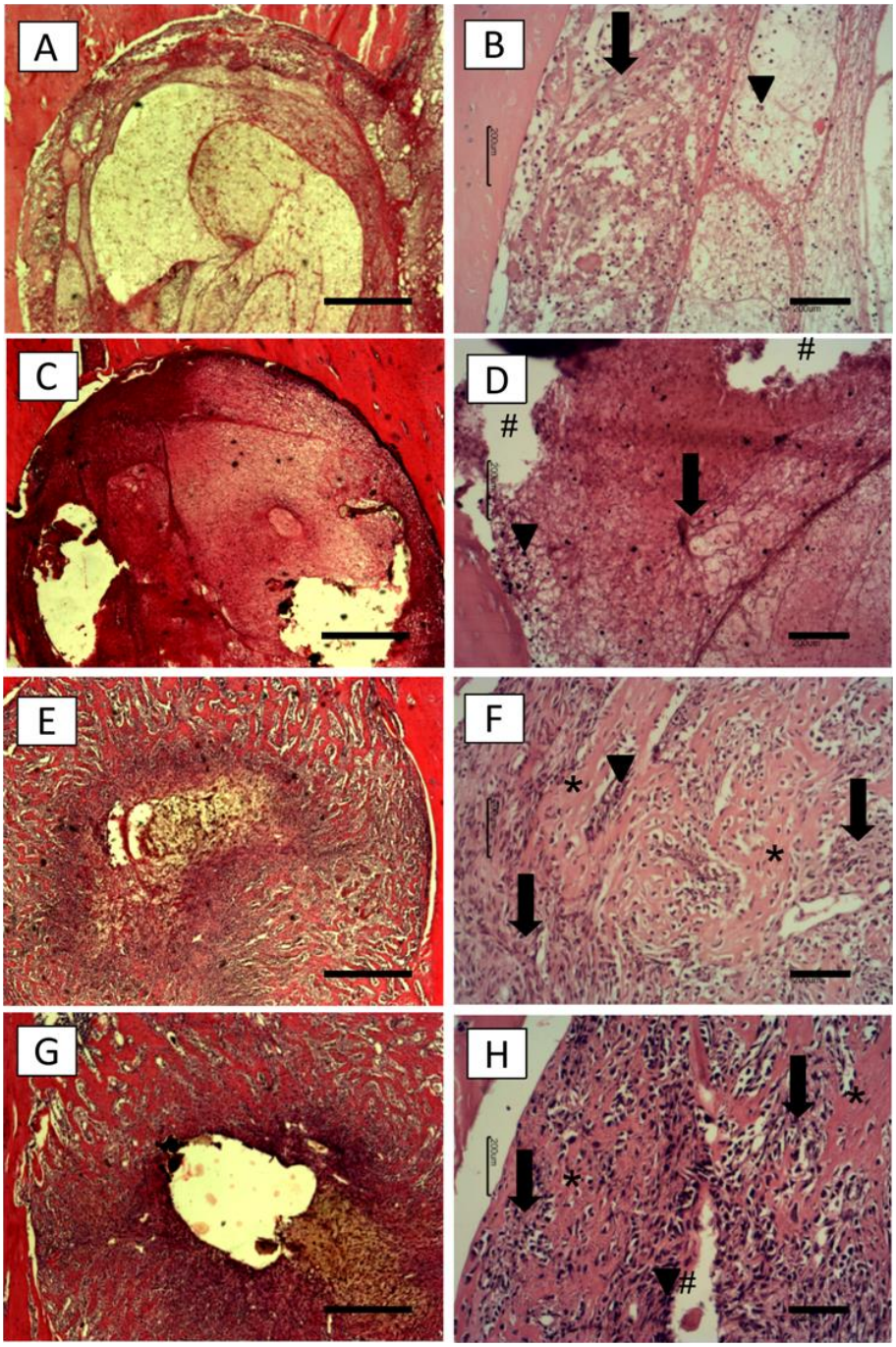

Fig. 4 Representative histological sections of tibial bone defects of the control (CG) and Biosilicate® Group (BG) 3 e 7 days after surgery: CG 3 days (a, b), BG 3 days (c, d), CG 7 days (e, f), BG 7 days (g, h). Newly formed bone (*), granulation tissue (black arrow), infiltrate of inflammatory cells (▼) and biomaterial (#). Bar represents 500 µm (a, c, e, g) and 200 µm (b, d, f, h). Hematoxylin and eosin staining.

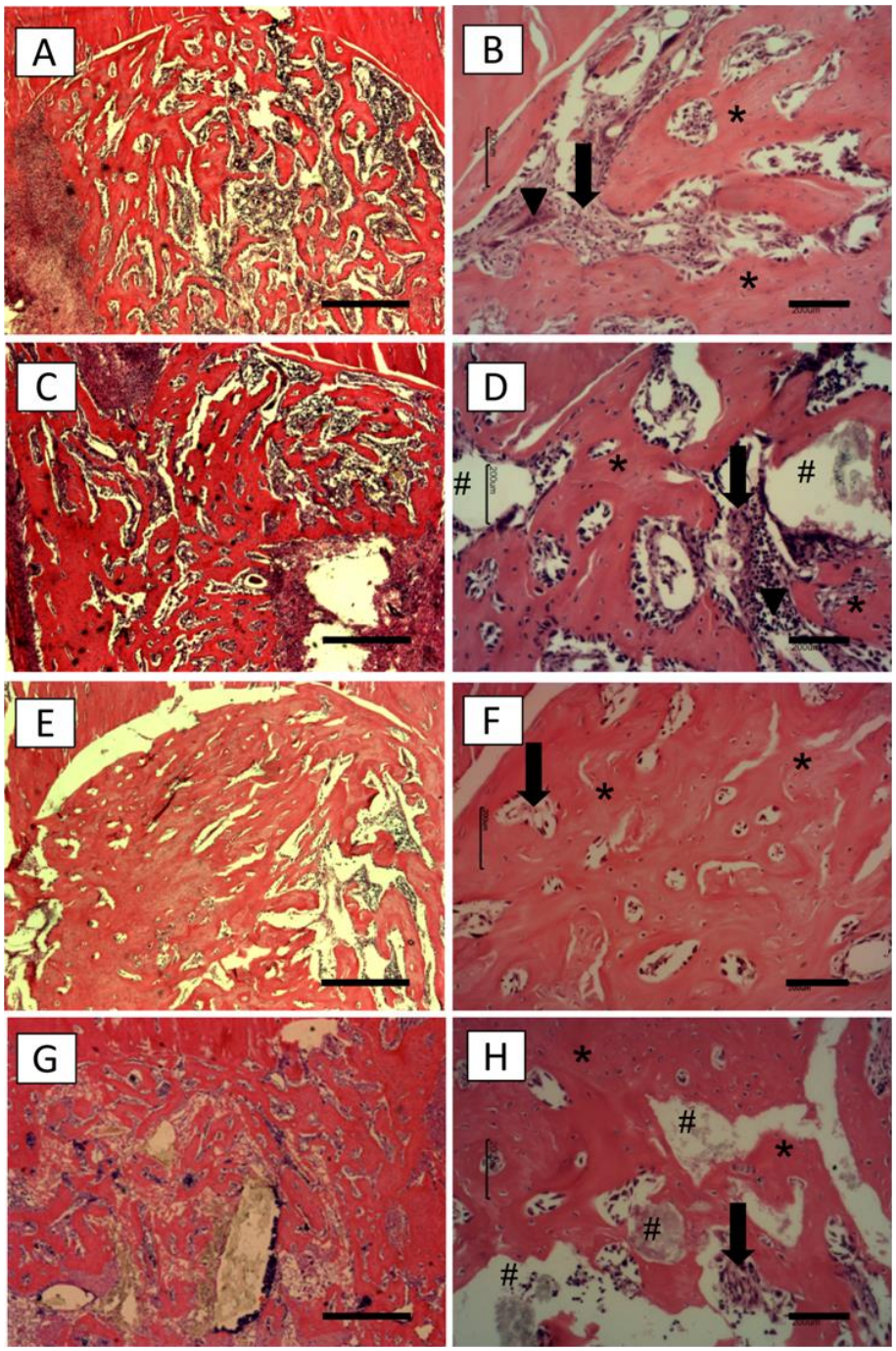

Fig. 5 Representative histological sections of tibial bone defects of the control (CG) and Biosilicate® Group (BG) 14 e 21 days after surgery: CG 14 days (a, b), BG 14 days (c, d), CG 21 days (e, f), BG 21 days (g, h). Newly formed bone (*), granulation tissue (black arrow), infiltrate of inflammatory cells (▼) and biomaterial (#). Bar represents 500 µm (a, c, e, g) and 200 µm (b, d, f, h). Hematoxylin and eosin staining.

4.4.4. IMMUNOHISTOCHEMISTRY

COX-2

COX-2 immunoexpression was observed mainly in the granulation tissue for both experimental groups, 3 and 7 days post-surgery (Fig. 6a, 6b, 6c, 6d). Fourteen days after surgery, for CG and BG, COX-2 expression was observed in the granulation tissue and in the osteoblast cells (Fig. 6e and 6f). At day 21 after surgery, CG showed COX-2 immunoexpression mainly in the osteoblasts (Fig. 6g). For BG, COX-2 immunoreactivity was detected in the granulation tissue and in the osteocytes (Fig. 6h).

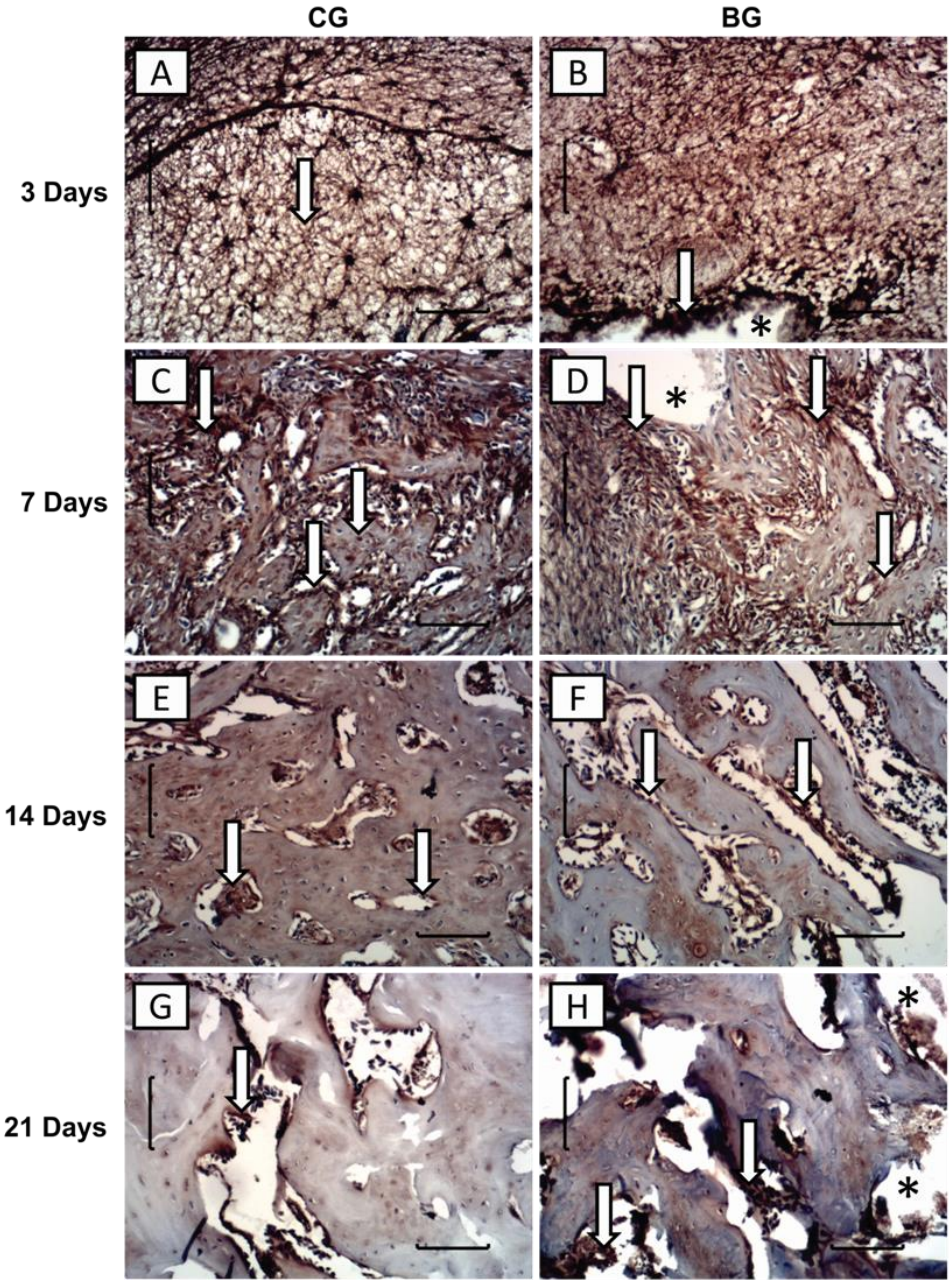

Fig. 6 Representative histological sections of cyclooxygenase-2 (COX-2) immunohistochemistry of the experimental groups (CG and BG) after 3, 7, 14 and 21 days post-surgery: CG 3 days (a), BG 3 days (b), CG 7 days (c), BG 7 days (d), CG 14 days (e), BG 14 days (f), CG 21 days (g), BG 21 days (h). COX-2 immunoexpression (arrow) and biomaterial (#). Bar represents 200 µm.

VEGF

Three days after surgery, VEGF immunoreactivity was observed in the granulation tissue in CG and BG (Fig. 7a, 7b). In this period, for BG, VEGF expression was more evident in the granulation tissue located around the material (Fig. 7b). In the other experimental periods (7, 14 and 21 days), VEGF expression was predominantly detected in the cells involving capillary walls for both groups CG and BG (Fig. 7c, 7d, 7e, 7f, 7g, 7h).

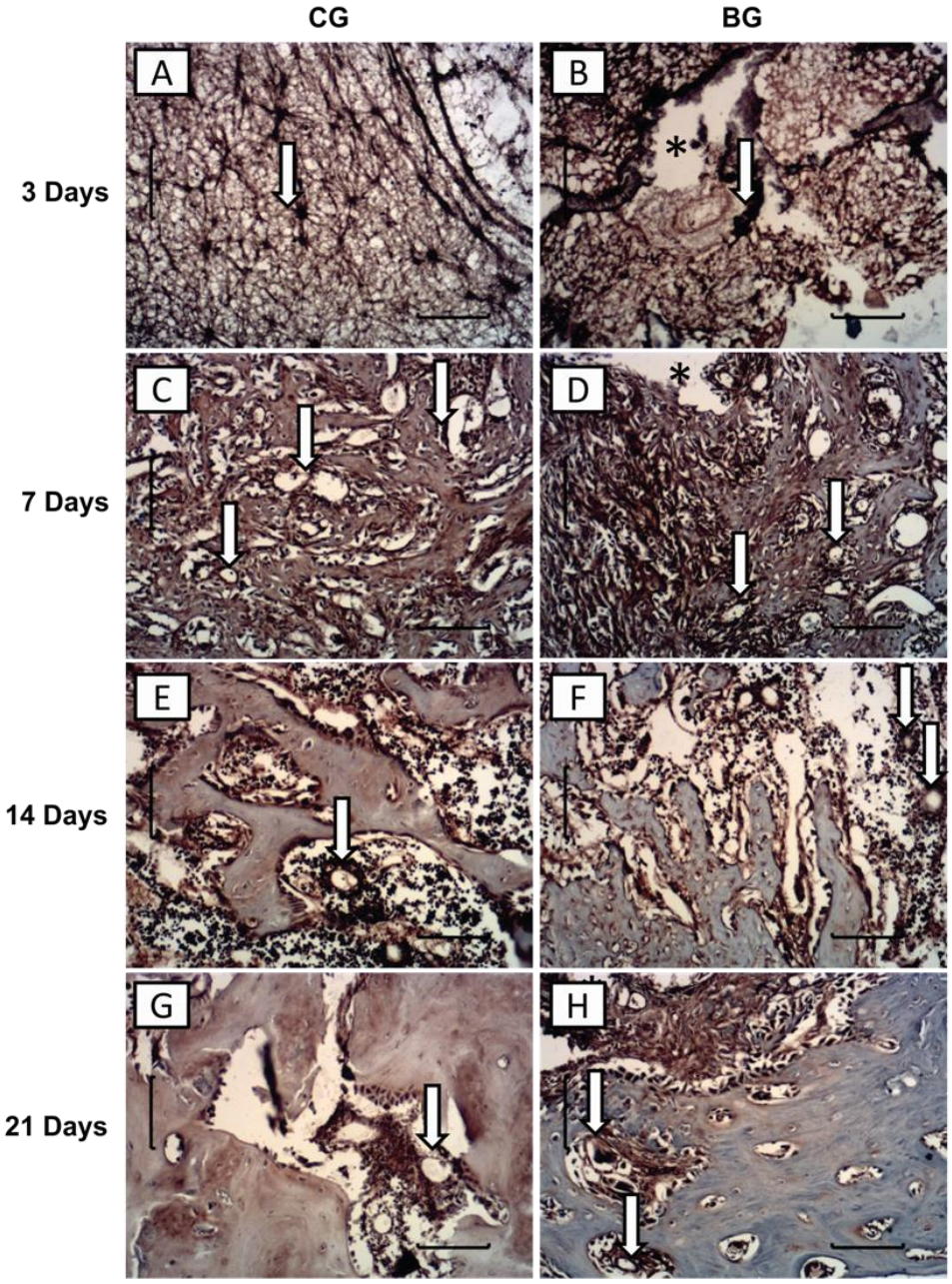

Fig. 7 Representative histological sections of vascular endothelial growth factor (VEGF) immunohistochemistry of the experimental groups (CG and BG) after 3, 7, 14 and 21 days post-surgery: CG 3 days (a), BG 3 days (b), CG 7 days (c), BG 7 days (d), CG 14 days (e), BG 14 days (f), CG 21 days (g), BG 21 days (h). VEGF immunoexpression (arrow) and biomaterial (#). Bar represents 200 µm.

Runx2

Similar to COX-2 and VEGF expression, Runx2 was predominantly detected in the granulation tissue for both CG and BG on day 3 after the surgery (Fig. 8a, 8b). In the same period, for BG, Runx2 immunoreactivity was mainly observed in the granulation tissue around the material (Fig. 8b). At day 7 after surgery, Runx2 immunoexpression was mainly detected in osteoblasts for CG (Fig. 8c) and in the granulation tissue for BG (Fig. 8d). Fourteen and 21 days after surgery, Runx2 expression was detected in osteocytes and osteoblasts for both CG (Fig. 8e, 8g) and BG (Fig. 8f and 8h).

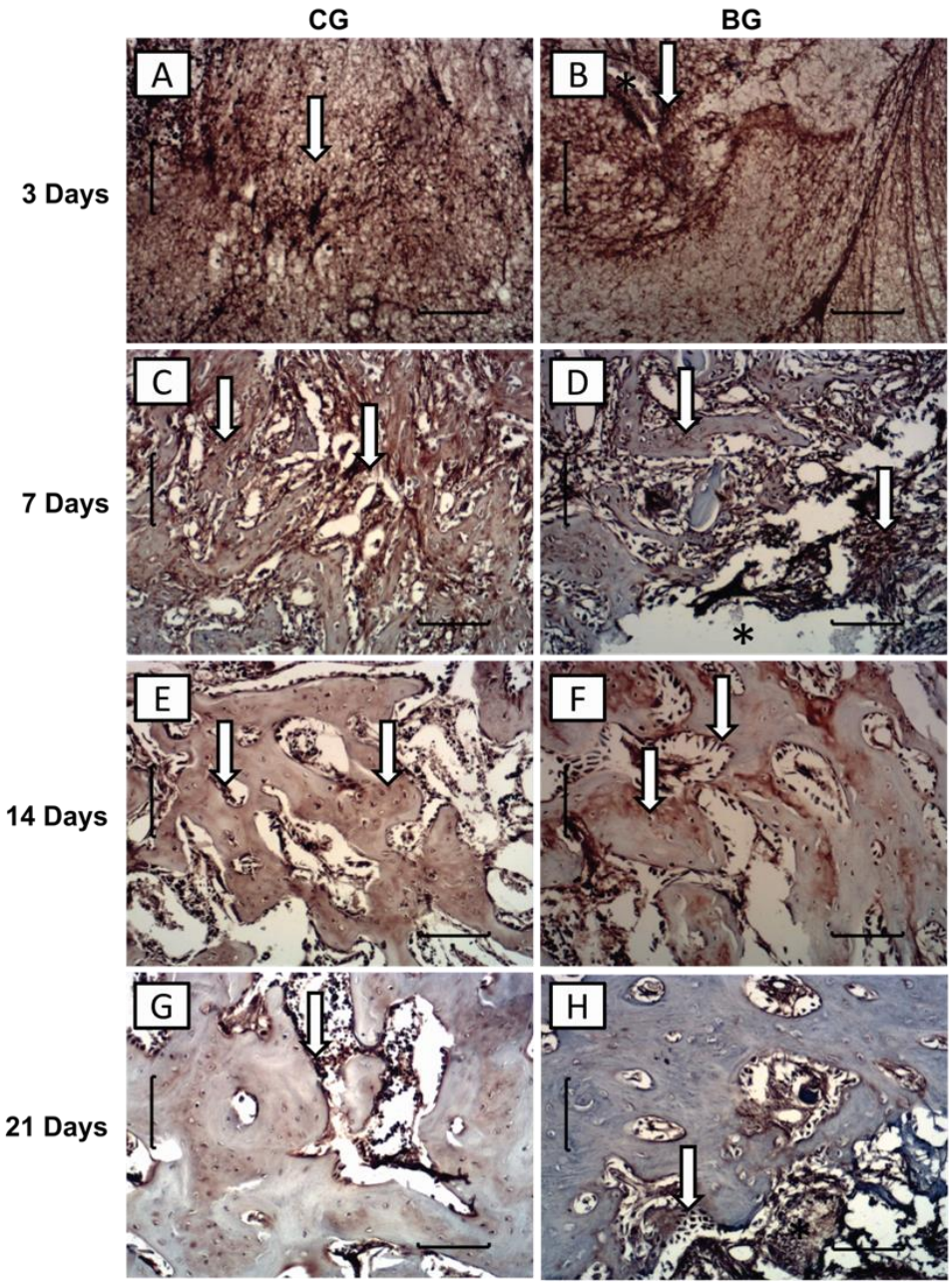

Fig. 8 Representative histological sections of runt-related transcription factor-2 (Runx2) immunohistochemistry of the experimental groups (CG and BG) after 3, 7, 14 and 21 days post-surgery: CG 3 days (a), BG 3 days (b), CG 7 days (c), BG 7 days (d), CG 14 days (e), BG 14 days (f), CG 21 days (g), BG 21 days (h). Runx2 immunoexpression (arrow) and biomaterial (#). Bar represents 200 µm.

4.4.5. IMMUNOENZYMATIC ASSESSMENT

The immunoenzymatic assessment showed no statistic difference in the levels of TNF-α comparing CG and BG in the experimental periods (Fig. 9). For IL-4, a significantly higher level of this cytokine was observed in BG when compared to CG, 14 days after implantation (Fig. 10). Moreover, the immunoenzymatic evaluation indicated a lower level of IL-10 (Fig. 11) in BG compared to CG, 21 days after the surgery.

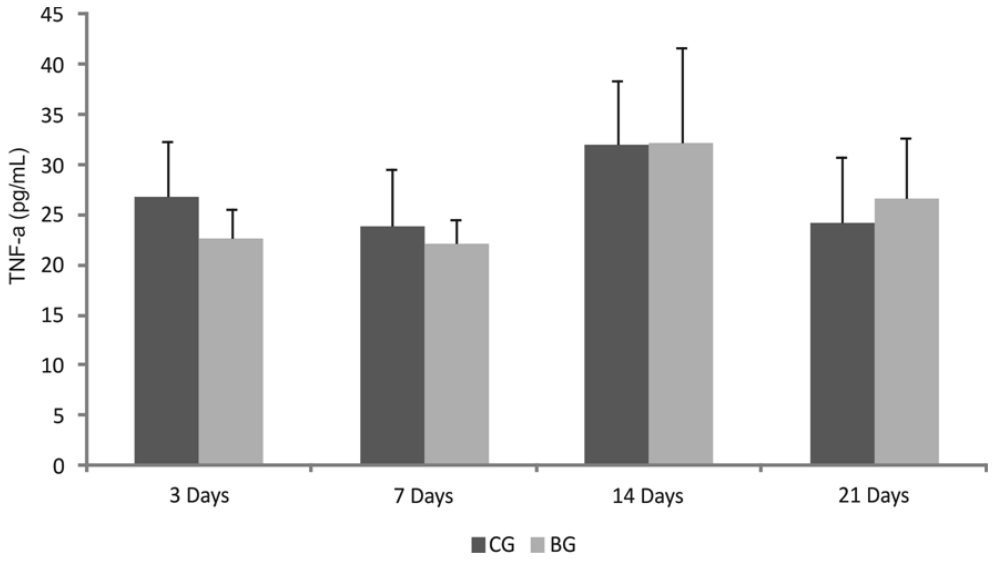

Fig. 9 Levels of TNF-α cytokines evaluated in the serum of rats undergoing implantation of the Biosilicate® scaffolds in different experimental periods.

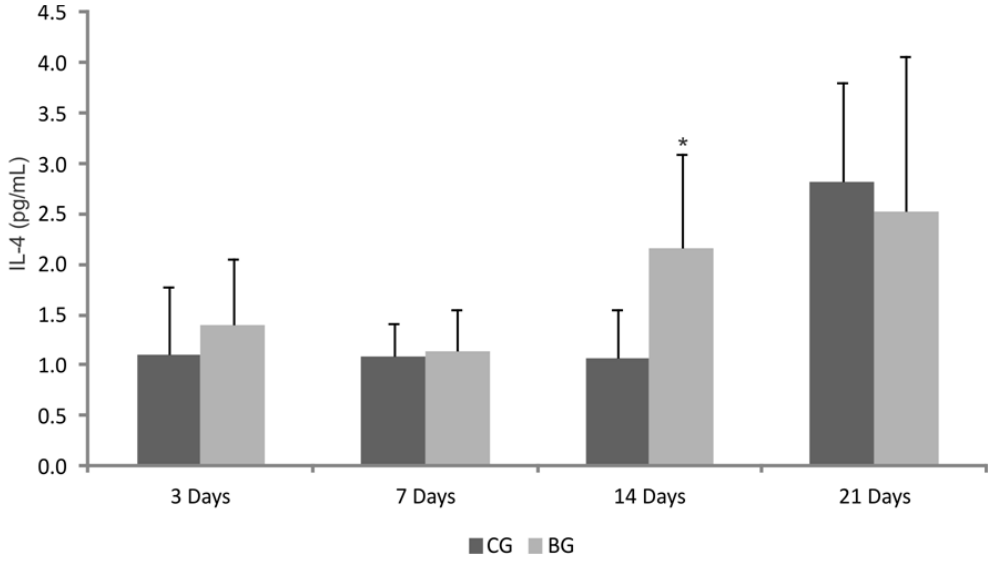

Fig. 10 Levels of IL-4 cytokines evaluated in the serum of rats undergoing implantation of the Biosilicate® scaffolds in different experimental periods. Significant differences of $p \leq 0.05$ are represented by an asterisk.

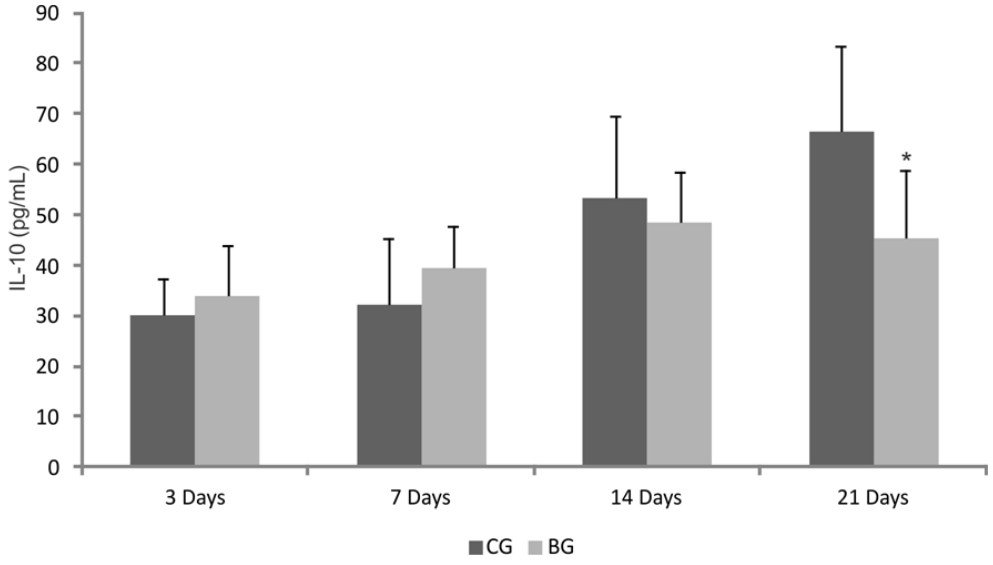

Fig. 11 Levels of IL-10 cytokines evaluated in the serum of rats undergoing implantation of the Biosilicate® scaffolds in different experimental periods. Significant differences of $p \leq 0.05$ are represented by an asterisk.

4.5. DISCUSSION

This study aimed to evaluate the biological *in vivo* response after the implantation of porous bioactive scaffolds in tibial bone defects in rats after 3, 7, 14 and 21 days. It was hypothesized that increasing the porosity in the bioactive scaffold would have more positive effects on bone tissue formation. The main findings showed that the porous bioactive scaffold degraded over the experimental set points and allowed formation of new bone tissues. In addition, the porous bioactive scaffold induced the immunoexpression of COX-2, VEGF and Runx2 and modulated the synthesis of systemic inflammatory cytokines, with an upregulation of anti-inflammatory cytokines IL-4 and downregulation of the anti-inflammatory cytokine IL-10.

Porous bioactive scaffolds have been of great interest in the bone tissue engineering field to be used as bone substitutes [16, 31, 32]. High bioactivity and adequate scaffold porosity are essential characteristics to stimulate osteoprogenitor cells and to support bone ingrowth [3, 16, 33]. Furthermore, resorption of the material with the same rate of the bone formation is required [34]. Several *in vivo* studies demonstrated that Biosilicate®, used in powder or scaffolds, was able to stimulate bone metabolism and accelerate the process of bone healing in different animal models, thus highlighting the osteogenic potential of the glass ceramic [25, 35, 36]. These findings are in line with the results of the current study which revealed a continuous newly bone tissue ingrowth at the defect area and in the spaces left by the degraded material. Many studies demonstrated that Biosilicate® scaffolds have bioactive properties [19-21]. Immediately upon the implantation, ions dissolution from the scaffold to bone tissue stimulates the formation of a hydroxyapatite layer, which

acts as a template for osteoblast growth, which can affect osteogenesis [16]. Furthermore, high porosity and adequate pore sizes are essential factors for an effective bone substitute material [26]. Scaffolds with pores between of 100 to 400 microns are of optimal size to allow bone ingrowth and to support neovascularization [37]. The pore size and porosity of the bioactive scaffold used in the present study indicate that it has morphological characteristics which make them suitable to be used as a bone graft.

Moreover, the histological findings demonstrated that the scaffold degraded over time and the degradation happened according to the rate of tissue ingrowth. Besides adequate porosity, proper scaffold degradation is also essential for the process to happen, since formation of new bone tissue needs space to grow in [38].

COX-2, VEGF and Runx2 immunoexpressions were increased in the porous bioactive scaffolds implanted animals. COX-2 and Runx2 have regulatory effects on the proliferation and differentiation of osteoblasts [39, 40], while the VEGF is the most important signal protein produced by cells that stimulates vasculogenesis and angiogenesis [41]. In the current study, the ions released from the scaffolds, such as silicon (Si) and calcium (Ca) may have provided the necessary stimuli to increase the expression of COX-2 and Runx2, and consequently lead to the proliferation of osteoblastic cells. Xynos *et al.* [33] observed that inorganic particles of Bioglass 45S5®, mainly Si and Ca, may carry specific morphogenic clues that stimulate the proliferation of osteoblastic cells. Furthermore, the increased VEGF expression may be also related to the ions dissolution of the porous bioactive scaffolds. These findings corroborate those of Matsumoto *et al.* [36] who demonstrated an increased VEGF immunoexpression in the calvaria defects in rabbits after Biosilicate® implantation.

Additionally, severe local and systemic inflammatory responses caused by the implantation of biomaterials may result in delay of the bone healing [34].The organic response is mainly related to the composition of the material, which may stimulate the expression of inflammatory factors such as interleukins and TNF-α. In the present study, the ELISA assay was used to measure the systemic reaction caused by the porous bioactive scaffold tibial implantation and demonstrated that no significant increase in TNF-α was observed in any experimental group. TNF-α is a factor which is involved in systemic inflammation and is mainly produced by activated macrophages [42]. The fact that the expression of this cytokine did not increase is an indicative that the porous bioactive scaffolds implantation did not induce any systemic inflammatory process.

In addition, porous bioactive scaffolds induced a higher expression of IL-4 on day 14 after implantation and a lower expression of IL-10 on day 21 after surgery. IL-4 and IL-10 are anti-inflammatory cytokines that can regulate the effects of the TNF-α [29]. Cytokines such as IL-4, indirectly promote the bone formation by increasing the expression of osteoprotegerin (OPG), inhibiting osteoclastogenesis [43]. In this context, the increase of the synthesis of IL-4 cytokines in the scaffold treated animals may have contributed to bone formation.

The results of this initial investigation confirmed the hypothesis that the high porous bioactive scaffold has an adequate porosity structure and is able to support bone tissue ingrowth, thus constituting a promising alternative to be used as bone grafts for tissue engineering. However, in the present study the comparison of the performance of the material was made using an empty control defect model. Future investigations should be performed using standard materials such as calcium phosphate or 45S5 Bioglass. Additionally, the biological performance of the scaffold

should be investigated in different bone defect models such as those of critical-size or compromised situations (e.g. osteoporosis).

4.6. CONCLUSIONS

In summary, the results indicated that the porous bioactive scaffold has good adequate porosity and proper degradability and bone-forming properties. The innovative scaffold enhanced the expression of vascular and osteogenic factors and did not induce any systemic inflammatory response. Further long-term studies should be carried out to provide additional information concerning the late stages of material degradation and the bone regeneration induced by the porous scaffold. Moreover, further researches are required to evaluate the biological performance of this new biomaterial in compromised situations to support the use of this promising scaffold for bone engineering applications.

4.7. ACKNOWLEDGMENTS

The authors thank FAPESP (Fundação de Amparo à Pesquisa do Estado de São Paulo) for their financial support.

4.8. REFERENCES

1. Phieffer LS, Goulet JA. Delayed Unions of the Tibia. J Bone Joint Surg Am. 2006;88:205-216.

2. Axelrad TW, Kakar S, Einhorn TA. New technologies for the enhancement of skeletal repair. Injury. 2007;38:S49-62.

3. Välimäki V, Yrjans JJ, Vuorio E, Aro HT: Combined effect of bone morphogenetic protein-2 gene therapy and bioactive glass microspheres in enhancement of new bone formation. J Biomed Mater Res. 2005;75:501-09.

4. Drosse I, Volkmer E, Seitz S, Seitz H, Penzkofer R, Zahn K, Matis U, Mutschler W, Augat P, Schieker M. Validation of a femoral critical size defect model for orthotopic evaluation of bone healing: a biomechanical, veterinary and trauma surgical perspective. Tissue Eng Part C Methods. 2008;14:79-88.

5. Bhatt RA, Rozental TD. Bone Graft Substitutes. Hand Clinics. 2012;28:457-468.

6. Nandi SK, Roy S, Mukherjee P, Kundu B, De DK, Basu D. Orthopaedic applications of bone graft & graft substitutes: a review. Indian J Med Res. 2010;132:15-30.

7. Dorozhkin S. Calcium orthophosphate-based biocomposites and hybrid biomaterials. J Mater Sci. 2009;44:2343-2387.

8. Hutmacher DW, Schantz JT, Lam CX, Tan KC, Lim TC. State of the art and future directions of scaffold-based bone engineering from a biomaterials perspective. J Tissue Eng Regen Med. 2007;1:245-60.

9. Renno AC, Bossini PS, Crovace MC, Rodrigues AC, Zanotto ED, Parizotto NA. Characterization and *in vivo* biological performance of biosilicate. Biomed Res Int, 2013, doi: 10.1155/2013/141427

10. De Long WG Jr, Einhorn TA, Koval K, McKee M, Smith W, Sanders R, Watson T. Bone grafts and bone graft substitutes in orthopaedic trauma surgery. A critical analysis. J Bone Joint Surg Am. 2007;89:649-58.

11. Hak DJ. The use of osteoconductive bone graft substitutes in orthopaedic trauma. J Am Acad Ortho Surg. 2007;15:525-536.

12. Ohtsuki C, Kamitakahara M, Miyazaki T. Bioactive ceramic-based materials with designed reactivity for bone tissue regeneration. J R Soc Interface. 2009;6:S349-60.

13. Hench LL, Xynos ID, Polak JM. Bioactive glasses for in situ tissue regeneration. J Biomater Sci Polym Ed. 2004;15:543-62.

14. Hu YC, Zhong JP. Osteostimulation of bioglass. Chin Med J. 2009;122:2386-9.

15. Xin R, Zhang Q, GAO, J. Identification of the wollastonite phase in sintered 45S5 bioglass and its effect on *in vitro* bioactivity. J Non Cryst Solids. 2010;356:1180-1184.

16. Hench LL, Polak JM. Third-generation biomedical materials. Science. 2002;295:1014-7.

17. Peitl Filho O, LaTorre GP, Hench LL. Effect of crystallization on apatite-layer formation of bioactive glass 45S5. J Biomed Mater Res. 1996:30:509-14.

18. Kido HW, Oliveira P, Parizotto NA, Crovace MC, Zanotto ED, Peitl-Filho O, Fernandes KP, Mesquita-Ferrari RA, Ribeiro DA, Renno AC. Histopathological, cytotoxicity and genotoxicity evaluation of Biosilicate® glass-ceramic scaffolds. J Biomed Mater Res A. 2013;101:667-73.

19. Moura J, Teixeira LN, Ravagnani C, Peitl O, Zanotto ED, Beloti MM, Panzeri H, Rosa AL, De Oliveira PT. *In vitro* osteogenesis on a highly bioactive glass–ceramic (Biosilicate®). J Biomed Mater Res A. 2007;82:545-557.

20. Bossini PS, Rennó AC, Ribeiro DA, Fangel R, Peitl O, Zanotto ED, Parizotto NA. Biosilicate® and low-level laser therapy improve bone repair in osteoporotic rats. J Tissue Eng Regen Med. 2011;5:229-37.

21. Granito RN, Renno AC, Ravagnani C, Bossini PS, Mochiuti D, Jorgetti V, Driusso P, Peitl O, Zanotto ED, Parizotto NA, Oishi J. *In vivo* biological performance of a novel highly bioactive glass-ceramic (Biosilicate®): a biomechanical and histomorphometric study in rat tibial defects. J. Biomed. Mater. Res. B Appl. Biomater. 2011;97:139-147.

22. Wu C, Zhu Y, Chang J, Zhang Y, Xiao Y. Bioactive inorganic-materials/alginate composite microspheres with controllable drug-delivery ability. J Biomed Mater Res B Appl Biomater. 2010;94:32-43.

23. Sachot N, Castaño O, Mateos-Timoneda MA, Engel E, Planell JA. Hierarchically engineered fibrous scaffolds for bone regeneration. J R Soc Interface. 2013;10:20130684.

24. Paşcu EI, Stokes J, McGuinness GB. Electrospun composites of PHBV, silk fibroin and nano-hydroxyapatite for bone tissue engineering. Mater Sci Eng C Mater Biol Appl. 2013;33:4905-16.

25. Pinto KN, Tim CR, Crovace MC, Matsumoto MA, Parizotto NA, Zanotto ED, Peitl O, Renno AC. Effects of Biosilicate® scaffolds and low-level laser therapy on the process of bone healing. Photomed Laser Surg. 2013;31:252-260.

26. Schieker M, Seitz H, Drosse I, Seitz S, Mutschler W. Biomaterials as Scaffold for Bone Tissue Engineering. Eur J Trau ma. 2006;32:114-24.

27. Zanotto ED, Ravagnani C, Peitl O, Panzeri H, Lara EH. Process and Compositions for Preparing Particulate, Bioactive or Resorbable Biosilicates for Use in the Treatment of Oral Ailments. Sao Carlos: Universidade Federal de Sao Carlos, Universidade de Sao Paulo; 2004. International Classification C03C10/00, WO 2004/074199 (INPI 03006441).

28. Crovace, MC. Obtencão de estruturas porosas altamente bioativas via sinterização do Biosilicate®. Dissertation (MSc in Materials Engineering) - Post-

Graduate Program in Science and Materials Engineering, Federal University of Sao Carlos, Sao Carlos; 2009. 120 pp.

29. Oliveira P, Ribeiro DA, Pipi EF, Driusso P, Parizotto NA, Renno AC. Low-level laser therapy does not modulate the outcomes of a highly bioactive glassceramic (Biosilicate®) on bone consolidation in rats. J. Mater. Sci. Mater. Med. 2010;21:1379-1384.

30. Pape HC, Marcucio R, Humphrey C, Colnot C, Knobe M, Harvey EJ. Trauma-induced inflammation and fracture healing. J Orthop Trauma. 2010;24:522-5.

31. Gauthier O, Müller R, von Stechow D, Lamy B, Weiss P, Bouler JM, Aguado E, Daculsi G. *In vivo* bone regeneration with injectable calcium phosphate biomaterial: a three-dimensional micro-computed tomographic, biomechanical and SEM study. Biomaterials. 2005;26:5444-53.

32. Link DP, Van den dolder J, Van den Beucken JJJP, Cuijpers VM, Wolke JGC, Mikos AG, Jansen JA. Evaluation of the biocompatibility of calcium phosphate cement/PLGA microparticle composites. J Biomed Mater Res A. 2008;87:760-769.

33. Xynos ID, Edgar AJ, Buttery LDK, Hench LL, Polak JM. Ionic products of bioactive glass dissolution increase proliferation of human osteoblasts and induce insulin-like growth factor II mRNA expression and protein synthesis. Biochem Biophys Res Commun. 2000;276:461-465.

34. Anderson JM, Mcnally AK. Biocompatibility of implants: lymphocyte/macrophage interactions. Semin Immunopathol. 2011;33:221-233.

35. Granito RN, Ribeiro DA, Rennó AC, Ravagnani C, Bossini PS, Peitl-Filho O, Zanotto ED, Parizotto NA, Oishi J. Effects of biosilicate and bioglass 45S5 on tibial bone consolidation on rats: a biomechanical and a histological study. J Mater Sci Mater Med. 2009;20:2521-6.

36. Matsumoto MA, Holgado LA, Renno ACM, Caviquioli G, Biguetti CC, Saraiva PP, Kawakami RY. A novel bioactive vitroceramic presents similar biological responses as autogenous bone grafts. J Mater Sci Mater Med. 2012;23:1447-1456.

37. Karageorgiou V, Kaplan D. Porosity of 3D biomaterial scaffolds and osteogenesis. Biomaterials. 2005;26:5474-91.

38. Salgado AJ, Coutinho OP, Reis RL. Bone tissue engineering: state of the art and future trends.Macromol Biosci. 2004;4:743-65.

39. Zhang X, Schwarz EM, Young DA, Puzas E, Rosier RN, O'keefe RJ. Cyclo-oxygenase-2 regulates mesenchymal cell differentiation into the osteoblast lineage and is critically involved in bone repair. J. Clin. Invest. 2002;109:1405-1415.

40. Komori T. Regulation of skeletal development by the Runx family of transcription factors. J Cell Biochem. 2005;95:445-53.

41. Keramarisa NC, Calorib GM, Nikolaoua VS, Schemitschc EH, Giannoudisa PV. Fracture vascularity and bone healing: A systematic review of the role of VEGF. Injury, Int. J. Care Injured. 2008;39:S45-S57.

42. Hallab NJ, Jacobs JJ. Biologic Effects of Implant Debris. Bulletin of the NYU for Joint Diseases. 2009;67:182-8.

43. Shioi A, Teitelbaum SL, Ross FP, Welgus HG, Suzuki H, Ohara J, Lacey DL. Interleukin 4 inhibits murine osteoclast formation *in vitro*. J Cell Biochem. 1991;47:272-7.

5. ESTUDO II

Porous poly (D,L-lactide-co-glycolide) acid/Biosilicate® composite scaffolds for bone tissue engineering

Hueliton Wilian Kido,[1] Patricia Brassolatti,[1] Carla Roberta Tim,[1] Paulo Roberto Gabbai-Armelin,[1] Angela Maria Paiva Magri,[6] Kelly Fernandes,[6] Paulo Sérgio Bossini,[6] Nivaldo Antônio Parizotto,[1] Murilo Camuri Crovace,[2] Iran Malavazi,[3] Anderson Ferreira da Cunha,[3] Ana Maria de Guzzi Plepis,[4] Fernanda de Freitas Anibal,[5] Ana Claudia Muniz Rennó[6]

[1]Department of Physiotherapy, Post-Graduate Program of Biotechnology, Federal University of São Carlos (UFSCar), São Carlos, SP, Brazil
[2]Department of Materials Engineering, Vitreous Materials Laboratory (LaMaV), Federal University of São Carlos (UFSCar), São Carlos, SP, Brazil
[3]Department of Genetics and Evolution, Federal University of São Carlos (UFSCar), São Carlos, SP, Brazil
[4]Institute of Chemistry of Sao Carlos, University of São Paulo (USP), São Carlos, SP, Brazil
[5]Department of Morphology and Pathology, Federal University of São Carlos (UFSCar), São Carlos, SP, Brazil
[6]Department of Biosciences, Federal University of São Paulo (UNIFESP), Santos, SP, Brazil

5.1. ABSTRACT

The aim of this study was to evaluate the effects of the Biosilicate® and poly (D,L-lactic-co-glycolic) acid composites on bone repair in a tibial bone defect model in rats by means of histological evaluation (histopathological, morphometric and immunohistochemical analysis) and osteogenic gene expression. Eighty male *Wistar* rats (12 weeks old, weighing ±300 g) were randomly divided into 2 groups: Biosilicate® group (BG) and Biosilicate®/PLGA group (BG/PLGA). Each group was euthanized at 3, 7, 14 and 21 days after surgery (n = 10 animals per time point). The main findings showed that the incorporation of PLGA into BG had a significant effect on the morphological structure of the material, leading to pore formation, decreasing pH and accelerating mass loss. Furthermore, histologic analysis revealed that the BG/PLGA showed increased material degradation, accompanied by higher bone formation compared to BG, after 21 days of implantation. In the immunohistochemistry, no statistically significant differences were detected between BG and BG/PLGA for Runx2, RANKL and OPG. In addition, qRT-PCR analysis showed that BG/PLGA induced an upregulation of the osteogenic genes related to BMP4, Runx2, ALP and OC. These results show that the BG/PLGA composite may be used as a bone graft for inducing bone repair.

Keywords: PLGA, Biosilicate®, composite, osteogenic genes, bone repair.

5.2. INTRODUCTION

Treating large bone defects represents a major challenge in traumatic and orthopedic surgery.[1] In this context, bone tissue engineering provides a promising therapeutic option to improve local bone healing response.[2] The gold standard treatment for critical size defects and fractures is autogenous bone grafting, which presents osteogenic, osteoinductive and osteoconductive properties.[3] However, the use of autologous bone involves some problems such as the need of an extra surgery, limited availability of donor tissue and risks of infection.[4] Considering these issues, synthetic bone grafts have been emerging as a promising alternative to be used as bone substitutes.[3,5,6] Engineered bone substitutes are attractive because they are biocompatible, have osteogenic properties and good biological performance without the aforementioned limitations.[4,5] Different kinds of synthetic materials, with many different characteristics have been studied including metals, ceramics, polymers and composite materials.[7,8]

Bioactive glasses (BGs), a group of silica-based materials, are able of rapidly bonding to bone tissue due to the fast ion exchange between the glass and the extracellular liquid, stimulating bone growth.[9-11] Moreover, BGs have also shown to have angiogenic capacity when combined with vascular endothelial growth factors.[5] Many *in vivo* studies and clinical trials have reported the benefits of BGs in the acceleration of bone repair.[10,12] Heikkila *et al.* (2011)[13] demonstrated that BGs granules can be clinically used as filler material for bone fractures in lateral tibial plateau compression fractures. Despite the stimulatory effects of BGs on bone metabolism and on fracture consolidation, its use has been restricted due to its poor

mechanical properties.[14] In this context, in this study a fully-crystallized bioactive glass-ceramic of the quaternary P_2O_5-Na_2O-CaO-SiO_2 system (Biosilicate®, patent application WO 2004/074199) was used. Full crystallization of the material lead to enhanced mechanical properties of the bulk material without losing the bioactive properties.[15,16]

Despite the excellent osteogenic properties of BGs, its handling properties and degradation rate constitute a disadvantage for several applications.[16,17] In order to overcome this limitation, some authors have introduced polymeric materials that degrades over time to create pores into BGs, enhancing degradation.[18,19] One of the most common biodegradable polymer is the form of poly (D,L-lactic-co-glycolic) acid (PLGA) microparticles.[19] Some animal studies demonstrated that the association of BGs and PLGA increases ceramic degradation and accelerates the regeneration of bone defects.[19-22]

Although the positive effects of BGs and PLGA on bone healing have been well described in the literature, the effects of the composite BGs/PLGA on bone metabolism are poorly understood. Also, the molecular and cellular modifications induced by BG/PLGA have not been described yet. In this context, this study aimed to evaluate the orthotopic *in vivo* response of BGs/PLGA composites, in rats. Matrices were implanted in a tibial condyle defect of rats. Histocompatibility, bone responses (orthotopic implants; histology and histomorphometry) and expression of genes related to bone consolidation were evaluated after 3, 7, 14 and 21 days of implantation.

5.3. MATERIALS AND METHODS

5.3.1. MATERIALS

For this study, pure Biosilicate® (BG, 100 wt %) and Biosilicate® associate to the acid terminated poly (DL-lactic-co-glycolic acid) (PLGA) microparticles (BG/PLGA, 70:30 wt %), were mixed with 280 µL of 2% Na_2HPO_4 for the preparation of the material. Acid-terminated poly (DL-lactic-co-glycolic acid) (PLGA) (Purasorb®, Purac, Gorinchem, Netherlands) with a lactic to glycolic acid ratio of 50:50 and a molecular weight (M_w) of 17 kDa was used for microparticle preparation. The employed BG (particle size: 1.3 µm) was provided by Vitreous Materials Laboratory (LaMaV, Department of Materials Engineering, Federal University of São Carlos, Sao Carlos, Sao Paulo, Brazil).

5.3.2. PREPARATION OF DENSE PLGA MICROPARTICLES

The single emulsion technique was used to prepare dense PLGA microparticles as described previously.[19] PLGA (0.2 g) was dissolved in 2 mL of dichloromethane (DCM) (Merck. Darmstadt, Germany) in a 20 mL glass tube. The solution was transferred into a stirred beaker with 0.3% poly vinyl alcohol (PVA) (88% hydrolyzed, MW 22000, Acros. Geel, Belgium) solution and then 50 mL of 2% isopropanol (IPN) (Merck) was added. After 1 hour, the microparticles were allowed to settle and were decanted. The microspheres were lyophilized and frozen until use.

5.3.3. PREPARATION OF PRE-SET COMPOSITES

BG (100%) and BG/PLGA (70/30 wt %) pre-set composites were made by mixing the materials using 280 µL of 2% Na_2HPO_4. The formulations were put inside

a 2 mL closed tip syringe (BD Plastipakt, São Paulo, Brazil) for mixing using an apparatus (Silamats, Ivoclar Vivadent, Barueri, Brazil). The syringe with the components was mixed for another 30 s and both samples were injected into Teflon molds (Ø8.0 mm x 2.0 mm for the in vitro study and Ø3.0 mm x 2.0 mm for the in vivo study). After overnight setting at room temperature, the samples were removed from the molds. Before use, the samples were sterilized by ethylene oxide (ACECIL®, Campinas, São Paulo, Brazil).

5.3.4. MASS LOSS QUANTIFICATION AND pH MEASUREMENTS

For the mass loss quantification and pH measurements studies, the materials were weighed and then immersed in 3 mL of phosphate buffered saline (PBS, 10 mM, pH 7.6) at 37ºC. After 3, 7, 14 and 21 days, the samples were subjected to analysis.

5.3.4.1. MASS LOSS QUANTIFICATION

According to each experimental period, the samples were removed from the medium and dried overnight before measuring the mass. Then, the samples were weighed and the percentage of mass loss was calculated by the difference between the initial and final value of the weight of the samples.

5.3.4.2. pH MEASUREMENTS

Directly after removal of the materials, the pH of the PBS medium was measured (Quimis, São Paulo, Brazil).

5.3.5. *IN VIVO* STUDY

This study was conducted in accordance with the Guide for Care and Use of Laboratory Animals and approved by the Animal Ethics Committee at the Federal University of São Carlos (protocol 050/2014). The animals were maintained at 19-23ºC on a 12:12-h light–dark cycle in the Animal Experimentation Laboratory of the Federal University of São Carlos. They were housed in plastic cages and had free access to water and standard food.

In order to perform this study 80 male *Wistar* rats (12 weeks old, weighing ±300 g) were used. These animals were randomly divided into two groups, with 40 animals each: Biosilicate® group (BG) and Biosilicate®/PLGA group (BG/PLGA). Each group was then divided into 4 four subgroups (n = 10 animals) euthanized at 3, 7, 14 and 21 days post-surgery.

5.3.6. TIBIAL BONE DEFECT

In order to induce the bone defect, animals were anesthetized with ketamine (40 mg/kg, Agener®, Brasília, Brazil) and xylazine (20 mg/kg, Syntec®, Cotia, Brazil) and the midregions of the tibias were shaved and disinfected with povidone iodine. A dermo-periosteal incision was performed to expose the tibia. Bone defects were performed 10 mm below the knee joint at the proximal metaphysis of the tibia. A 3-mm diameter cavity defect was made in both tibias, using a spherical burr (12,500 rpm) under copious irrigation with saline solution. The cutaneous flap was replaced and sutured with 4-0 nylon monofilament (Shalon®, São Luis de Montes Belos, GO, Brazil), and the skin was disinfected with povidone iodine.[23] The health status of the rats was daily monitored. After a period of 3, 7, 14 and 21 days of surgery, rats were

euthanized with an intra-peritoneal injection of general anesthetic and the tibias were removed for analysis.

5.3.7. HISTOPATHOLOGICAL ANALYSIS

For the histopathological analysis, the right tibias were fixed in 10% buffer formalin (Merck, Darmstadt, Germany) for 24 h, decalcified in 4 % EDTA (Merck, Darmstadt, Germany) and embedded in paraffin blocks. Three micrometrical slices were obtained in a serially longitudinal sectioned pattern and stained with Hematoxylin and Eosin (HE stain, Merck, Darmstadt, Germany). Histopathological evaluation was performed under a light microscope (Olympus, Optical Co. Ltd, Tokyo, Japan.). Any changes in the bone defect, such as presence of woven bone, medullar tissue, inflammatory process, granulation tissue, or even tissues undergoing hyperplastic, metaplastic and/or dysplastic transformation were investigated per each animal.

5.3.8. MORPHOMETRIC ASSESSMENT

The morphometry of the area of newly formed bone in the regions of bone repair which were previously identified through qualitative histopathological observation was then measured in a blind fashion by one expert pathologist using an image analysis system Motican 5.0 (Meiji camera, Santa Clara, USA). In order to perform the analysis, one slice per animal was stained with HE (Merck,Darmstadt, Germany). Three areas of the region of the bone defect were selected. The one that corresponded to the regions which were closer to the defect wall were named C1 and C2 and the one which corresponded to the central region of the defect was named C3. Newly formed bone was measured at 10x magnification. After the measurement,

areas were added, resulting in the total area of newly formed bone in the defect. This analysis was established in a previous study.[23-25]

5.3.9. IMMUNOHISTOCHEMISTRY

Histological sections (5 µm) were deparaffinized using xylene and rehydrated in graded ethanol. Afterwards, each specimen was pre-treated in a Steamer with buffer Diva Decloaker (Biocare Medical, CA, USA) for 5 min for antigen retrieval. The material was pre-incubated with 0.3% hydrogen peroxide (Labsynth®, Diadema, Brazil) in phosphate-buffered saline (PBS) solution for 30 min in order to inactivate endogenous peroxidase and then blocked with 5% normal goat serum in PBS solution for 20 min. Three sections of each specimen were incubated for 2 h with polyclonal primary antibody anti-Runt-related transcription factor-2 (Runx2), anti-activator of nuclear factor kappa-B ligand (RANKL) and anti-osteoprogesterin (OPG), all at a concentration of 1:100 (Santa Cruz Biotechnology, Santa Cruz, USA). Afterwards, the sections were incubated with biotin conjugated secondary antibody anti-rabbit IgG (Vector Laboratories, Burlingame, CA, USA) at a concentration of 1:200 in PBS for 30 min, followed by the application of preformed avidin biotin complex conjugated to peroxidase (Vector Laboratories, Burlingame, CA, USA) for 30 min. A solution of 3-3′-diaminobenzidine solution (0.05%) and Harris hematoxylin was applied.

The expression of related transcription factor-2 (Runx2), activator of nuclear factor kappa-B ligand (RANKL) and osteoprogesterin (OPG), was assessed qualitatively (presence and location of the immunomarkers) in three pre-determined fields using an optical light microscope (Leica Microsystems AG, Wetzlar, Germany). According to previous studies, the quantity of positive cells per field was described by

a scoring scale from 1 to 4 (1 = absent, 2 = weak, 3 = moderate, and 4 = intense) (Matsumoto *et al.*, 2012; Tim *et al.*, 2013; Pinto *et al.*, 2013). The analysis was performed by 2 observers (AMPM and HWK) in a blinded way.[25-27]

5.3.10. RNA ISOLATION AND cDNA SYNTHESIS

For the RNA isolation, left tibias were dissected and rapidly frozen in liquid nitrogen. The ends of each tibia were removed and the region of the bone defect was stored (-80ºC) until analysis. Total RNA was extracted from the bone defect using the Trizol reagent (1 ml, Invitrogen, Carlsbad, USA) according to the manufacturer's instructions. Trizol reagent (1 ml, Invitrogen, Carlsbad, USA) was added to the sample and the mixture was transferred to a polypropylene tube and incubated (room temperature, 5 min). Chloroform (0.2 ml, Sigma, Saint Louis, USA) was added, mixed vigorously, and the mixture was transferred to a 2 ml tube (Eppendorf, Hamburg, Germany) and centrifuged (28ºC, 15 min). The nucleic acid phase was decanted and an equal volume of RNase-free 70 % ethanol was added. Potential DNA contamination was removed by Turbo DNA-free (Invitrogen, Carlsbad, USA). The purity was assessed by determining the ratio of the absorbance at 260 and 280 nm. The integrity of the RNA was confirmed by inspection of ethidium bromide stained18S and 28S ribosomal RNA under ultraviolet light. The total RNA (1 µg) was applied as template for cDNA synthesis using the High-capacity cDNA Reverse Transcription (Life Technologies, Carlsbad, USA) following the manufacturer's instructions. Oligonucleotide primers were designed for RPS18 (NM_181374.2), Bone Morphogenetic Protein 4 (NM_012827.2), Runt-related Transcription Factor 2 (NM_053470.2), Alkaline Phosphatase (J03572.1) and Osteocalcin (NM_013414.1) (Table 2) using the Primer Express Software 2.0 (Applied Biosystems, Foster City,

USA). All real-time primers were initially tested against standards and a standard curve was generated.

Table 2 Primers and the expected PCR product size at indicated annealing temperatures for each gene analyzed

Gene	Forward primer	Reverse primer	Annealing temperature (ºC)
RPS18	GTGATCCCCGAGAAGTTC	AATGGCAGTGATAGCGAA	60
BMP4	TTACCTCAAGGGAGTGGAAATTG	CCATCGTGGCCAAAAGTGA	60
Runx2	TTATGTGTGCCTCCAACCTGTGT	GGTTTCTTTCCCCCTCAATTTGT	60
ALP	GGTTTCTTTCCCCCTCAATTTGT	CCCAGGCACAGTGGTCAAG	60
OC	ACGAGCTAGCGGACCACATT	CCCTAAACGGTGGTGCCATA	60

BMP4: bone morphogenetic protein 4, Runx2: runt-related transcription factor 2, ALP: alkaline phosphatase, OC: osteocalcin.

5.3.11. QUANTITATIVE REAL-TIME POLYMERASE CHAIN REACTION

The cDNA samples were subjected to quantitative real-time polymerase chain reaction (qRT-PCR) using an Applied Biosystems StepOne^{TM} Real-Time PCR System (Life Technologies, Carlsbad, USA). The optimized PCR conditions were: initial denaturation at 94ºC for 10 min, followed by 40 cycles consisting of denaturation at 94ºC for 15 s, annealing at 60ºC for 1 min, and extension at 72ºC for 45 s, with a final extension step at 72ºC for 2 min. Negative control reactions with no template (deionized water) were also included in each run. For each gene, all samples were simultaneously amplified in duplicate in one assay run. Analysis of relative gene expression was performed using the $2^{-\Delta\Delta CT}$ method (Livak; Schmittgen, 2001). RPS18 was used as a housekeeping gene to normalize our expression data.

5.3.12. STATISTICAL ANALYSIS

Data were expressed as mean values and the standard error (SE) of the mean values for each sample. The normal distribution of all variables was checked using the Shapiro-Wilk's W test. For parametric samples, test t student was used to

evaluate the variance between groups. For nonparametric samples, the Mann–Whitney test was used. All analyses were performed on Excel (2007) and STATISTICA 7.0. For all the tests, the significance level of 5% ($p \leq 0.05$) was considered.

5.4. RESULTS

5.4.1. MATERIAL CHARACTERIZATION

Figure 12 illustrates the morphological structure of BG (Fig. 12A) and BG/PLGA (Fig. 12B) samples. Morphological examination using SEM revealed that PLGA particles presented a spherical shape and were homogenously distributed. PLGA could be clearly differentiated from BG particles (Fig. 12B).

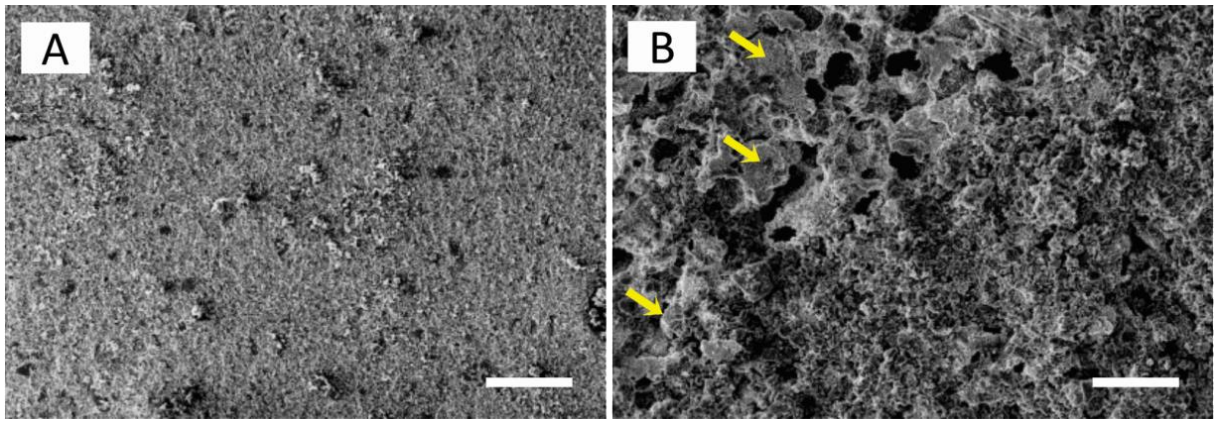

Fig. 12 SEM micrographs of the BG (A) and BG/PLGA (B) samples. PLGA particles are indicated by arrows. Bars represent 100 µm. Magnification: 500x.

5.4.2. MASS LOSS QUANTIFICATION

Mass loss evaluation indicated a decrease of 14 and 17% for BG and BG/PLGA, respectivelly, at day 3. Mass loss progressed during the other experimental periods for BG, presenting a ~18% loss after 21 days of immersion. On

the other hand, the mass loss continued faster for BG/PLGA (up to ~25% after 21 days). At all experimental periods, mass loss of the BG/PLGA was significantly higher compared to BG ($p = 0.0005$ at day 3; $p = 0.0035$ at day 7; $p = 0.0071$ at day 14 and $p = 0.0373$ at day 21) (Fig. 13).

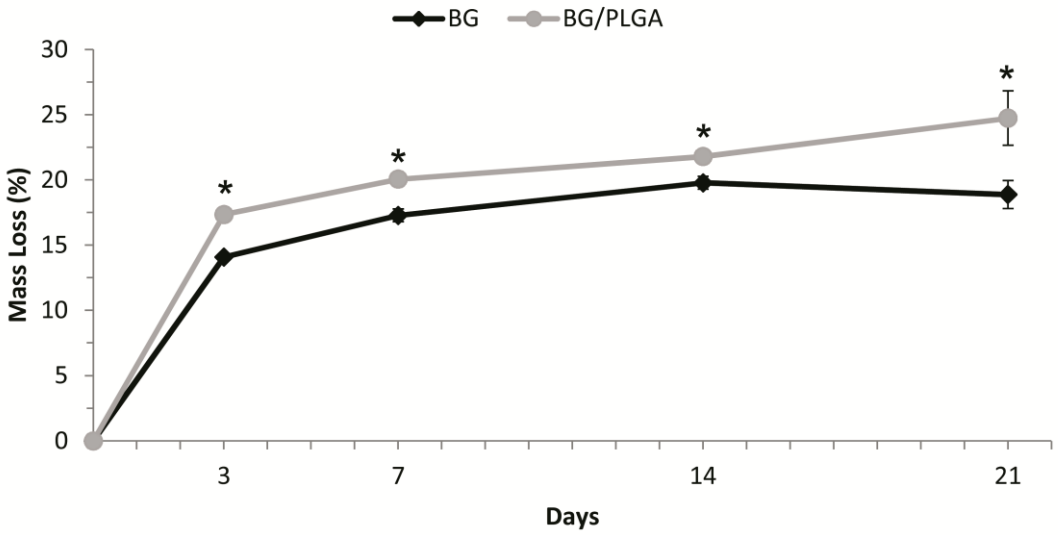

Fig. 13 Mass loss measurements for BG and BG/PLGA samples. (*) BG compared to BG/PLGA ($p \leq 0.05$).

5.4.3. PH MEASUREMENTS

The results of the pH measurements upon incubation in PBS (pH 7.60) are presented in Figure 14. For BG, a high increase in pH was observed after 3 days of incubation when compared BG/PLGA (12.25). For the following experimental periods, pH values maintained stable for BG (~12). For BG/PLGA, pH increased until 10.6 in the first experimental period, reaching a value of 9.68, 21 days after the immersion. Furthermore, pH values were statistically different for BG compared to BG/PLGA in all experimental periods ($p \leq 0.001$).

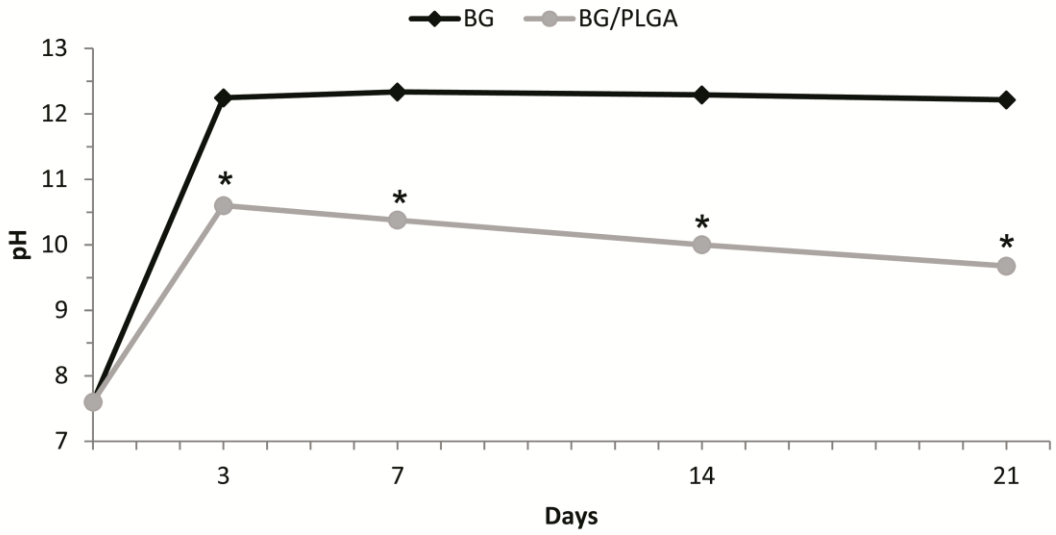

Fig. 14 Behaviour of pH of the incubation medium for BG and BG/PLGA samples. (*) BG compared to BG/PLGA ($p \leq 0.05$).

5.4.4. HISTOPATHOLOGICAL ANALYSIS

Representative histological sections of all experimental groups are depicted in Figure 15.

3 days

Three days after surgery, histological evaluation revealed that BG and BG/PLGA presented initial signs of degradation mainly in the edges of the materials (Fig. 15A, 15B). This degradation was more evident in BG/PLGA implant (Fig. 15B). It was also observed an intense presence of granulation tissue in both groups and some inflammatory cells (Fig. 15A, 15B).

7 days

Seven days post-surgery, both BG and BG/PLGA presented a progressive material degradation (Fig. 15C, 15D). The material degradation was more intense for BG/PLGA compared to BG (Fig. 15C, 15D). Through the histopathological analysis was also noticed, in the border of the defect, for both groups, a more organized

granulation tissue and some inflammatory cells (Fig. 15C, 15D). In this experimental period, newly formed bone was presented mainly in the edges of the defect for BG and BG/PLGA (Fig. 15C, 15D).

14 days

In BG, 14 days after implantation (Fig. 15E), it could be observed similar patterns of material degradation compared to BG in the previous period (Fig. 15C). Fourteen days post-surgery, BG showed granulation tissue and woven bone between the defect border and the implant (Fig. 15E). In regards to BG/PLGA, implant degradation evidently continued 14 days post-implantation compared to other experimental periods, especially in the borders of the material (Fig. 15E, 15F). Moreover, BG/PLGA presented a more intense material degradation and a greater amount of granulation tissue when compared to BG (Fig. 15E, 15F). Also, BG/PLGA and BG showed a moderate presence of bone tissue between the defect borders and the implants (Fig. 15F).

21 days

The histopathological evaluation showed, 21 days after surgery, similar patterns of degradation for BG comparing to the previous time points in this same group (Fig. 15G). Some organized granulation tissue was also observed around the biomaterial and a more organized bone tissue was found in the defect border compared to the other experimental periods (Fig. 15G, 15H). BG/PLGA (Fig. 15H) presented a greater amount of neoformed bone and granulation tissue when compared to BG (Fig. 15G). In addition, BG/PLGA particles were almost completely degraded, in contrast to BG which presence was still intense in the defect area (Fig. 15G, 15H).

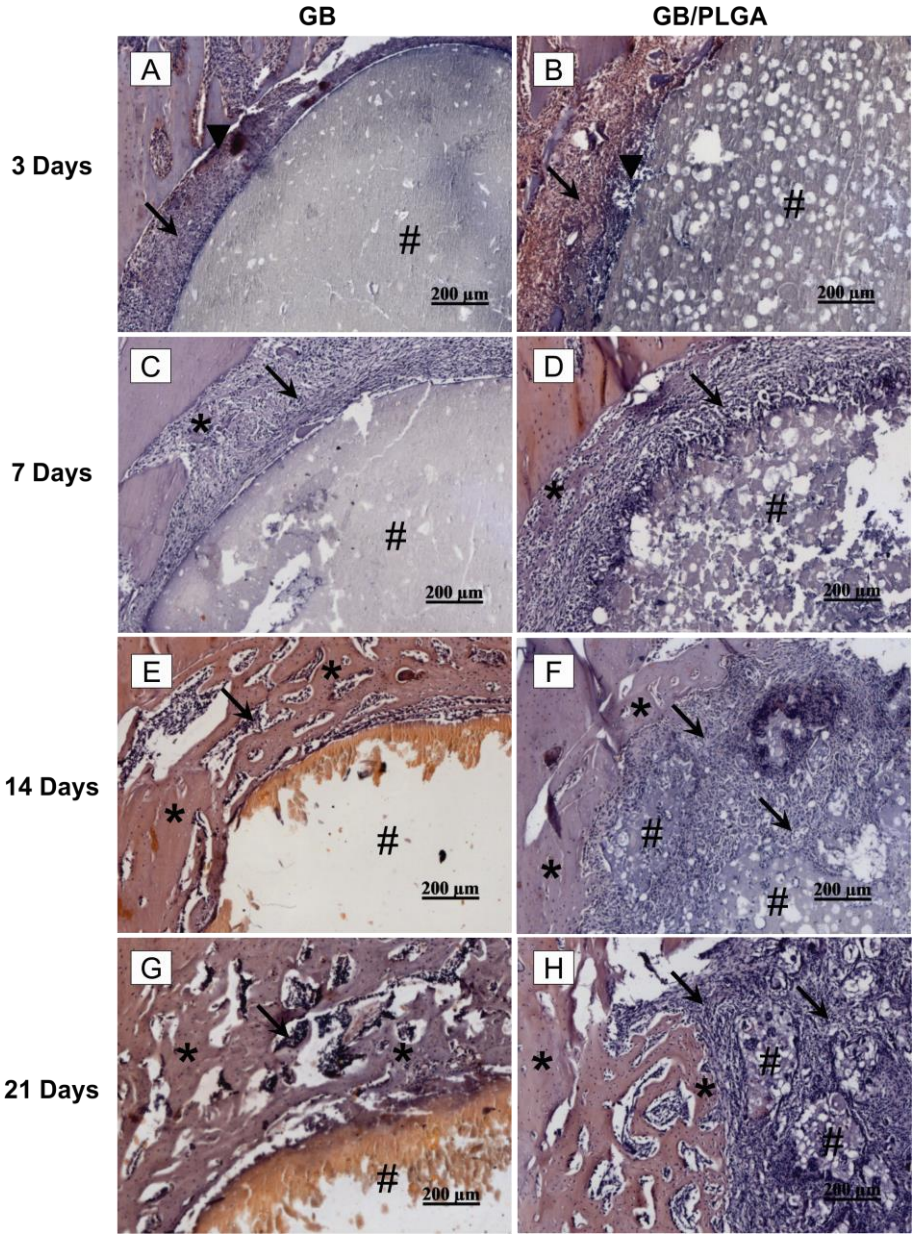

Fig. 15 Representative histological sections of tibial bone defects of the Biosilicate® (BG) and Biosilicate®/PLGA (BG/PLGA) group at 3, 7, 14 and 21 days after surgery, demonstrating newly formed bone (*), granulation tissue (black arrow), infiltrate of inflammatory cells (▼) and biomaterial (#). BG 3 days (A), BG/PLGA 3 days (B), BG 7 days (C), BG/PLGA 7 days (D), BG 14 days (E), BG/PLGA 14 days (F), BG 21 days (G), BG/PLGA 21 days (H). Hematoxylin and eosin staining. Magnification: 100x.

5.4.5. MORPHOMETRIC ASSESSMENT

Figure 16 demonstrates the mean and standard error (SE) of the area of newly formed bone during the experimental periods. No significant difference was found between BG and BG/PLGA at 3, 7, 14 days after surgery. However, BG/PLGA presented a statistically higher area of newly formed bone when compared to BG at 21 days after implantation.

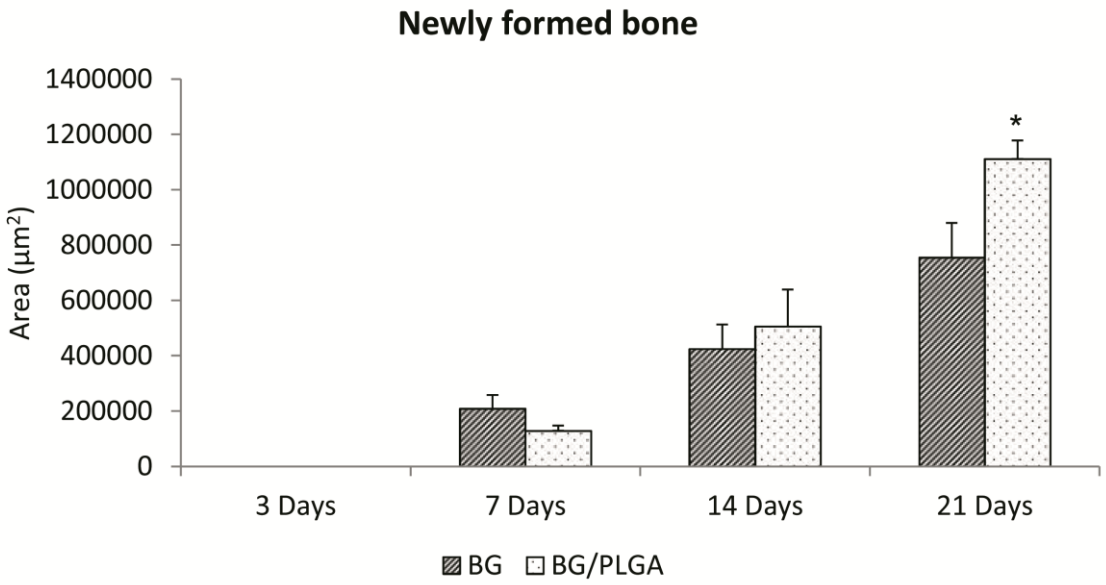

Fig. 16 Means and SE of the morphometric assessment. Biosilicate® group (BG) and Biosilicate®/PLGA group (BG/PLGA). (*) BG compared to BG/PLGA ($p \leq 0.05$).

5.4.6. IMMUNOHISTOCHEMISTRY

Runx2

Runx2 immunomarking was predominantly detected in the granulation tissue in the edges of the bone defect for both BG and BG/PLGA 3 (Fig. 17A, 17B) and 7 days (Fig. 17C, 17D). Fourteen days after surgery, BG and BG/PLGA showed Runx2 immunomarking mainly in the granulation tissue around the biomaterial (Fig. 17E,

17F). Furthermore, in BG/PLGA, it was also observed Runx2 immunomarking in the granulation tissue in the center of the bone defect between the particles of the biomaterial. On day 21 after surgery, Runx2 immunomarking in BG could be observed in the granulation tissue between the material and the newly bone formed (Fig. 17G). In this period, the Runx2 immunomarking for BG/PLGA was mainly observed in the central region of the defect around the particles of the biomaterial (Fig. 17H).

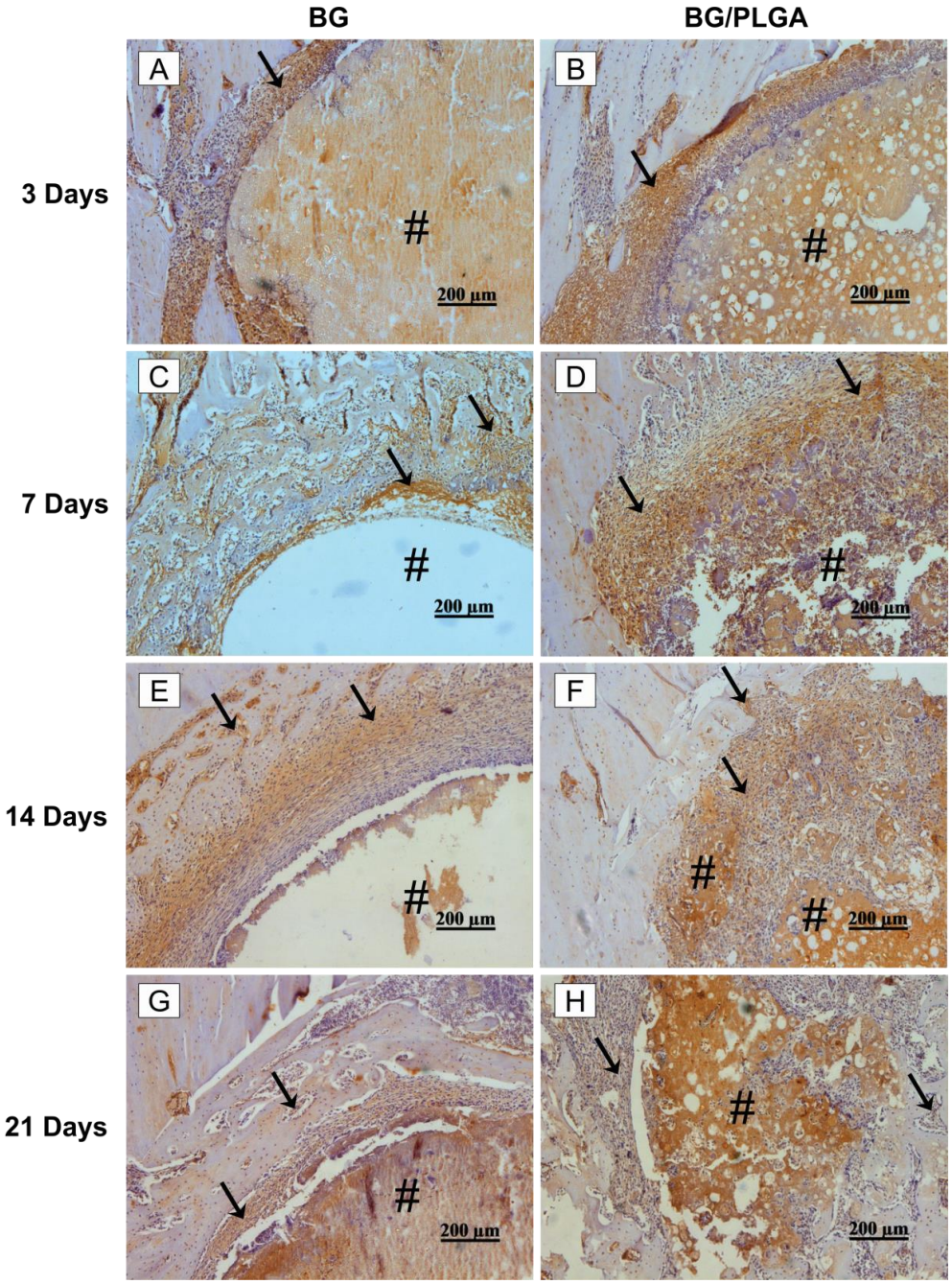

Fig. 17 Representative histological sections of runt-related transcription factor-2 (Runx2) immunohistochemistry of the experimental groups (BG and BG/PLGA) at 3, 7, 14 and 21 days after surgery: BG 3 days (A), BG/PLGA 3 days (B), BG 7 days (C), BG/PLGA 7 days (D), BG 14 days (E), BG/PLGA 14 days (F), BG 21 days (G), BG/PLGA 21 days (H). Runx2 immunomarking (arrow) and biomaterial (#).

RANKL

RANKL immunomarking was observed mainly in the granulation tissue in the peripheral region of the bone defect in BG and BG/PLGA, at 3 and 7 days after surgery (Fig. 18A, 18B, 18C, 18D). Fourteen days after surgery, BG showed RANKL immunoreactivity in the granulation tissue around the implant and close to the newly formed bone tissue in the edges defect (Fig. 18E). In BG/PLGA, immunoreactivity was detected for RANKL in the granulation tissue which was in the edges of the defect and around the particles of the biomaterial 14 days after surgery (Fig. 18G). Twenty one days after implantation, a RANKL expression in the granulation tissue which was between the implant and the newly bone formed was verified in BG. In the same period, in BG/PLGA, RANKL immunomarking was observed predominantly in the granulation tissue in the central region of the bone defect (Fig. 18H).

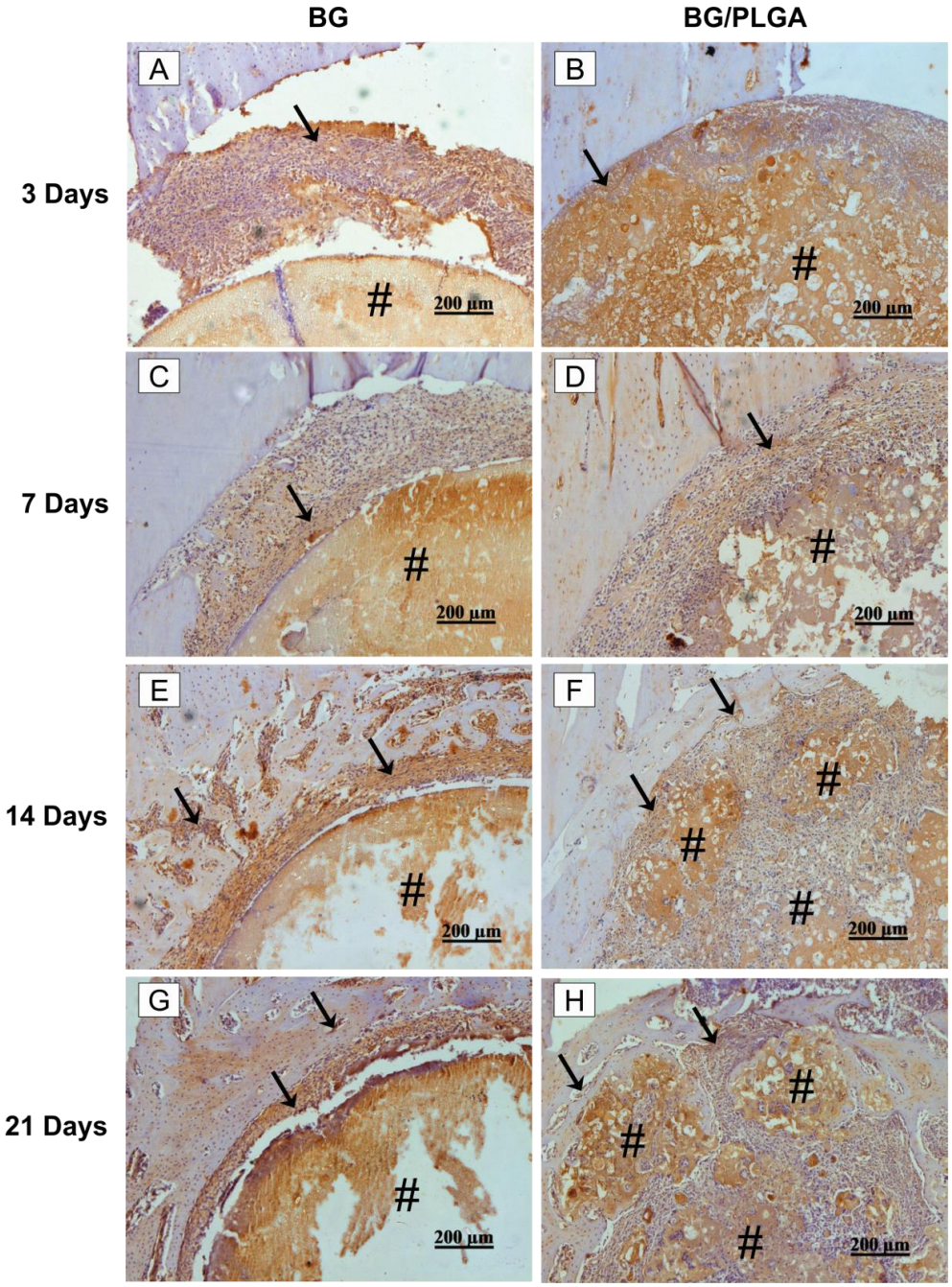

Fig. 18 Representative histological sections of activator of nuclear factor kappa-B ligand (RANKL) immunohistochemistry of the experimental groups (BG and BG/PLGA) at 3, 7, 14 and 21 days after surgery: BG 3 days (A), BG/PLGA 3 days (B), BG 7 days (C), BG/PLGA 7 days (D), BG 14 days (E), BG/PLGA 14 days (F), BG 21 days (G), BG/PLGA 21 days (H). RANKL immunomarking (arrow) and biomaterial (#).

OPG

Similar to Runx2 and RANKL immunomarking, OPG was predominantly detected in the granulation tissue in the peripheral region of the bone defect for both BG and BG/PLGA on day 3 and 7 after surgery (Fig. 19A, 19B, 19C, 19D). Fourteen days after surgery, BG and BG/PLGA showed OPG immunomarking mainly in the granulation tissue around the biomaterial (Fig. 19E, 19F). On day 21 after surgery, in BG, OPG immunomarking could be observed in the granulation tissue between the material and the newly bone formed (Fig. 19G). In this period, BG/PLGA showed OPG immunomarking predominantly in the granulation tissue in the central region of the bone defect (Fig. 19H).

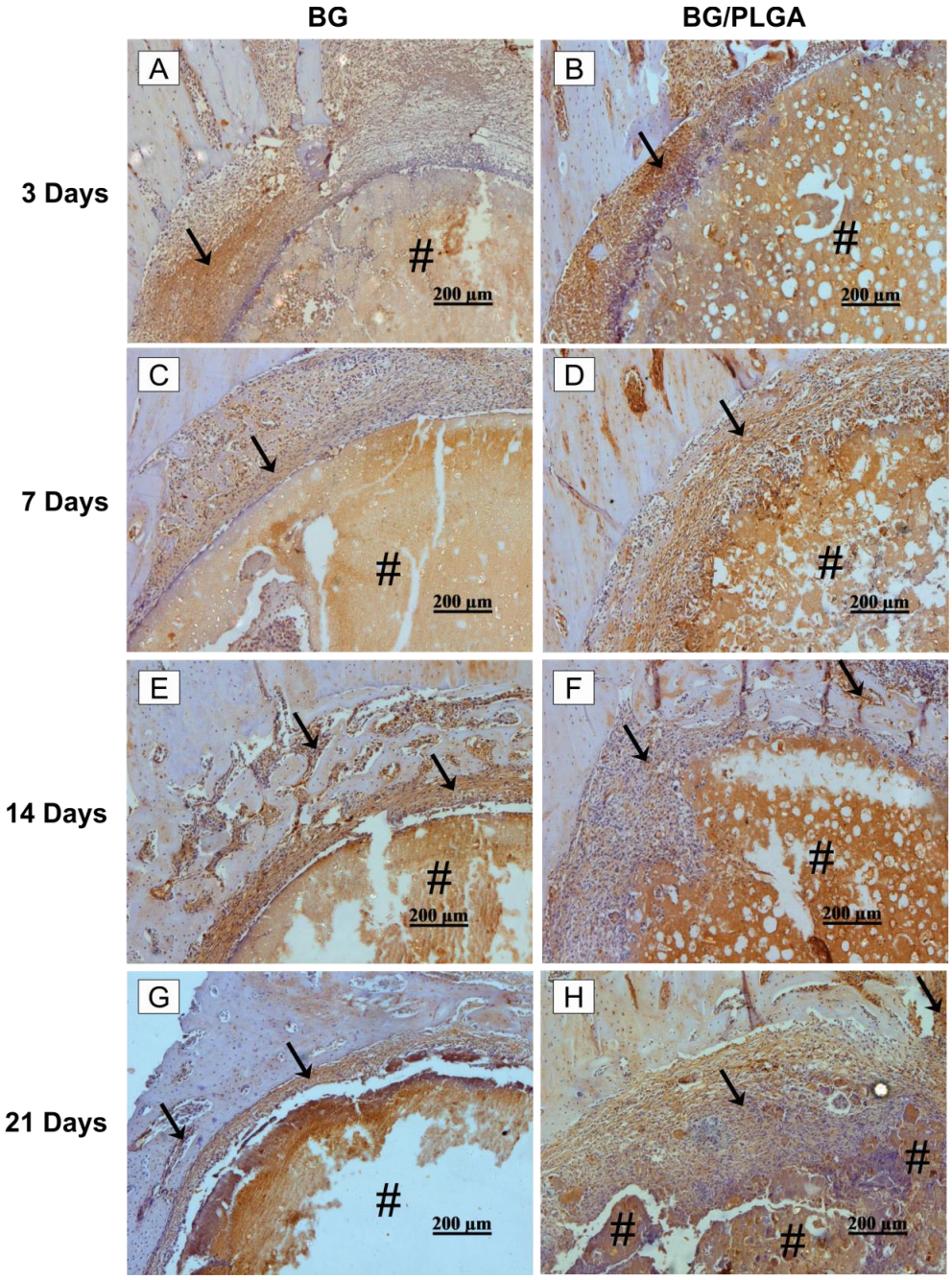

Fig. 19 Representative histological sections of Osteoprogesterin (OPG) immunohistochemistry of the experimental groups (BG and BG/PLGA) at 3, 7, 14 and 21 days after surgery: BG 3 days (A), BG/PLGA 3 days (B), BG 7 days (C), BG/PLGA 7 days (D), BG 14 days (E), BG/PLGA 14 days (F), BG 21 days (G), BG/PLGA 21 days (H). OPG immunomarking (arrow) and biomaterial (#).

5.4.7. QUANTITATIVE IMMUNOHISTOCHEMICAL ANALYSIS

No statistically significant differences were detected among the groups (BG and BG/PLGA) for Runx2 (Fig. 20A), RANKL (Fig. 20B) and OPG (Fig. 20C) immunomarking in the evaluated periods (3, 7, 14 and 21 days).

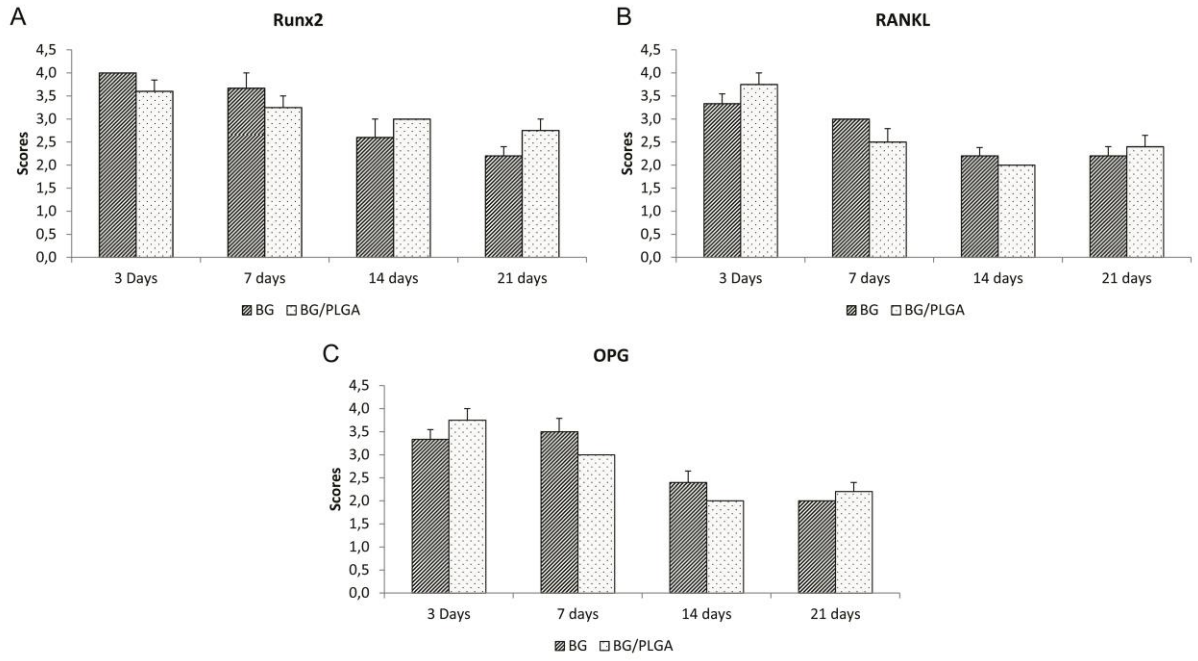

Fig. 20 Mean and SE scores for immunomarking of (A) runt-related transcription factor-2 (Runx2), (B) activator of nuclear factor kappa-B ligand (RANKL) and (C) osteoprogesterin (OPG).

5.4.8. qRT-PCR EVALUATION

Figure 21 represents the gene expression in BG and BG/PLGA after 3, 7, 14 and 21 days of implantation.

Day 3

Three days after implantation, no statistical difference was observed between BG and BG/PLGA for BMP4, Runx2, ALP and OC expression (Fig. 21A-21D).

Day 7

Seven days after surgery, no significantly statistical difference in the BMP4, ALP and OC expression was observed when compared BG/PLGA and BG (Fig. 21C, 21D). Furthermore, in this period, BG presented significantly higher values of the Runx2 expression when compared to BG/PLGA.

Day 14

After 14 days of implantation, no significantly statistical difference was observed in the expression levels of OC gene compared to BG/PLGA with BG (Fig. 21D). However, in the same period, BG/PLGA presented significantly higher values of BMP4, Runx2, and ALP expression when compared to the BG (Fig. 21A, 21B and 21C).

Day 21

After 21 days of surgery, no significantly statistical difference was observed in the BMP4, Runx2 and ALP expression in the groups evaluated (Fig. 21A, 21B). BG/PLGA presented higher values of the OC expression when compared to BG (Fig. 21D).

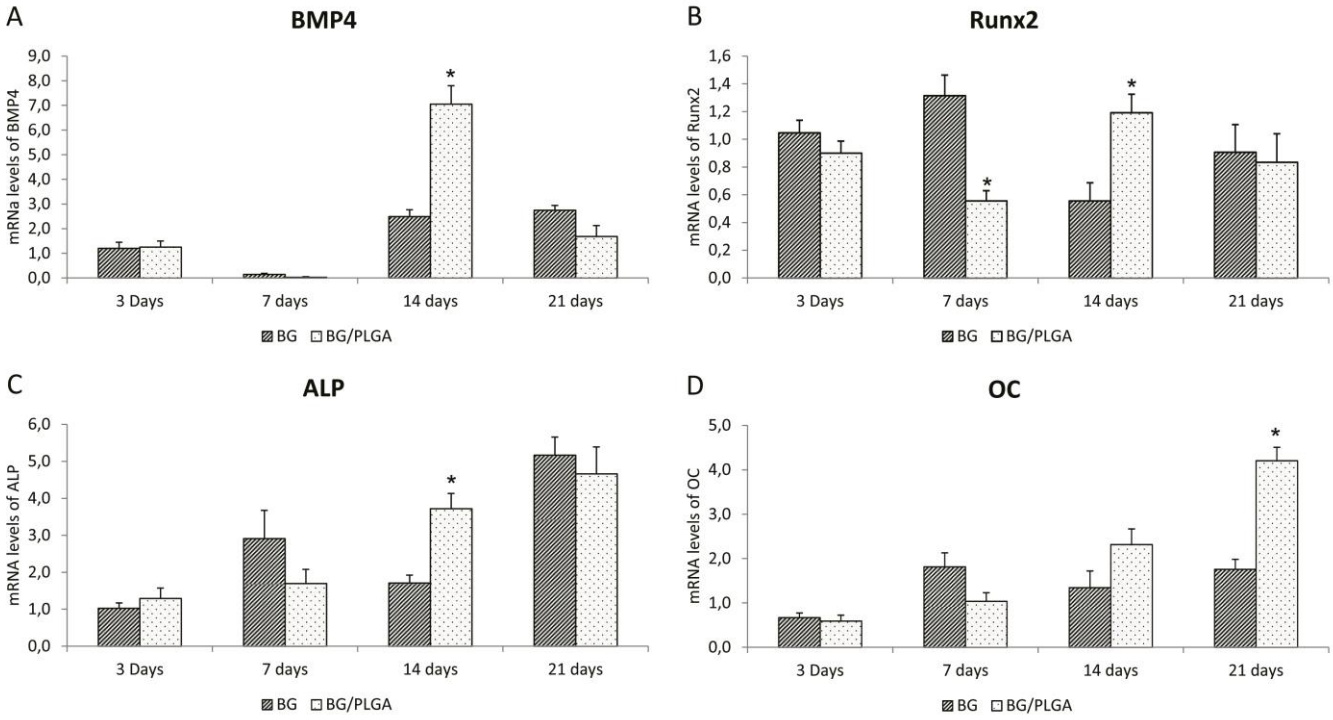

Fig. 21 Relative expression levels of BMP4 (A), Runx2 (B), ALP (C) and OC (D) in Biosilicate® group (BG) and Biosilicate®/PLGA group (BG/PLGA) measured by real-time PCR. (*) BG compared to BG/PLGA ($p \leq 0.05$).

5.5. DISCUSSION

This study aimed to investigate a BG/PLGA based composite in terms of morphological characteristics, pH and mass loss measurements, and further analyze the effects of this biomaterial on tibial bone repair in rats after 3, 7, 14 and 21 days. The main findings showed that the incorporation of PLGA into BG had a significant effect on the morphological structure of the material, decreasing pH and accelerating mass loss (increased degradation). Furthermore, histologic analysis revealed that the BG/PLGA showed increased material degradation, accompanied by higher bone formation when compared to BG, after 21 days of implantation. The immunohistochemical analysis indicated no statistically significant differences

between BG and BG/PLGA for Runx2, RANKL and OPG in all periods. In addition, qRT-PCR analysis showed that BG/PLGA induced downregulation of Runx2 at day 7, upregulation of BMP4, Runx2 and ALP at day 14 and upregulation of OC at day 21.

The inclusion of PLGA microspheres as a porogen additive is a promising strategy for bone tissue engineering due to the well-known biocompatibility of this polymer[19,29,30] and its capacity of inducing macroporosity and accelerating the degradation of biomaterials.[17,19] The degradation properties of a biomaterial are crucial for its successful performance and must be in balance with the tissue growth. The degradation rate of a biomaterial can influence cell growth, tissue regeneration, and host response.[31]

The mass loss evaluation showed a significant decrease in mass for both materials 3 days after immersion, but the materials did not collapse. This event may also be associated to the rapid ion release which is initiated after the contact of BG with fluids, starting the degradation of the material.[32,33] It is also suggested that the enhanced mass loss found for BG/PLGA composites when compared to BG in all periods may be related to the hydrolytic cleavage of the PLGA in the presence of water.[19] This event causes loss of integrity of the polymer, and consequently, the formation of porous structures, generating a higher implant surface area. The higher surface area leads to a more rapid dissolution when compared to dense bioactive glass.[34]

The medium containing BG/PLGA presented a decrease in the pH value when compared to BG. The acidification provided by PLGA degradation may have contributed to the pH decrease[19] in a highly alkaline medium generated by BG.[9] PLGA in the presence of water undergoes hydrolysis of its esters covalent bonds,

leading to the loss of the polymer integrity and, consequently, the degradation of the acid monomers (lactic and glycolic acid), which contributes to the acidification of the medium.[19,35] The acidification induced by PLGA, bringing the pH value closer to the physiological one, may favor the bone repair, since the variation of this factor can induce structural changes in bone proteins and, consequently, influence the activity of these macromolecules.[36,37]

The histological results indicated a higher progressive degradation for BG/PLGA when compared to BG, and substitution of the material by neoformed bone from the border to the central area of the defect. The higher amount of newly formed bone observed for BG/PLGA may be related to the increased degradation induced by PLGA microspheres. These results corroborate with those of Felix Lanao *et al*. (2011)[19] that indicate the incorporation of PLGA into calcium phosphate ceramics (CPC) as a factor that clearly accelerates material degradation and bone formation (Felix Lanao *et al*., 2011). The degradation of the material, accompanied by liberation of space in the defect area, is essential for tissue ingrowth.[38] Furthermore, BG/PLGA degradation may have provided an increased release of Biosilicate® particles, contributing to the bone formation induced by the bioactivity of this material.[39]

The qualitative immunohistochemical analysis indicated for Runx2, RANKL and OPG a more evident immunomarking for these markers in the granulation tissue. These finding corroborates with Tim *et al.* (2014)[25] and Pinto *et al.* (2013)[27] who also observed an intense immunomarking of osteogenic markers in this tissue. Although no statistical difference was found in the quantitative immunohistochemical analysis between BG and BG/PLGA, a tendency in decreasing Runx2, RANKL and OPG immunolabeling was observed overtime for both BG and BG/PLGA. Most probably, the decrease in the amount of cells (constituting the granulation tissue) with

increasing implantation time was accompanied by the reduction of the immunomarking, since these cells are responsible synthesis of the immunomarkers (proteins).[40]

The qRT-PCR analysis revealed downregulation of Runx2 expressions at day 7 and upregulation of BMP4, RUNX-2 and ALP expressions in BG/PLGA which were significantly different when compared to BG at day 14. These genes are related to attraction, differentiation and proliferation of osteoblasts.[41-44] It is suggested that the accelerated degradation of BG induced by PLGA, manly at day 14 after implantation, led to an increased release of ions leached from the material (calcium and sodium), stimulating the expression of BMP4, RUNX-2 and ALP genes.[17,45] Xynos *et al.* (2001)[45] observed that the ionic products of the Bioglass® 45S5 dissolution had a direct effect on the gene-expression profile of human osteoblasts, inducing relevant genes for the osteoblast metabolism and bone homeostasis. On the other hand, OC presented a statistically higher expression in BG/PLGA when compared to BG only after 21 days. This data can be clearly justified by the fact that this gene is later expressed,[46,47] since it is related to the mineralization process in the site of the bone injury.[48]

These results show that the present composite may be used as a bone graft for inducing bone repair. Nevertheless, since this work is limited to non-critical size bone defects using healthy animals, further studies on this new biomaterial, regarding critical size bone defect models (CSD) and compromised conditions (e.g. osteoporosis), are required in order to evaluate its *in vivo* efficacy.

5.6. CONCLUSION

BG/PLGA composites were obtained, presenting accelerated degradation which induced higher expressions (compared to plain BG) of osteogenic genes related to attraction, differentiation and proliferation of osteoblast in the defect area. As a consequence of all these improved processes, a higher amount of newly formed bone was found for the groups treated using the composites at day 21 after implantation. These promising results justify additional biological studies using other kind of experimental models and compromised conditions to deeply understand the behavior of this new composite toward its use in bone engineering applications.

5.7. ACKNOWLEDGMENTS

The authors thank FAPESP (Fundação de Amparo à Pesquisa do Estado de São Paulo) for their financial support.

5.8. REFERENCES

1. Furia JP, Rompe JD, Cacchio A, Maffulli N. Shock wave therapy as a treatment of nonunions, avascular necrosis, and delayed healing of stress fractures. Foot Ankle Clin. 2010;15:651-662.

2. Eldesoqi K, Henrich D, El-Kady AM, Arbid MS, Abd El-Hady BM, Marzi I, Seebach C. Safety evaluation of a bioglass-polylactic acid composite scaffold seeded with progenitor cells in a rat skull critical-size bone defect. PLoS One. 2014;9:e87642.

3. Lichte P, Pape HC, Pufe T, Kobbe P, Fischer H. Scaffolds for bone healing: concepts, materials and evidence. Injury. 2011;42:569-73.

4. Dias MI, Lourenço P, Rodrigues A, Azevedo J, Viegas C, Ferreira A, Cabrita AS. The effect of the quantitative variation of autologous spongy bone graft applied for bone regeneration in an experimental model of tibia osteotomy. Acta Med Port. 2007;20:37-46.

5. Välimäki V, Yrjans JJ, Vuorio E, Aro HT: Combined effect of bone morphogenetic protein-2 gene therapy and bioactive glass microspheres in enhancement of new bone formation. J Biomed Mater Res. 2005;75:501-09.

6. Drosse I, Volkmer E, Seitz S, Seitz H, Penzkofer R, Zahn K, Matis U, Mutschler W, Augat P, Schieker M. Validation of a femoral critical size defect model for orthotopic evaluation of bone healing: a biomechanical, veterinary and trauma surgical perspective. Tissue Eng Part C Methods. 2008;14:79-88.

7. Cheng N, Wang Y, Zhang Y, Shi B. The osteogenic potential of mesoporous bioglasses/silk and non-mesoporous bioglasses/silk scaffolds in ovariectomized rats: in vitro and in vivo evaluation. PLoS One 2013; 12:e81014.

8. Zwingenberger S, Nich C, Valladares RD, Yao Z, Stiehler M, Goodman SB. Recommendations and considerations for the use of biologics in orthopaedic surgery. BioDrugs. 2012;26:245-56.

9. Hench LL,Polak JM. 2002, Third-generation biomedical materials, Science, 295: 1014-1017.

10. Day RM, Maquet V, Boccaccini AR, Jerome R,Forbes A. In vitro and in vivo analysis of macroporous biodegradable poly(D,L-lactide-co-glycolide) scaffolds containing bioactive glass, J Biomed Mater Res A 2005;75:778-787.

11. Jones JR. Review of bioactive glass: from Hench to hybrids, Acta Biomater 2013;9:4457-4486.

12. Bossini PS, Rennó AC, Ribeiro DA, Fangel R, Peitl O, Zanotto ED, Parizotto NA. Biosilicate® and low-level laser therapy improve bone repair in osteoporotic rats. J Tissue Eng Regen Med. 2011 5:229-37.

13. Heikkilä JT, Kukkonen J, Aho AJ, Moisander S, Kyyrönen T, Mattila K. Bioactive glass granules: a suitable bone substitute material in the operative treatment of depressed lateral tibial plateau fractures: a prospective, randomized 1 year follow-up study. J Mater Sci Mater Med. 2011;22:1073-80.

14. Peitl O, Zanotto ED, Hench LL. Highly bioative P2O5-Na2OCaO-SiO2 glass ceramics. Journal of Non-Crystalline Solids 2001;292:115-126.

15. Peitl O, Zanotto ED, Serbena FC, Hench LL. "Compositional and Microstructural Design of Highly Bioactive P2O5-Na2O-CaO-SiO2 Glass

Ceramics", Acta Biomaterialia 2012;1-49.

16. Granito RN, Rennó AC, Ravagnani C, Bossini PS, Mochiuti D, Jorgetti V, Driusso P, Peitl O, Zanotto ED, Parizotto NA, Oishi J. In vivo biological performance of a novel highly bioactive glass-ceramic (Biosilicate®): A biomechanical and histomorphometric study in rat tibial defects. J Biomed Mater Res B Appl Biomater. 2011;97:139-47.

17. Renno AC, van de Watering FC, Nejadnik MR, Crovace MC, Zanotto ED, Wolke JG, Jansen JA, van den Beucken JJ. Incorporation of bioactive glass in calcium phosphate cement: An evaluation. Acta Biomater. 2013;9:5728-39.

18. Liao H, Walboomers XF, Habraken WJEM, Zhang Z, Li Y, Grijpma DW, et al. Injectable calcium phosphate cement with PLGA, gelatin and PTMC microspheres in a rabbit femoral defect. Acta Biomater 2011;7:1752-9.

19. Félix Lanao RP, Leeuwenburgh SC, Wolke JG, Jansen JA. Bone response to fast-degrading, injectable calcium phosphate cements containing PLGA microparticles. Biomaterials. 2011;32:8839-47.

20. Habraken WJEM, Wolke JGC, Mikos AG, Jansen JA. PLGA microsphere/calcium phosphate cement composites for tissue engineering: in vitro release and degradation characteristics. J Biomater Sci Polym Ed 2008;19:1171-88.

21. Ruhé P, Boerman O, Russel F, Mikos A, Spauwen P, Jansen J. In vivo release of rhBMP-2 loaded porous calcium phosphate cement pretreated with albumin. J Mater Sci Mater Med 2006;17:919-27.

22. Plachokova A, Link D, van den Dolder J, van den Beucken J, Jansen J. Bone regenerative properties of injectable PGLA–CaP composite with TGF- b1 in a rat augmentation model. J Tissue Eng Regen Med 2007;1:457-64.

23. Bossini PS, Rennó AC, Ribeiro DA, Fangel R, Ribeiro AC, Lahoz Mde A, Parizotto NA. Low level laser therapy (830nm) improves bone repair in osteoporotic rats: similar outcomes at two different dosages. Exp Gerontol. 2012;47:136-42.

24. Matsumoto MA, Ferino RV, Monteleone GF, Ribeiro DA. Low-level laser therapy modulates cyclo-oxygenase-2 expression during bone repair in rats. Lasers Med Sci. 2009;24:195-201.

25. Tim CR, Pinto KNZ, Rossi BRO, Fernandes K, Matsumoto MA, Parizotto NA, Rennó ACM. Low-level laser therapy enhances the expression of osteogenic factors during bone repair in rats. Lasers Med Sci 2014:29:147-156.

26. Matsumoto, M.A.; Caviquioli, G.; Biguetti, C.C.; Holgado, L.A.; Saraiva, P.P.; Rennó, A.C.M.; Kawakam, R.Y. A novel bioactive vitroceramic presents similar biological responses as autogenous bone grafts. J. Mater. Sci. Mater. Med 2012;23:1447-1456.

27. Pinto KN, Tim CR, Crovace MC, Matsumoto MA, Parizotto NA, Zanotto ED, Peitl O, Rennó AC. Effects of Biosilicate® scaffolds and low-level laser therapy on the process of bone healing. Photomed Laser Surg. 2013;31:252-60.

28. Livak KJ, Schmittgen TD. Analysis of Relative Gene Expression Data Using Real Time Quantitative PCR and the $2^{-\Delta\Delta CT}$ Method. Methods 2001;25:402-408.

29. Link DP, van den Dolder J, van den Beucken JJ, Cuijpers VM, Wolke JG, Mikos AG, et al. Evaluation of the biocompatibility of calcium phosphate cement/PLGA microparticle composites. J Biomed Mater Res A 2008;87:760e9.

30. Wang S, Shi X, Gan Z, Wang F. Preparation of PLGA Microspheres with Different Porous Morphologies. Chinese Journal of Polymer Science 2015;33:128-136.

31. Ren T, Ren J, Jia X, Pan K. The bone formation in vitro and mandibular defect repair using PLGA porous scaffolds. J Biomed Mater Res A. 2005;74:562-9.

32. Kokubo T, Kushitani H, Sakka S, Kitsugi T,Yamamuro T. Solutions able to reproduce in vivo surface-structure changes in bioactive glass-ceramic A-W, J Biomed Mater Res 1990;24:721-734.

33. Jones J. Review of bioactive glass: from Hench to hybrids. Acta Biomater,2013;9:4457-86.

34. Jones JR, Gentleman E, Polak J. Bioactive Glass Scaffolds for Bone Regeneration. Elements 2007;3:393-399.

35. Félix Lanao RP, Sariibrahimoglu K, Wang H, Wolke JG, Jansen JA, Leeuwenburgh SC. Accelerated calcium phosphate cement degradation due to incorporation of glucono-delta-lactone microparticles. Tissue Eng Part A. 2014;20:378-88.

36. Dimitriou R, Tsiridis E, Giannoudis PV. Current concepts of molecular aspects of bone healing. Injury. 2005;36:1392-404.

37. Luca L, Rougemont AL, Walpoth BH, Gurny R, Jordan O. The effects of carrier nature and pH on rhBMP-2-induced ectopic bone formation. J Control Release. 2010;147:38-44.

38. van de Watering FCJ, van den Beucken JJJP, Walboomers XF, Jansen JA. Calcium phosphate/poly(D,L-lactic-co-glycolic acid) composite bone substitute materials: evaluation of temporal degradation and bone ingrowth in a rat critical-sized cranial defect. Clin Oral Implants Res 2012;23:151-9.

39. Moura J, Teixeira LN, Ravagnani C, Peitl O, Zanotto ED, Beloti MM, et al. In vitro osteogenesis on a highly bioactive glass-ceramic (Biosilicate). J Biomed Mater Res A 2007;82A:545-57.

40. Maeda H, Wada N, Nakamuta H, Akamine A. Human periapical granulation tissue contains osteogenic cells. Cell Tissue Res (2004) 315:203–208. Biomed. Mater. 2013;8:035012.

41. Wang M. Developing bioactive composite materials for tissue replacement. Biomaterials. 2003;24:2133-51.

42. Hadjidakis DJ, Androulakis II. Bone remodeling. Ann N Y Acad Sci, Nova York 2006;1092:385-396.

43. Proff P. Römer P. The molecular mechanism behind boné remodelling: a review. Clinical Oral Investigations 2009;13:355-362.

44. Nakamura T, Naruse M, Chiba Y, Komori T, Sasaki K, Iwamoto M, Fukumoto S. Novel hedgehog agonists promote osteoblast differentiation in mesenchymal stem cells. J Cell Physiol. 2015;230:922-9.

45. Xynos ID, Edgar AJ, Buttery LD, Hench LL, Polak JM. Gene-expression profiling of human osteoblasts following treatment with the ionic products of Bioglass 45S5 dissolution. J Biomed Mater Res. 2001;55:151-7.

46. Wang C, Duan Y, Markovic B, Barbara J, Howlett CR, et al. Phenotypic expression of bone-related genes in osteoblasts grown on calcium phosphate ceramics with different phase compositions. Biomaterials 2004;25:2507-2514.

47. Lee H-R, Kim H-J, Ko J-S, Choi Y-S, Ahn M-W, et al. (2013) Comparative Characteristics of Porous Bioceramics for an Osteogenic Response In Vitro and In Vivo. PLoS ONE 2013;8:e84272.

48. Chen L, Jacquet R, Lowder E, WJ Landis. Refinement of collagen - mineral interaction: A possible role for osteocalcin in apatite crystal nucleation, growth and development. Bone 2015;71:7-16.

PARTE III

6. CONSIDERAÇÕES FINAIS

7. REFERÊNCIAS BIBLIOGRÁFICAS

ANEXOS

6. CONSIDERAÇÕES FINAIS

Baseado nos resultados dos dois estudos é possível chegar as seguintes conclusões:

- Os *scaffolds* de Biosilicato® apresentaram uma estrutura porosa e uma taxa de degradação adequada para a formação de tecido ósseo. Além disso, os *scaffolds* de Biosilicato® foram capazes de induzir a síntese de fatores vasculares e osteogênicos e não induziu qualquer resposta inflamatória sistémica.

- Os compósitos de BG/PLGA apresentaram uma maior taxa de degradação quando comparado ao BG. Tal característica encontrada em BG/PLGA pode ter induzido uma maior expressão de genes osteogênicos relacionados a atração, diferenciação e proliferação de osteoblastos na área do defeito, conduzindo a uma maior formação de tecido ósseo no período de 21 dias após implantação quando comparado a BG.

Diante do exposto, é possível concluir que ambas os materiais utilizados neste estudo, *scaffold* de Biosilicato® altamente poroso e compósito de Biosilicato® e PLGA, foram eficazes em estimular o reparo de um defeito ósseo tibial em ratos, demonstrando serem alternativas promissoras para tratamento de fraturas ósseas.

7. REFERÊNCIAS BIBLIOGRÁFICAS

BHATT, R.A.; ROZENTAL, T.D. Bone Graft Substitutes. **Hand Clinics**, v. 28, p. 457-468, 2012.

BOSSINI P.S.; RENNÓ, A.C.M.; RIBEIRO, D.A.; FANGEL, R.; RIBEIRO, A.C.; LAHOZ, M.A.; PARIZOTTO, N.A. Low level laser therapy (830 nm) improves bone repair in osteoporotic rats: Similar outcomes at two different dosages. **Experimental Gerontology**, v. 47, p. 136-142, 2012.

BOSSINI, P.S.; RENNÓ, A.C.; RIBEIRO, D.A.; PEITL, O.; ZANOTTO, E.D.; PARIZOTTO, N.A. Biosilicato® and low-level laser therapy improve bone repair in osteoporotic rats. **J Tissue Eng Regen Med**, v. 5, p. 229-37, 2011.

CHEN, J.P.; TSAI, M.J.; LIAO, H.T. Incorporation of biphasic calcium phosphate microparticles in injectable thermoresponsive hydrogel modulates bone proliferation and differentiation. **Colloids Surf B Biointerfaces**, v. 1, p. 120-9, 2013.

CHEN, Q.; ROETHER, J.A.; BOCCACCINI, A.R. Tissue engineering scaffolds from bioactive glass and composite materials. In: Ashammakhi, N.; REIS, R.; CHIELLINI, F. (eds.) Topics in Tissue Engineering, v. 4, 2008.

CROVACE, M.C. **Obtenção de estruturas porosas altamente bioativas via sinterização do Biosilicato®**. 2009. 141f. Dissertação (Mestrado em Engenharia de

Materiais) - Programa de Pós-Graduação em Ciência e Engenharia de Materiais, Universidade Federal de São Carlos, São Carlos, 2009.

DE LONG, W.G. Jr.; EINHORN, T.A.; KOVAL, K.; MCKEE, M.; SMITH, W.; SANDERS, R.; WATSON, T. Bone grafts and bone graft substitutes in orthopaedic trauma surgery. A critical analysis. **J Bone Joint Surg Am**, v. 89, p. 649-58, 2007.

DIMITRIOU, R.; TSIRIDIS, E.; GIANNOUDIS, P.V. Current concepts of molecular aspects of bone healing. **Injury**, v. 36, p. 1392-1404, 2005.

DREIFKE, M.B.; EBRAHEIM, N.A.; JAYASURIYA, A.C. Investigation of potential injectable polymeric biomaterials for bone regeneration. **J Biomed Mater Res A**., v. 101, p. 2436-47, 2013.

FELIX LANAO, R.P.; LEEUWENBURGH, S.C.G.; WOLKE, J.G.C.; JANSEN, J.A. Bone response to fast-degrading, injectable calcium phosphate cements containing PLGA microparticles. **Biomaterials**, v. 32, p. 8839-8847, 2011.

FILLINGHAM, Y.A.; LENART, B.A.; GITELIS, S. Function after injection of benign bone lesions with a bioceramic. **Clin Orthop Relat Res**, v. 470, p. 2014-20, 2012.

FURIA, J.P.; ROMPE, J.D.; CACCHIO, A.; MAFFULLI, N. Shock wave therapy as a treatment of nonunions, avascular necrosis, and delayed healing of stress fractures. **Foot Ankle Clin**, v. 15, p. 651-662, 2010.

GIANNOUDIS, P.V.; EINHORN, T.A.; MARSH, D. Fracture healing: the diamond concept. **Injury**, v. 38, p. S3-6, 2007.

GRANITO, R.N.; RIBEIRO, D.A.; RENNÓ, A.C. M.; RAVAGNANI, C.; BOSSINI, P.S.; PEITL-FILHO, O.; ZANOTTO, E.D.; PARIZOTTO, N.A.; OISHI, J. Effects of biosilicate and bioglass 45S5 on tibial bone consolidation on rats: a biomechanical and a histological study. **J Mater Sci: Mater Med**, v. 20, p. 2521-2526, 2009.

HABRAKEN, W.J.; WOLKE, J.G.; MIKOS, A.G.; JANSEN, J.A. PLGA microsphere/calcium phosphate cement composites for tissue engineering: in vitro release and degradation characteristics. **J Biomater Sci Polym**, v. 19, p. 1171-1188, 2008.

HADJIARGYROU, M.; KENNETH, M.; RYABY, J.P.; RUBIN, C. Enhancement of fracture healing by low intensity ultrasound. **Clin Orthop Relat Res***,* v. 355, p. 216-229, 1998.

HAK, D.J. The use of osteoconductive bone graft substitutes in orthopaedic trauma. **J Am Acad Ortho Surg**, v. 15, p. 525-536, 2007.

HENCH, L.L.; POLAK, J.M. Third-generation biomedical materials. **Science**, v. 295, p. 1014-7, 2002.

JONES, J. Review of bioactive glass: from Hench to hybrids. **Acta Biomater**, v. 9, p. 4457-86, 2013.

JONES, J.R.; GENTLEMAN, E.; POLAK, J. Bioactive Glass Scaffolds for Bone Regeneration. **Elements**, v. 3, p. 393-399, 2007.

KARAGEORGIOU, V.; KAPLAN, D. Porosity of 3D biomaterial scaffolds and osteogenesis. **Biomaterials**, v. 26, p. 5474-91, 2005.

KHAN, Y.; YASZEMSKI, M.J.; MIKOS, A.G.; LAURENCIN, C.T. Tissue engineering of bone: material and matrix considerations. **J Bone Joint Surg Am**, v. 1, p. 36-42, 2008.

KIDO, H.W.; OLIVEIRA, P.; PARIZOTTO, N.A.; CROVACE, M.C.; ZANOTTO, E.D.; PEITL-FILHO, O.; FERNANDES, K.P.; MESQUITA-FERRARI, R.A.; RIBEIRO, D.A.; RENNO A.C. Histopathological, cytotoxicity and genotoxicity evaluation of Biosilicate® glass-ceramic compósitos. **J Biomed Mater Res A**, v. 101, p. 667-73, 2013.

KLOTING, N.; FOLLAK, N.; KLOTING, I. Is there an autoimmune process in bone? Gene expression studies in diabetic and nondiabetic BB rat as well as BB rat-related and-unrelated rat strains. **Physiol Genomics**. 24:59-64, 2005.

LEACH, J.K; KAIGLER, D.; WANG, Z.; KREBSBACH, P.H.; MOONEY, D.J. Coating of VEGF-releasing scaffolds with bioactive glass for angiogenesis and bone regeneration. **Biomaterials**, v. 27, p. 3249-55, 2006.

LIVAK, K.J.; SCHMITTGEN, T.D. Analysis of Relative Gene Expression Data Using Real Time Quantitative PCR and the $2^{-\Delta\Delta CT}$ Method. **Methods**, v. 25, p. 402-408, 2001.

MATSUMOTO, M.A.; FERINO, R.F.; MONTELEONE, G.F.; RIBEIRO, D.A. Low-level laser therapy modulates cyclo-oxygenase-2 expression during bone repair in rats. **Laser Med. Sci.**, v. 24, p. 195-201, 2009.

MATSUMOTO, M.A.; CAVIQUIOLI, G.; BIGUETTI, C.C.; HOLGADO, L.A.; SARAIVA, P.P.; RENNÓ, A.C.M.; KAWAKAM, R.Y. A novel bioactive vitroceramic presents similar biological responses as autogenous bone grafts. **J. Mater. Sci. Mater. Med.,** v. 23, p. 1447-1456, 2012.

MOURA, J.; TEIXEIRA, L.N.; RAVAGNANI, C.; PEITL-FILHO, O.; ZANOTTO, E.D.; BELOTI, M.M.; PANZERI, H.; ROSA, A.L.; OLIVEIRA, P.T. In vitro osteogenesis on a highly bioactive glassceramic (Biosilicato®**). J Biomed Mater Res A**, v. 82, p. 545-57, 2007.

NO, Y.J.; ROOHANI-ESFAHANI, SI.; ZREIQAT, H. Nanomaterials: the next step in injectable bone cements. **Nanomedicine (Lond)**, v. 8, p. 1745-64, 2014.

PAPE, H.C.; MARCUCIO, R.; HUMPHREY, C.; COLNOT, C.; KNOBE, M.; HARVEY, E.J. Trauma-Induced Inflammation and Fracture Healing. J Orthop **Trauma**, v. 24, p. 9, 2010.

PHIEFFER, L.S.; GOULET, J.A. Delayed Unions of the Tibia. **J Bone Joint Surg Am**, v. 88, p. 205-216, 2006.

PINTO, K.N.; TIM, C.R.; CROVACE, M.C.; MATSUMOTO, M.A.; PARIZOTTO, N.A.; ZANOTTO, E.D.; PEITL, O.; RENNÓ, A.C. Effects of Biosilicate scaffolds and low-level laser therapy on the process of bone healing. **Photomed Laser Surg**, v. 31, p. 252-60, 2013.

PLACHOKOVA, A.; LINK, D.; VAN DEN DOLDER, J.; VAN DEN BEUCKEN, J.; JANSEN, J. Bone regenerative properties of injectable PGLA-CaP composite with TGF- b1 in a rat augmentation model. **J Tissue Eng Regen Med**, v. 1, p. 457-64, 2007.

PULEO, D.A.; HOLLERAN, L.A.; DOREMUS, R.H.; BIZIOS, R. Osteoblast responses to orthopedic implant materials in vitro. **J Biomed Mater Res**, v. 25, p. 711-723, 1991.

RATH, B.; NAM, J.; KNOBLOCK, T.J.; LANNUTTI, J.J.; AGARWALL, S. Compressive forces induce osteogenic gene expression in calvarial osteoblasts. **J Biomech**, v. 41, p. 1095-1103, 2008.

RENNO, A.C.; NEJADNIK, M.R.; van de WATERING, F.C.; CROVACE, M.C.; ZANOTTO, E.D.; HOEFNAGELS, J.P.; WOLKE, J.G.; JANSEN, J.A.; van den BEUCKEN, J.J. Incorporation of bioactive glass in calcium phosphate cement: material characterization and in vitro degradation. **J Biomed Mater Res A**, v. 101, p. 2365-73, 2013.

RENNO, A.C.; van de WATERING, F.C.; NEJADNIK, M.R.; CROVACE, M.C.; ZANOTTO, E.D.; WOLKE, J.G.; JANSEN, J.A.; van den BEUCKEN, J.J. Incorporation of bioactive glass in calcium phosphate cement: An evaluation. **Acta Biomater**, v. 9, p. 5728-39, 2013.

SCHIEKER, M.; SEITZ, H.; DROSSE, I.; SEITZ, S.; MUTSCHLER. W. Biomaterials as Scaffold for Bone Tissue Engineering. **Eur J Trauma**, v. 32, p. 114-24, 2006.

SONG, S.L.; HUTMACHER, D.; NURCOMB, V.; COOL, SM. Temporal expression of protoeglycans in the rat limb during bone healing. **Gene**, v. 379, p. 92-100, 2006.

TIM, C.R. **Efeitos do laser de baixa intensidade e do scaffold de Biosilicato® no processo de reparação óssea.** 2011. 78 f. Dissertação (Mestrado em Biotecnologia) – Programa de Pós-Graduação em Biotecnolgia, Universidade Federal de São Carlos, São Carlos, 2009.

TIM, C.R.; PINTO, K.N. Z.; ROSSI, B.R.O.; FERNANDES, K.; MATSUMOTO, M.A.; PARIZOTTO, N.A. RENNÓ, A.C.M. Low-level laser therapy enhances the expression of osteogenic factors during bone repair in rats. **Lasers Med Sci**, 2013.

WU, C.C.; YANG, K.C.; YANG, S.H.; LIN, M.H.; KUO, T.F.; LIN, F.H. In vitro studies of composite bone filler based on poly (propylene fumarate) and biphasic α-tricalciumphosphate/hydroxyapatite ceramic powder. **Artif Organs**, v. 36, p. 418-28, 2012.

XIN, R.; ZHANG, Q.; GAO, J. Identification of the wollastonite phase in sintered 45S5 bioglass and its effect on in vitro bioactivity. **J Non Cryst Solids**, v. 356, p. 1180-1184, 2010.

YAOITA, H.; ORIMO, H.; HHIRAI, Y.; SHIMADA, T. Expression of bone morphogenetic proteins and rat distal-less homolog genes following rat femoral fracture. **J Bone Miner Metab**, v. 18, n. 2, p. 63-70, 2000.

ZANOTTO, E.D. et al. **Process and compositions for preparing particulate, bioactive or resorbable biosilicates for use in the treatment of oral ailments.** Fundação Universidade Federal de São Carlos; Universidade de São Paulo. Int. C. C03C10/00, 20, WO2004/074199, 2004.

ANEXOS

ANEXO A – Parecer da Comissão de Ética no Uso de Animais – Estudo I

UNIVERSIDADE FEDERAL DE SÃO CARLOS
PRÓ-REITORIA DE PESQUISA
Comissão de Ética no Uso de Animais
Via Washington Luís, km. 235 - Caixa Postal 676
Fones: (016) 3351.8025 / 3351.9679
Fax: (016) 3351.8025
CEP 13560-970 - São Carlos - SP - Brasil
ceua@ufscar.br - www.propq.ufscar.br

Parecer da Comissão de Ética no Uso de Animais

nº 046/2012

Protocolo nº. 042/2012

A Comissão de Ética no Uso de Animais da Universidade Federal de São Carlos - CEUA/UFSCar **APROVOU** o projeto de pesquisa intitulado *"Ação da Vitrocerâmica Bioativa (Biosilicato) no Processo de Reparação Óssea"*, submetido pelo pesquisador *Hueliton Wilian Kido.*

São Carlos, 14 de setembro de 2012.

Profa. Dra. Luciana Thie Seki Dias

Presidente da Comissão de Ética no Uso de Animais

ANEXO B – Parecer da Comissão de Ética no Uso de Animais – Estudo II

UNIVERSIDADE FEDERAL DE SÃO CARLOS
PRÓ-REITORIA DE PESQUISA
Comissão de Ética no Uso de Animais
Via Washington Luís, km. 235 - Caixa Postal 676
Fones: (016) 3351.8025 / 3351.9679
Fax: (016) 3351.8025
CEP 13560-970 - São Carlos - SP - Brasil
ceua@ufscar.br - www.propg.ufscar.br

Parecer da Comissão de Ética no Uso de Animais
nº 050/2014

A Comissão de Ética no Uso de Animais da Universidade Federal de São Carlos - CEUA/UFSCar **APROVOU** o projeto de pesquisa *Incorporação do Ácido Poli-Láctico-Co-Glicólico (PLGA) na vitrocerâmica bioativa (Biosolicato®); efeitos sobre o processo de reparo ósseo*, submetido pelo pesquisador **Hueliton Wilian Kido.**

São Carlos, 15 de Dezembro de 2014

Profa. Dra. Azair Liane Matos do Canto de Souza

Presidente da Comissão de Ética no Uso de Animais

ANEXO C – Artigo publicado – Estudo I

J Mater Sci: Mater Med (2015) 26:74
DOI 10.1007/s10856-015-5411-9

BIOCOMPATIBILITY STUDIES

Porous bioactive scaffolds: characterization and biological performance in a model of tibial bone defect in rats

Hueliton Wilian Kido · Carla Roberta Tim · Paulo Sérgio Bossini · Nivaldo Antônio Parizotto · Cynthia Aparecida de Castro · Murilo Camuri Crovace · Ana Candida Martins Rodrigues · Edgar Dutra Zanotto · Oscar Peitl Filho · Fernanda de Freitas Anibal · Ana Claudia Muniz Rennó

Received: 5 May 2014 / Accepted: 6 November 2014

Abstract The aim of this study was to evaluate the effects of highly porous Biosilicate® scaffolds on bone healing in a tibial bone defect model in rats by means of histological evaluation (histopathological and immunohistochemistry analysis) of the bone callus and the systemic inflammatory response (immunoenzymatic assay). Eighty Wistar rats (12 weeks-old, weighing ±300 g) were randomly divided into 2 groups (n = 10 per experimental group, per time point): control group and Biosilicate® group (BG). Each group was euthanized 3, 7, 14 and 21 days post-surgery. Histological findings revealed a similar inflammatory response in both experimental groups, 3 and 7 days post-surgery. During the experimental periods (3–21 days post-surgery), it was observed that the biomaterial degradation, mainly in the periphery region, provided the development of the newly formed bone into the scaffolds. Immunohistochemistry analysis demonstrated that the Biosilicate® scaffolds stimulated cyclooxygenase-2, vascular endothelial growth factor and runt-related transcription factor 2 expression. Furthermore, in the immunoenzymatic assay, BG presented no difference in the level of tumor necrosis factor alpha in all experimental periods. Still, BG showed a higher level of interleukin 4 after 14 days post-implantation and a lower level of interleukin 10 in 21 days post-surgery. Our results demonstrated that Biosilicate® scaffolds can contribute for bone formation through a suitable architecture and by stimulating the synthesis of markers related to the bone repair.

H. W. Kido · C. R. Tim · N. A. Parizotto
Department of Physiotherapy, Post-Graduate Program of Biotechnology, Federal University of São Carlos (UFSCar), São Carlos, SP, Brazil
e-mail: hueliton_kido@yahoo.com.br

P. S. Bossini · A. C. M. Rennó (✉)
Department of Biosciences, Federal University of São Paulo (UNIFESP), Ana Costa, 95, Santos, SP, Brazil
e-mail: a.renno@unifesp.br

C. A. de Castro
Department of Physiological Sciences, Federal University of São Carlos (UFSCar), São Carlos, SP, Brazil

M. C. Crovace · A. C. M. Rodrigues · E. D. Zanotto · O. P. Filho
Department of Materials Engineering, Vitreous Materials Laboratory (LaMaV), Federal University of São Carlos (UFSCar), São Carlos, SP, Brazil

F. de Freitas Anibal
Department of Morphology and Pathology, Federal University of São Carlos (UFSCar), São Carlos, SP, Brazil

1 Introduction

Although bone tissues have the ability of healing themselves, multiple factors may impair fracture consolidation, including fractures beyond critical size dimension, bone loss caused by diseases, infections or tumor resections, which may lead to the development of pseudoarthosis or even non-union fractures [1]. In this context, several surgical procedures are required to treat such clinical conditions, which are related to considerable morbidity and increased health care needs [2]. Bone grafts to enhance bone repair have been emerging as a promising alternative and include the use of autografts, allografts and synthetic bone substitutes [3–5].

Nevertheless, the limited availability of autogenous bone implants and the possibility of infectious diseases or tissue rejection associated to the use of allogenous implants are pivotal restrictions related to bone healing therapies [6].

Published online: 29 January 2015